REGULARIZED STRUCTURAL EQUATION MODELING FOR INDIVIDUAL-LEVEL DIRECTED FUNCTIONAL CONNECTIVITY

Stephanie T. Lane

A dissertation submitted to the faculty of the University of North Carolina at Chapel Hill in partial fulfillment of the requirements for the degree of Doctor of Philosophy in the Department of Psychology and Neuroscience (Quantitative).

Chapel Hill
2017

Approved by:

Kathleen Gates

Patrick Curran

Kenneth Bollen

Kelly Giovanello

Donglin Zeng

ABSTRACT

Stephanie T. Lane: Regularized structural equation modeling for individual-level directed functional connectivity.
(Under the direction of Kathleen Gates and Patrick Curran).

Within functional magnetic resonance imaging (fMRI) research, one method for evaluating functional brain architecture is directed functional connectivity analysis. Given the potentially exploratory nature of directed functional connectivity modeling, data-driven strategies for identifying individual-level models are necessary. One promising method, the unified SEM, is rooted in the structural equation modeling framework. By representing both the lagged and contemporaneous directed relationships present among regions of interest, it allows for the estimation of individual-level models of connectivity. In this study, I present the *regularized* unified SEM as an alternative to existing methods, where an individual-level model is selected from a range of possible models with varying degrees of penalization. This method is compared to other existing methods for establishing directed functional connectivity, including an established stepwise model building procedure for the unified SEM as well as the graphical vector autoregressive model. In this evaluation, the regularized unified SEM using the adaptive LASSO outperforms all other methods on simulated time series data, as well as on simulated blood oxygen level dependent (BOLD) data. Performance is optimal in the presence of a long time series, a small number of variables, and a sparse network.

TABLE OF CONTENTS

LIST OF TABLES

LIST OF FIGURES

LIST OF ABBREVIATIONS

ALASSO	adaptive least absolute shrinkage and selection
HRF	hemodynamic response function
LASSO	least absolute shrinkage and selection
ML	maximum likelihood
ROI	region of interest
S	sparsity of network
T	number of time points
TR	temporal resolution
uSEM	unified structural equation model
V	number of variables
VAR	vector autoregressive

CHAPTER 1: INTRODUCTION

Within psychological science, a renewed appreciation for investigating processes at the level of the individual has emerged. In the last several decades, a handful of methods have been proposed to examine change at the level of the individual (e.g., p-technique factor analysis; Nesselroade & Ford, 1985); however, these lines of research have historically occupied a relatively small portion of methodological research in psychology. Nonetheless, the desire to model processes at the level of the individual, as opposed to the level of a group or sample, is increasingly evident in applications ranging from ecological momentary assessment data (e.g., Beltz et al., 2016; Wright et al., 2014) to blood oxygen level dependent (BOLD) data from functional magnetic resonance imaging (e.g., Price et al., 2016). Moreover, this individual-level focus is not only present within traditional psychometric models (e.g., structural equation models), but is also present within emerging research in network conceptualizations of psychological outcomes over time (e.g., Borsboom & Cramer, 2013). Thus, it may be said that there is increasing appreciation for *intra*individual variation, as opposed to *inter*individual variation.

Here, we are not conceptualizing individual variation as a quantifiable amount of deviation from some nomothetic process, but we are instead endorsing the notion that an individual is characterized by her own process (Cattell, 1966). That is, in this context, intraindividual variation does not simply refer to the error variation present for a given individual. Nowhere is this perspective so evident as Molenaar (2004), where

it is argued that the structure identified from a group process may be generalized to an individual only under very strict conditions. More precisely, a process is said to be "ergodic" if the structures of interindividual variation and intraindividual variation are equivalent. However, in the presence of a nonergodic process, we may not validly pool over individuals, arrive at one model characterizing the processes underlying the full sample, and then use that model to make inferences at the level of the individual. In such an instance, dedicated analysis of the individual may instead be used to reliably recover within-person processes over time.

The desire to make inferences at the level of the individual is particularly evident in person-specific connectivity modeling within fMRI research. Specifically, one goal of connectivity modeling is to reveal the directed relationships capturing temporal processes between pre-defined regions of interest (ROIs) in the brain, where these relationships are the result of underlying dependencies in the neural signal (Friston et al., 2013). Within the context of connectivity modeling, there is a critical distinction between *functional* and *effective* connectivity. Where functional connectivity implies some mutual information or statistical dependence between two systems over time, effective connectivity explicitly refers to the *causal* influence that one system exerts over another over time (Friston et al., 2013).

Importantly, the establishment of functional connectivity does not offer information regarding the source of the dependence between regions, but rather that the dependence between regions exists. At the most basic level, functional connectivity between ROIs of interest could be represented using a correlation matrix. In contrast, effective connectivity analysis seeks to make explicit claims of causality and requires more sophisticated model-

ing approaches, such as the dynamic causal model (Friston et al., 2003). Finally, *directed* functional connectivity may be established when identifying statistical dependencies which possess directionality but do not directly model the neuronal activity or imply causality. This is in contrast to nondirected functional connectivity, in which bidirectional correlation may be used. For the purposes of the present project, all discussion will be limited to *directed* functional connectivity analysis. Therefore, we will seek to make inferences regarding the temporal ordering of relationships, but we do not make statements regarding causality.

Since the inception of the Human Connectome Project, an overarching goal has been to establish a "blueprint" of connectivity that exists across *all* persons (Van Essen et al., 2013). However, it has also been acknowledged that there is a sizable amount of the connectome that may be specific to the individual (Barch et al., 2013), yielding more of an individual-specific "fingerprint" of connectivity (Finn et al., 2015). Moreover, this individual variability, whether at the level of network-wide measures (e.g., centrality, degree) or at the level of individual weights characterizing connection strength within a network structure, has been found to be predictive of a host of cognitive and behavioral outcomes (van den Heuvel et al., 2009). Subsequently, researchers increasingly wish to identify functional connectivity at the level of the individual. A variety of efforts have been made toward this goal, many of which have been evaluated in recent years (Smith et al., 2011). Of these methods, many are able to detect the presence of a relationship between pairs of regions of interest (e.g., correlation); however, few are able to detect the *direction* of a relationship (Smith et al., 2011). Thus, it is well established that there is a need for methods which can identify both the presence and direction of relationships

between regions of interest.

Given the inherently exploratory nature of identifying individual-level network-like models to inform connectivity, there exists a need for principled unsupervised, or data-driven, methods to arrive at models characterizing connectivity at the individual level. However, within psychological science, much work has warned against the use of specification searches in covariance structure modeling (MacCallum, 1986), as well as the use of measures of model modification to make data-driven modifications to a model (MacCallum et al., 1992). Specifically, it is known that the dangers of these specification searches are most pronounced when the initial model is farthest from the data-generating model. Additional concerns regard the notion that these models may be infrequently cross-validated in practice, yielding models which may capitalize on the unique idiosyncrasies of a single sample.

The use of time series data affords unique opportunities to ameliorate concerns surrounding data-driven specification searches in two ways. Addressing the first concern requires understanding the characteristics of BOLD data. That is, when considering a time series of BOLD activation, it is readily apparent that there will be an effect representing the extent to which a variable will predict itself at the next time point. This effect, where a variable at $time - 1$ predicts itself at $time$, is known as an autoregressive effect. In a specification search, by beginning the search procedure with freely estimated autoregressive effects at the start of estimation, the search is able to start in a more optimal position. Specifically, the inclusion of autoregressive effects likely begins the search closer to the data-generating, or true, model. A second consideration with the use of time series data is the presence of multiple individuals, or multiple "samples." That is, the

presence of multiple individuals is analogous to the presence of multiple data sets in the context of cross-sectional data. Therefore, cross-validation can be conceptualized across each individual's data set, as opposed to across each study's data set. Consequently, cross-validation may occur to assess the presence of relationships which may consistently exist in a homogeneous sample.

Importantly, while some of the issues concerning specification searches have been addressed, indicating that models may be reliably recovered, other issues have not been addressed. All of the methods considered in the course of this study, whether existing methods or newly proposed methods, fall broadly under the category of a "specification search." The current study introduces, for the first time, a regularized unified structural equation model (uSEM), a penalized estimation procedure, for identifying individual-level models characterizing both lagged and contemporaneous (instantaneous) processes within time series data. Additionally, the performance of the regularized uSEM performance is compared to a similar method rooted in the structural equation modeling framework, the stepwise unified SEM. The stepwise uSEM has also been previously referred to as the automated unified SEM; here, the term "stepwise uSEM" will be used to maintain clarity, as many data-driven or unsupervised search procedures may be considered "automated" in nature.

Previously, the stepwise uSEM has been used with success for neuroimaging data from within the group iterative multiple model estimation (GIMME) framework (Gates & Molenaar, 2012), in which shared information across other individuals in a given sample is used to inform a subset of relationships within each individual's automated uSEM. However, because the interest here is in individual-level modeling, the individual-

level stepwise uSEM, using no shared information across the sample, will be used. The performance of the regularized uSEM will also be compared to the graphical vector autoregressive model (graphical VAR; Eichler, 2005; Wild et al., 2010) rooted in the Gaussian graphical modeling framework. Like the other methods investigated in this study, the graphical VAR model was introduced to identify models representing sparse connectivity (or relationships) among variables of interest. As these three methods use lagged information from the time series to predict current values, all methods may be considered more broadly rooted in the Granger Causality framework. It is to a discussion of these respective methods I now turn, prefaced by a introduction of the notion of Granger Causality.

Granger Causality

Given that BOLD data constitute a time series that could be characterized as both stationary (after preprocessing) and stochastic, Granger Causality analysis has been applied with some success in the past. The concept of Granger Causality supposes that a variable X is said to "Granger-cause" a variable Y if past (or contemporaneous) values of X provide information about the future prediction of Y after controlling for past values of Y (Granger, 1969). However, the use of modeling rooted in a Granger Causality framework, such as vector autoregressive modeling, has not been without contention in neuroscience (Friston et al., 2013). Of primary concern is the rate at which data are sampled. In the context of fMRI data, the sampling rate is the speed with which scans are obtained (Friston et al., 2013).

This sampling rate is specifically of concern given the rate of measurement relative to the process under observation; that is, the rate of measurement of the fMRI

signal (seconds) is longer than the speed of the neural process under observation (milliseconds). In time series modeling more broadly, it is known that when the rate of measurement is longer than the process under observation, effects may surface contemporaneously (Granger, 1969). Thus, there exists a need for methods that are able to not only establish directionality with respect to lagged relationships, but also with respect to contemporaneous relationships, given that many effects of interest may surface contemporaneously.

Furthermore, it has been argued that Granger Causality modeling can be successfully applied to neuroimaging data when proper care is taken (Gates et al., 2010; Friston et al., 2013; Seth et al., 2013, 2015). Multiple methods that have been popularized in the neuroimaging literature rest on the concept of Granger causality, including the unified structural equation model and the graphical VAR. Here, I will introduce one existing variant of the uSEM, the stepwise uSEM, as well as the graphical VAR. This discussion will be followed by the introduction of the proposed regularized uSEM, which also stems from a Granger Causality framework.

Unified Structural Equation Model

The aptly named unified SEM (Kim et al., 2007) "unifies" the estimation of both the lagged relationships and the contemporaneous relationships present among observed variables. This framework was specifically introduced to meet the challenges of analyzing multi-subject, multivariate fMRI data (Kim et al., 2007). Because the fMRI signals contained in a typical fMRI time series are temporally correlated, a conventional SEM modeling only contemporaneous relationships is not well suited for the analysis of fMRI data. This is due to violation of the assumption of independent observations. Specifically,

observations are sequentially correlated in time.

At its core, the unified SEM is a structural vector autoregressive model (SVAR; Chen et al., 2011) estimated within a structural equation modeling framework. By fitting the SVAR within an SEM framework, we are able to circumvent the usual process of identifying an SVAR. That is, a typical SVAR is obtained by using Cholesky decomposition on the covariance of the errors in a standard VAR model, thereby transforming a VAR into an SVAR (Lütkepohl, 2005). A known feature of SVARs fitted in this way is that the solutions are nonunique and instead rely upon the ordering of the series (Beltz & Molenaar, 2016; Lütkepohl, 2005). By fitting the SVAR as a uSEM, we avoid these nonunique solutions.

While structural equation modeling has been previously discussed as a potential solution for modeling directed functional connectivity, it has occasionally been dismissed within the literature for being either entirely confirmatory (Varoquaux & Craddock, 2013) or for its ability to only represent contemporaneous relationships (McIntosh & Gonzalez-Lima, 1994). Here, the incorporation of the lagged relationships in the unified SEM obviates the criticism that it may only handle contemporaneous relationships. Additionally, the potential for incorporating different model-building or estimation procedures that could be used with the unified SEM addresses the criticism that SEM may be confirmatory-only.

First, the constituent parts of the unified SEM may be defined. The multivariate autoregressive process may be defined as:

$$\boldsymbol{\eta}_t = \boldsymbol{\phi}_1 \boldsymbol{\eta}_{t-1} + ... + \boldsymbol{\phi}_q \boldsymbol{\eta}_{t-q} + \boldsymbol{\zeta}_t \tag{1}$$

where $\boldsymbol{\eta}_t$ is the $p \times 1$ vector of observed (or latent) variables at time t, $\boldsymbol{\phi}$ is a $p \times p$ parameter matrix containing the longitudinal temporal (or lagged) relationships, and $\boldsymbol{\zeta}_t$ is a $p \times 1$ vector of white noise. Within the $\boldsymbol{\phi}$ matrix, the coefficients along the diagonal represent the autoregressive process for each variable; that is, these coefficients represent the effect a variable has on itself at a future time point. Similarly, the off-diagonal coefficients represent the cross-lagged relationships between variables. These coefficients may be freed, fixed, or constrained. The contemporaneous, or instantaneous, activity among variables can then be represented by a conventional SEM,

$$\boldsymbol{\eta}_t = \mathbf{A}\boldsymbol{\eta}_t + \boldsymbol{\epsilon}_t \tag{2}$$

where $\boldsymbol{\eta}_t$ is the $p \times 1$ vector of observed (or latent) variables at time t, $\mathbf{A}$ is a $p \times p$ matrix containing the contemporaneous relationships among ROIs, and $\boldsymbol{\epsilon}_t$ is a $p \times 1$ vector assumed to be white noise. The diagonal of $\mathbf{A}$ is set to zero to reflect that a variable cannot predict itself in contemporaneous time. That is, a variable may not exert an instantaneous effect on itself. The combined expression for the unified SEM can be defined as:

$$\boldsymbol{\eta}_t = \mathbf{A}\boldsymbol{\eta}_t + \Sigma_{u=1}^{q}\boldsymbol{\phi}_u\boldsymbol{\eta}_{t-u} + \boldsymbol{\zeta}_t \tag{3}$$

where lagged relationships may be represented up to order q and all else is defined as before, with $E(\boldsymbol{\zeta}_t) = 0$ and error covariance $\boldsymbol{\theta}_{\boldsymbol{\zeta}}$. A path diagram representing the structure of the unified SEM is shown in Figure 1, where current variables are represented by η_t, lagged variables are represented by η_{t-1}, contemporaneous effects are represented by solid lines, and lagged effects are represented by dashed lines.

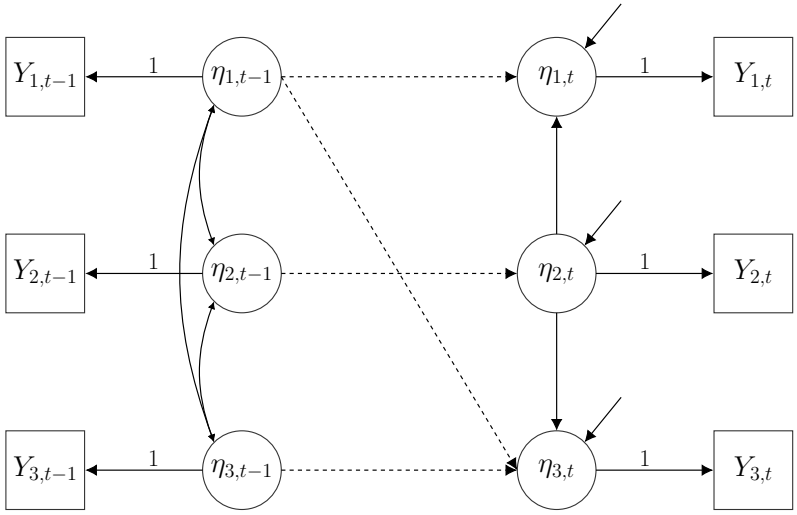

Figure 1: Three-Variable uSEM: Detailed Depiction

A more common representation of the unified SEM collapses the directed lagged and contemporaneous effects into a single path diagram, where the phantom variables (latent variables regressed into observed variables with a fixed loading of 1) are omitted from the diagram and all relationships are depicted simultaneously. This depiction, as seen in Figure 2, will be used moving forward to simplify presentation in the presence of more variables.

In the context of modeling fMRI data, the unified SEM is frequently simplified to include only lagged associations of order $q = 1$ given the speed of the BOLD signal relative to the speed of data collection. That is, the neural signal underlying the BOLD signal responds on the order of milliseconds, where a standard amount of time between scans is two seconds. Thus, in resting-state data, there may be few instances in which activity two

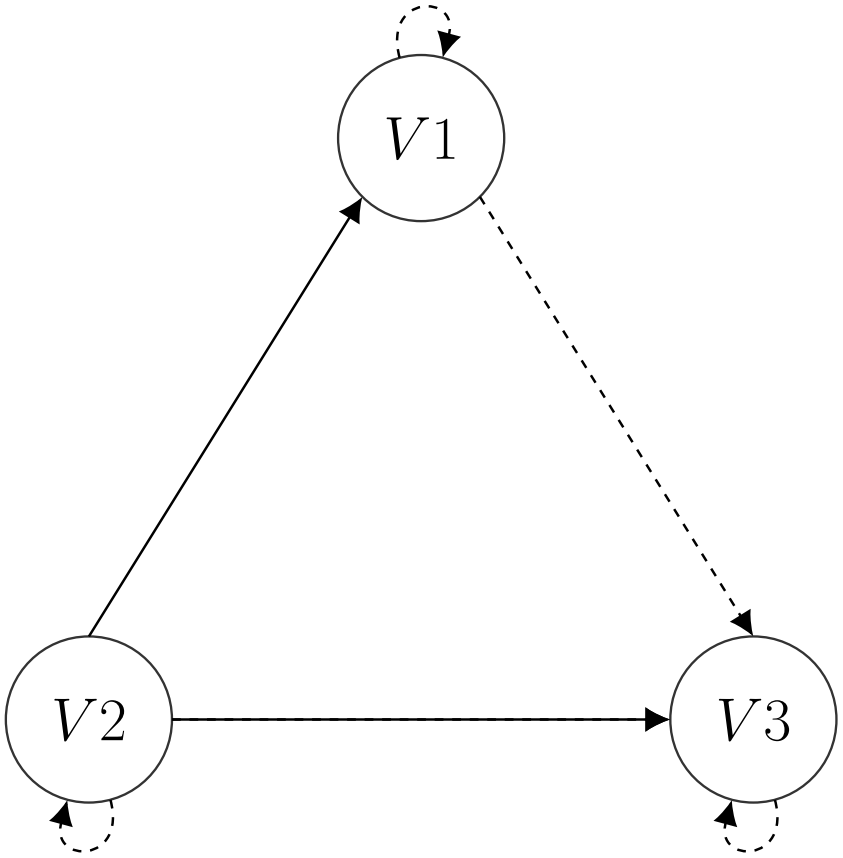

Figure 2: Three-Variable uSEM: Simplified Depiction

scans ago in time predicts the activity in the current scan.[1]

The unified SEM may be more concisely written as

$$\boldsymbol{\eta} = \mathbf{B}\boldsymbol{\eta} + \boldsymbol{\zeta} \tag{4}$$

where $\boldsymbol{\eta}$ is composed of $[\boldsymbol{\eta}_{t-1}, \boldsymbol{\eta}_t]$, such that the lagged time series and contemporaneous time series are horizontally concatenated. Similarly, $\boldsymbol{\zeta}$ is composed of $[\boldsymbol{\zeta}_{t-1}, \boldsymbol{\zeta}_t]$, where $\boldsymbol{\zeta}_{t-1}$ is a $\mathbf{0}$ vector. The $\mathbf{B}$ matrix, as depicted in Gates et al. (2016), is of dimension $2p \times 2p$,

[1] A researcher can confirm that additional lags are not necessary by performing white noise tests.

such that:

$$\mathbf{B} = \underbrace{\begin{bmatrix} 0 & \cdots & 0 & 0 & \cdots & 0 \\ \vdots & \ddots & \vdots & \vdots & \ddots & \vdots \\ 0 & \cdots & 0 & 0 & \cdots & 0 \\ \phi_{11} & \phi_{12} & \cdots & 0 & A_{12} & \cdots \\ \phi_{21} & \vdots & \phi_{1p} & A_{21} & \vdots & A_{1p} \\ \vdots & \ddots & \ddots & \vdots & \ddots & \ddots \\ \phi_{p1} & \cdots & \phi_{pp} & A_{p1} & \cdots & 0 \end{bmatrix}}_{\begin{matrix} \textit{Lagged} \end{matrix}\quad\quad\quad \underbrace{\phantom{\begin{matrix} 0 & \cdots & 0 \\ \vdots & \ddots & \vdots \\ 0 & \cdots & 0 \end{matrix}}}_{\textit{Contemporaneous}}} \tag{5}$$

Here, the upper left and upper right quadrant reflect that a lagged variable cannot be predicted by another lagged variable, nor can it be predicted by a variable measured at a future point in time. That is, no directed relationships are permitted where a variable at *time* would predict a variable at $time - 1$. The lower left quadrant represents the $\boldsymbol{\phi}$ matrix containing the lagged relationships (both autoregressive and cross-lagged), while the lower right quadrant represents the $\mathbf{A}$ matrix containing the contemporaneous relationships. Again, the diagonal of the lower right quadrant is set to zero to reflect that no variable may predict itself at the same time point.

Similarly, the $\boldsymbol{\Psi}$ matrix may be defined, such that:

$$\boldsymbol{\Psi} = \underbrace{\begin{bmatrix} \psi_{11} & & & & & \\ \psi_{21} & \ddots & & & & \\ \vdots & \ddots & \ddots & & & \\ \psi_{p1} & \cdots & \psi_{p(p-1)} & & & \\ 0 & \cdots & 0 & 0 & & \\ \vdots & \ddots & \vdots & \ddots & \ddots & \\ 0 & \cdots & 0 & 0 & \cdots & \psi_{(2p)(2p)} \end{bmatrix}}_{\textit{Lagged}} \underbrace{\qquad\qquad}_{\textit{Contemporaneous}} \tag{6}$$

where the $\boldsymbol{\Psi}$ matrix contains the variance and covariance matrix of the regression errors. Specifically, the off-diagonal elements represent covariances and the diagonal elements represent variances. Thus, the variances are estimated for all variables, lagged and contemporaneous, and covariances are estimated among the lagged variables. However, covariances are neither estimated among lagged and contemporaneous variables nor among contemporaneous variables. Put differently, as the lagged variables are considered exogenous variables, only exogenous covariances are allowed.

Finally, the covariance matrix $\boldsymbol{\Sigma}$ may be represented using conventional SEM notation, such that

$$\boldsymbol{\Sigma} = \boldsymbol{\Lambda}(\mathbf{I} - \mathbf{B})^{-1}\boldsymbol{\Psi}(\mathbf{I} - \mathbf{B}')^{-1}\boldsymbol{\Lambda}' + \boldsymbol{\Theta} \tag{7}$$

If the time series were composed of latent variables, $\boldsymbol{\Lambda}$ would represent the relation of the observed variables to the latent variables. In the context of neuroimaging data, a latent

variable could represent a broader network of regions within the brain (e.g., default mode network), and each observed variable could represent a region of interest that belongs to that network. In other contexts within psychological research, a latent variable may represent a construct such as depression, and each observed variable may be an item evaluating some aspect of depressive symptomatology. In this project, however, only single observed variables will be considered; no multiple-indicator latent factors will be considered (see Chapter 4, Future Directions, however, for further discussion). Therefore, when the time series is composed of observed variables, $\mathbf{\Lambda}$ is reduced to an identity matrix of dimension $2p \times 2p$. Similarly, $\mathbf{\Theta}$ drops out of the equation, as we are not modeling measurement error; therefore, $\mathbf{\Theta} = 0$.

Stepwise Unified Structural Equation Model

Model Building Procedure

Though multiple methods of automated model building are possible, one classic approach makes use of a forward-selection model building procedure driven by modification indices, also known as LaGrange multipliers (Sörbom, 1989). Within structural equation modeling, a modification index indicates the extent to which the model fit would improve if a given parameter (currently fixed to zero) were freely estimated (Jöreskog & Sörbom, 1986). One automated procedure for identifying individual-level models using modification indices is a forward-selection procedure which begins with a null model, where all lagged and all contemporaneous relationships are set to zero. In order to aid the search, the autoregressive relationships representing a variable's influence on itself from the previous time point may be freed, as prior work has shown that beginning the model search with these relationships freely estimated aids with the recovery of directionality, even when

these effects are small in magnitude (Lane et al., under revision). Regardless of the null model used at the start of estimation, the forward-selection procedure proceeds to iteratively add directed paths, both lagged and contemporaneous, which improve the likelihood ratio test. The model selection terminates when no modification index possesses a p-value lower than a pre-specified threshold for α. This automated procedure, adding relationships one at a time in a forward-selection process, was popularized in LISREL, though its use has been met with great criticism (MacCallum, 1986).

A variation of this procedure is used in Gates et al. (2010), where fit indices are used as the stopping criteria (instead of p-values alone) and a pruning stage is added. Specifically, the search proceeds as previously specified, adding directed relationships which most improve the likelihood ratio test. However, instead of stopping when no modification index possesses a p-value lower than a prespecified α, it instead terminates when the model is "excellent" as indexed by two of four standard fit indices used in structural equation modeling: the NNFI (also known as the TLI) (Bentler & Bonnett, 1980), CFI (Bentler, 1990), RMSEA (Steiger, 1990), and SRMR (Jöreskog & Sörbom, 1981). Specifically, estimation is terminated when the CFI and TLI are greater than .95 and the RMSEA and SRMR are less than .05. These fit indices will be used at stopping criteria in Chapters 2 and 3; therefore, full details regarding the specification of each index of fit is displayed below.

The RMSEA is estimated by $\hat{\epsilon_a}$, which is the square root of the discrepancy per degree of freedom:

$$\hat{\epsilon_a} = \sqrt{max\left\{ \left(\frac{F(S, \Sigma(\hat{\theta})}{df} - \frac{1}{N-1} \right), 0 \right\}} \tag{8}$$

where the minimum of the fit function is represented by $F(S, \Sigma(\hat{\theta}))$, df is the number of degrees of freedom represented by $m(m+1)/2 - t$ (where $m = 2p$ and p is the number of variables for the unified SEM), and N is the sample size. The SRMR may be expressed as:

$$SRMR = \sqrt{\frac{\sum_{i=1}^{p} \sum_{j=1}^{i} [(s_{ij} - \hat{\sigma}_{ij})/s_{ii}s_{jj}]^2}{m(m+1)/2}} \tag{9}$$

where s_{ij} is an element of the sample covariance matrix, $\hat{\sigma}_{ij}$ is an element of the model-implied covariance matrix, m is twice the number of observed variables (current and lagged), and all elements are standardized by dividing the residuals by the standard deviations of the observed variables (e.g., s_{ii}).

The CFI may be defined as:

$$CFI = 1 - \frac{max[(\chi_t^2 - df_t), 0]}{max[(\chi_t^2 - df_t), (\chi_i^2 - df_i), 0]} \tag{10}$$

where χ_t^2 is the chi-square corresponding to the baseline model, or independence model, and χ_t^2 is the chi-square corresponding to the fitted model. Finally, the TLI may be defined as:

$$TLI = \frac{(\chi_i^2/df_i) - (\chi_t^2/df_t)}{(\chi_i^2/df_i) - 1} \tag{11}$$

Once a model is achieved that satisfies two of these four fit indices, a pruning stage is added to the classic LISREL search procedure, where any directed relationships no longer significant at $p = .05$ are removed from the model. After this pruning stage, if the model fit is no longer excellent, then the search proceeds one final time until a model again satisfies two of four of these criteria.

As previously mentioned, chief among the criticism of such a method is that it is frequently difficult to cross-validate a model which was arrived at via specification search. The first concern regarding cross-validation may be ameliorated when considering that each individual may be considered his or her own sample, and researchers may assess the degree of concordance among individual-level models if seeking evidence for some group-level pattern of effects. Indeed, MacCallum et al. (1992) recommend the use of parallel samples when using specification searches, and time series data collected from multiple individuals allow for exactly this possibility.

Furthermore, as previously discussed, prior work has shown that specification searches are most dangerous when the initial model is far from the true, data-generating model. Similarly, in the context of neuroimaging data, autoregressive effects are consistently present and large in magnitude due to the lagged nature of the hemodynamic response following neural activation. Thus, by beginning the model search with the autoregressive effects freely estimated, we start the model closer to the true model. For all models tested in the present study, the autoregressive effects will be freely estimated. The aforementioned automated procedure using modification indices is implemented in the group iterative multiple model estimation algorithm, GIMME (Gates & Molenaar, 2012), and its use for neuroimaging data has been met with success.

However, as the model-building procedure makes use of forward or stepwise selection, there is concern for how well the procedure may perform if incorrect paths are selected near the beginning of model selection (Beltz & Molenaar, 2016). An approach such as GIMME largely makes use of a group-level structure in order to guide individual-level model selection, as the group-level model assists in picking out signal from noise

in selecting individual-level paths. However, imposing a group-level structure could foreseeably arrive at paths that are not significant for a sizable minority of the sample. Indeed, as the use of GIMME is predicated on the assumption of an underlying group-level model, it will ultimately make use of a truly individual-level stepwise uSEM when no group-level structure exists. Additionally, if a better individual-level search can be implemented, the need for a group-level structure to guide individual-level search may be obviated. Therefore, all models within this project will only consider and use data from a single individual, $N = 1$.

Graphical Vector Autoregressive Model

A related model, the graphical vector autoregressive model, has also been previously introduced for the analysis of single-subject, multivariate time series data (Eichler, 2005; Wild et al., 2010). The graphical VAR, also known as a sparse time series chain graphical model (Abegaz & Wit, 2013), has seen applications ranging from reconstructing genetic networks (Abegaz & Wit, 2013) to estimating temporal relations within experience sampling data (Wild et al., 2010). Much like the unified SEM, the graphical VAR relies on the concept of Granger causality and utilizes information regarding temporal dependence within time series data. Further, the graphical VAR utilizes graphical modeling to represent directed relationships among variables. That is, it is rooted in the framework of Gaussian Graphical Modeling, which has been recently presented as an alternative to structural equation modeling for representing covariance structures (Epskamp et al., 2016). Specifically, the graphical VAR makes use of a Gaussian Graphical Model to describe contemporaneous relationships leftover after modeling temporal (lagged) relationships using a network of directed regression coefficients.

First, the graphical VAR searches across all possible constrained VAR models and selects the model that optimizes some target criterion (e.g., AIC: Wild et al., 2010, EBIC or BIC: Chen & Chen, 2008; Epskamp, 2016). In the graphical portion of the model, the contemporaneous relationships are denoted via *undirected* connections among the errors. That is, no statement of directionality is made with respect to instantaneous relationships. In contrast, the lagged, or temporal, relationships are denoted via directed connections. Though the graphical VAR can be expanded to include lagged relationships beyond an order of 1, I restrict our discussion here to a lag of order 1 for consistency and scope.

The graphical VAR using a lag of order 1 can be represented as:

$$\mathbf{y}_t = \boldsymbol{\Omega}\mathbf{y}_{t-1} + \boldsymbol{\epsilon}_t \tag{12}$$

where $\mathbf{y}_t$ is a vector of values across multiple variables at time t, $\boldsymbol{\Omega}$ contains the lagged, or "between-time" effects, and $\boldsymbol{\epsilon}_t$ is an error vector. Within contemporaneous time, $(\boldsymbol{\epsilon}_t \sim \mathbf{0}, \boldsymbol{\kappa})$, where $\boldsymbol{\kappa}$ represents the nondirected contemporaneous, or lag-0, relationships. The graphical VAR lends itself well to interpretation, as both the $\boldsymbol{\Omega}$ and $\boldsymbol{\kappa}$ matrices may be standardized post-estimation to represent partial directed correlation (PDC) and partial contemporaneous (nondirected) correlations (PCC), respectively. That is, the elements of the $\boldsymbol{\kappa}$ matrix may be rescaled as:

$$PCC(y_{i,t}, y_{j,t}) = -\frac{K_{ij}}{\sqrt{K_{ii}K_{jj}}} \tag{13}$$

where the PCC represents the correlation between a given pair of variables at the same point in time, partialling out the linear effects of all other variables, both contemporaneous

and lagged. Similarly, the elements of the $\mathbf{\Omega}$ matrix containing the lagged relationships may be standardized by

$$PDC(y_{i,t}, y_{j,t-1}) = \frac{\omega_{ij}}{\sqrt{\Sigma_{ii} K_{jj} + \omega_{ij}^2}} \tag{14}$$

where Σ_{ii} represents a diagonal element of the variance-covariance matrix of the residuals, after inverting the concentration matrix $\boldsymbol{\kappa}$, and all other terms are defined as before. The PDC represents the linear relationship between a dependent variable y at time t and a predictor variable y at time $t-1$, net the linear effect of all other variables at time $t-1$ (Wild et al., 2010). Figure 3 depicts an example network structure from the `graphicalVAR` package (Epskamp, 2016), where the contemporaneous and lagged structures are depicted separately. Note that the lagged relationships are depicted by one-headed arrows, where the contemporaneous relationships are depicted by nondirected edges. In this simple diagram representing typical output from `graphical VAR` package, positive weights are depicted using green edges and negative weights are depicted using red edges.

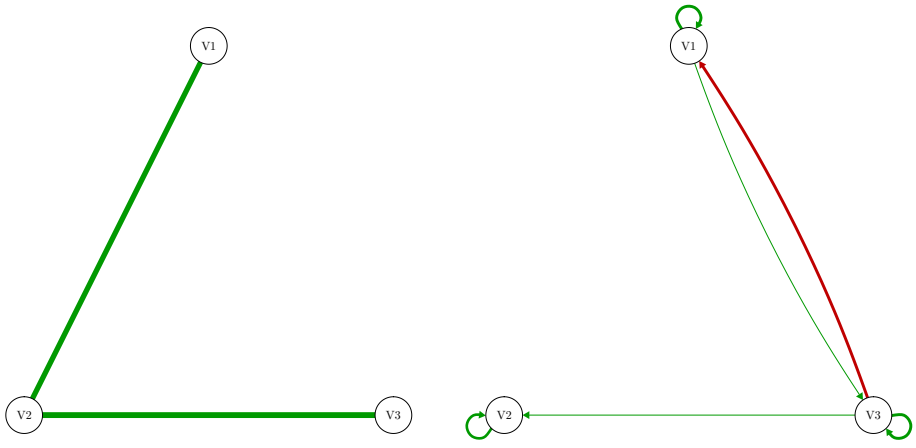

Figure 3: Graphical VAR: Partial Contemporaneous and Partial Directed Correlations

Much like the stepwise uSEM, the graphical VAR lends itself to multiple options for proceeding with model building, and several options have been proposed. For example, a simple constrained search using forward selection in combination with some information criteria, such as the AIC or BIC, was proposed in an earlier variation of the graphical VAR (Eichler, 2005). As with the unified SEM, it is possible to fit an entirely confirmatory model derived from some *a priori* hypothesis. However, in the context of establishing functional connectivity, researchers frequently do not have a concrete, *a priori* structure in mind. Therefore, an exploratory variation of the graphical VAR will be investigated here.

Specifically, a variant of the graphical VAR will be investigated, where the least absolute shrinkage and selection operator (LASSO; Tibshirani, 1996) is used in combination with the Bayesian Information Criteria (BIC; Schwarz et al., 1978), for model selection. A general expression for the LASSO in the context of regression can be written as:

$$\hat{\beta}_{lasso} = \text{argmin}\Big\{ \sum_{i=1}^{N} \Big(y_i - \beta_0 - \sum_{j=1}^{p} x_{ij}\beta_j \Big)^2 + \lambda \sum_{j=1}^{p} |\beta_j| \Big\} \tag{15}$$

provided an outcome vector, $\mathbf{y}$, and a matrix of predictors, $\mathbf{X}_{n\times p}$, where β_0 is the intercept term and β_j is the coefficient for the prediction of y using x_j, and λ is the tuning parameter controlling the degree of regularization. In the case of the graphical VAR, the vector $\mathbf{y}$ would represent the observed variables at time, $\mathbf{y}_t$, and $\mathbf{X}$ would represent the vector of $\mathbf{y}$ variables at $t-1$. Because the LASSO forces some parameter estimates to zero as the level of penalization increases, it serves as not only a method to induce sparsity, but also as a method to perform variable selection.

In this specification of the graphical VAR, the LASSO penalty is incorporated into estimation to act as a variable selection procedure, such that small coefficients are shrunk to zero. The LASSO stands in contrast to an alternative approach, such as ridge regression, in which coefficients are shrunk toward zero but do not reach zero (Hoerl & Kennard, 1970). Though the ridge penalty has been shown to outperform the LASSO in minimizing prediction error (mean square error; MSE), it yields a less interpretable solution. Therefore, the ridge penalty will not be investigated in the present study.

The implementation of both penalties fall into the category of a *regularization* procedure, which aims to increase the sparsity, and therefore, the parsimony and generalizability of a solution (Jacobucci et al., 2016). With the LASSO, the degree of regularization is set by a tuning parameter, λ. Higher values of λ will result in more parsimonious model; at the extreme, the highest value of λ will result in a model in which all connections are zero. When λ is zero, no regularization takes place. Ideally, an optimal value of λ will be selected in order to maximize true connections and minimize spurious connections (Epskamp & Fried, 2016).

In the graphical VAR, the procedure is as follows: a range of networks are first estimated using various levels of the LASSO tuning parameters, resulting in a variety of potential models. If we assume that $\boldsymbol{\epsilon} \sim N(\mathbf{0}, \boldsymbol{\kappa})$, then we may express the conditional density of the tth observation as:

$$f_c(\mathbf{y}_t|\mathbf{y}_{t-1}; \boldsymbol{\Omega}, \boldsymbol{\Theta}) = (2\pi)^{p/2}\det(\boldsymbol{\Theta})^{1/2}e^{-\frac{1}{2}(\mathbf{y}_t-\boldsymbol{\Omega}\mathbf{y}_{t-1})'\boldsymbol{\Theta}(\mathbf{y}_t-\boldsymbol{\Omega}\mathbf{y}_{t-1})} \tag{16}$$

where $\mathbf{y}_t$ is a vector representing the levels of p variables measured at time t, $\boldsymbol{\Theta}$ represents

the inverse of $\boldsymbol{\kappa}$, the variance-covariance matrix of the residuals, and all other terms are defined as before (Abegaz & Wit, 2013). Thus, the objective function for minimization may be expressed as:

$$\ell_{pen}(\boldsymbol{\Omega}, \boldsymbol{\Theta}) = \log\det - tr(\mathbf{S}_{\boldsymbol{\Omega}}\boldsymbol{\Theta}) - \Sigma_{i\neq j}^{p} P_{\lambda}(|\theta_{ij}|) - \Sigma_{i,j}^{p} P_{\rho}(|\omega_{ij}|) \tag{17}$$

where

$$\mathbf{S}_{\boldsymbol{\Omega}} = (1/T)\Sigma_{t=1}^{T}(\mathbf{y}_t - \boldsymbol{\Omega}\mathbf{y}_{t-1})(\mathbf{y}_t - \boldsymbol{\Omega}\mathbf{y}_{t-1})', \tag{18}$$

$P_{\lambda}(\cdot)$ and $P_{\rho}(\cdot)$ are penalty functions for $\boldsymbol{\Theta}$ and $\boldsymbol{\Omega}$ respectively, and θ_{ij} and ω_{ij} are elements of these matrices (Abegaz & Wit, 2013). Though several penalty functions are possible, the L_1 penalty representing the LASSO is used here. The convex L_1 penalty may be represented as

$$P_{\lambda}(\theta) = \lambda|\theta|, \tag{19}$$

which may be substituted into the prior expression to yield the optimization problem which allows for sparse estimates of both $\boldsymbol{\Omega}$ and $\boldsymbol{\Theta}$:

$$\max(\boldsymbol{\Theta}, \boldsymbol{\Omega})\big\{\log\det(\boldsymbol{\Theta}) - \mathrm{tr}(\mathbf{S}_{\boldsymbol{\Omega}}\boldsymbol{\Theta}) - \lambda\Sigma_{i\neq j}^{p}|\theta_{ij}| - \rho\Sigma_{i,j}^{p}\omega_{ij}\big\} \tag{20}$$

where λ and ρ control the level of sparsity for the lagged matrix, $\boldsymbol{\Omega}$, and the inverted contemporaneous matrix, $\boldsymbol{\Theta}$. For this optimization problem, an efficient coordinate descent algorithm is used, full details of which can be found in Rothman et al. (2010).

In order to select the optimal model from this range of models, the BIC (Schwarz

et al., 1978) or extended BIC (Chen & Chen, 2008) is used. In prior simulation work, the EBIC has been shown to successfully select the correct model (Epskamp et al., 2016). The original BIC (Schwarz et al., 1978) would select the model that minimizes the following expression:

$$BIC = -2 \log L_n \hat{\theta}(s) + \nu(s) \log n, \tag{21}$$

where $\hat{\theta}(s)$ is the maximum likelihood estimator of $\theta(s)$, $\nu(s)$ is the number of components in model s, and n is the number of observations. The extended BIC extends this equation to include:

$$BIC_\gamma = -2 \log L_n \hat{\theta}(s) + \nu(s) \log n + 2\gamma \log \tau(S_j), \tag{22}$$

where γ is a hyperparameter controlling the sparsity of the solution, τ is the size of the model space S_j, and S_j is the collection of all models with j variables (Chen & Chen, 2008). When γ is set to zero, the extended BIC corresponds to the original BIC. For purposes of consistency across methods, the γ parameter will be set to zero, yielding the original BIC.

Thus, in each iteration, instead of optimizing the likelihood function, the penalized likelihood is instead optimized, where the tuning parameters λ and ρ control the level of penalization (Epskamp et al., 2016). The optimal model following this procedure is identified by selecting the model with the lowest BIC value.

The graphical VAR approach is characterized by several advantages. First, it is well-suited for the analysis of time series data with a large number of variables where a relatively sparse solution is desired. Additionally, the presence of multiple tuning pa-

rameters allows for a more continuous selection of models, where there may be multiple possible optimal models, depending on the desired level of sparsity. Moreover, the use of the LASSO for variable selection avoids the use of a forward-selection or stepwise procedure, which may miss the optimal model by adding only one relationship in each iteration. Finally, a VAR(1) model allows all directed lagged and all nondirected contemporaneous relationships among variables to be present prior to the regularization procedure offered by the LASSO. Note that for the purposes of this dissertation, λ and ρ will be set to equality in the graphical VAR, yielding equally penalized lagged and contemporaneous relationships.

Importantly, there are several desirable characteristics that are not offered by the graphical VAR. First, the parameterization is such that the contemporaneous relationships are expressed via off-diagonal elements in the variance-covariance matrix of the residuals. Thus, there are no directed contemporaneous relationships; instead, sparse nondirected contemporaneous relationships are modeled to simply account for any leftover relationships after modeling directed lagged processes. However, in the pursuit of *directed* functional connectivity, it is precisely these missing directed contemporaneous elements that are frequently of interest, as many effects surface contemporaneously. Thus, it may be desirable to combine the most useful elements of the data-driven unified SEM and the graphical VAR into a hybrid model: the regularized unified structural equation model.

Regularized Unified Structural Equation Modeling

Though the topic of regularization has been long-discussed in other modeling contexts, such as graphical modeling (Friedman et al., 2008) and regression (Tibshirani,

1996), it has received less attention within structural equation modeling, and psychometrics more broadly. However, with the increasing presence of "big data" within psychological research, more research into methods for automatic variable selection and models with many variables relative to the number of individuals is warranted. To this end, there exists increased discussion regarding what regularization has to offer various models popular in psychological research, ranging from regression (McNeish, 2015) to traditional factor analysis or structural equation modeling (Jacobucci et al., 2016).

In the context of multiple regression, regularization may be used to perform variable selection when the number of predictors exceeds the number of individuals, or when a small set of predictors (out of many possible) is desired. In the context of confirmatory factor analysis, where an underlying, or latent, variable is related to a given number of observed variables via a factor loading, regularization may be used to either force loadings to zero (e.g., LASSO penalty) or force loadings close to zero (e.g., ridge penalty). Using regularization in this example may be a more principled way to induce sparsity than an alternative approach, such as forcing a simple structure to exist, which could have the unintentional consequence of inflating covariances among latent factors (Hsu et al., 2014). Both examples highlight ways in which regularization may be introduced to psychological audiences using familiar models.

With respect to structural equation modeling, regularization may be applied to the latent variable portion of a structural equation model as well as the measurement model portion. Given that this project pertains to the structural relationships present in a time series composed of observed variables, I will focus my discussion on this case. Unlike a VAR(1) model, the unified SEM does not allow for all possible paths to be present at the

beginning of model estimation. In the unified SEM, if the specified model contained all autoregressive relationships, all possible cross-lagged relationships, and all possible contemporaneous relationships, it would suffer from underidentification.

This fact largely informs why previous strategies for data-driven identification of relationships within structural equation modeling (e.g., Gates et al., 2010) have utilized forward-selection procedures, where relationships are added sequentially until a final model is established, or stepwise procedures, where relationships are added sequentially and subsequently pruned until a final model is established. In contrast, backward-elimination procedures, where all possible relationships exist at the start of model estimation and are sequentially eliminated, have received less discussion. Given that the proposed regularized uSEM is able to begin estimation with an underidentified model and gradually arrive at a sparse model via the introduction of parameter penalties, it offers a unique solution to arriving at a sparse individual-level model.

First, the regularization procedure begins by presenting the unified SEM using matrices expressed in reticular action model, or RAM, notation (McArdle, 2005). The use of RAM notation is beneficial here for two reasons. First, it offers a direct correspondence between the matrix and graphical specifications of the unified SEM, yielding easily interpretable matrices. Second, the direct, or structural, relations are captured in a single matrix which may be used for regularization. Note that this is in contrast to the traditional LISREL notation, which would separate the directed effects into two matrices: the exogenous and the endogenous effects.

Briefly, RAM notation decomposes any structural equation model into three matrices: the filter (F) matrix, the asymmetric (A) matrix, and the symmetric (S) matrix.

The filter matrix contains a 1 for each manifest variable and zeros elsewhere; thus, for our observed-variable unified SEM, the filter matrix would be equivalent to an identity matrix. The asymmetric matrix contains any regressions among variables; for the unified SEM, this matrix would take the form of the $\mathbf{B}$ matrix presented in Equation (5) containing regressions of variables at *time* on variables at $time - 1$ and regressions of variables at *time* on other variables at *time*. Finally, the symmetric matrix contains all variances and covariances; this matrix aligns with the $\mathbf{\Psi}$ previously presented in Equation (6), where lagged variables are allowed to freely covary. Using these matrices, the expected covariance matrix can then be computed as:

$$\mathbf{\Sigma} = \mathbf{F}(\mathbf{I} - \mathbf{A})^{-1}\mathbf{S}(\mathbf{I} - \mathbf{A})^{-1\prime}\mathbf{F}'. \tag{23}$$

In turn, this expected covariance matrix may then be placed into the maximum likelihood loss function, such that

$$F_{ML} = \log(\det(\mathbf{\Sigma})) + \text{tr}(\mathbf{S} * \mathbf{\Sigma}^{-1}) - \log(\det(\mathbf{S})) - p \tag{24}$$

where S is the sample covariance matrix and p is the number of variables. In order to incorporate regularization into this loss function, we modify it accordingly:

$$F_{reg} = F_{ML} + \lambda P(\cdot), \tag{25}$$

where $P(\cdot)$ is a general function for penalizing the parameters. In this instance, the LASSO ($||\cdot||$), which penalizes the sum of the absolute values of the parameters, and adaptive LASSO, which introduces a parameter-specific penalty in the sum of the absolute values of the parameters, are used given the interest in variable selec-

tion.

Borrowing the structure from Equation 15, we may express the *adaptive* LASSO penalty in a simple regression context as:

$$\hat{\beta}_{adaptivelasso} = \text{argmin}\Big\{ \sum_{i=1}^{N} \Big(y_i - \beta_0 - \sum_{j=1}^{p} x_{ij}\beta_j \Big)^2 + \lambda \sum_{j=1}^{p} \hat{w}_j |\beta_j| \Big\} \tag{26}$$

where $\hat{w}_j$ is a weight equal to $1/|\hat{\beta}_j|$. With the introduction of the weight vector $\hat{\mathbf{w}}$ in the adaptive LASSO, each estimate possesses a data-dependent weight (Zou, 2006). It is known that compared to the standard LASSO, the adaptive LASSO is able to reduce bias (Zou, 2006) through these parameter-specific weights. Specifically, the standard LASSO is known to introduce bias in larger coefficients, as all estimates are penalized uniformly. Thus, large coefficients are less biased in the final model. By optimizing the fit function containing parameter-specific penalties on the **B** matrix containing all directed relationships, we now have the regularized unified SEM.

Given the goal of a sparse, data-driven model, the regularized uSEM offers several benefits. First, we are able to begin estimation with a model containing all possible bidirectional structural relations. Additionally, we are able to utilize the benefits of the SEM framework to utilize traditional measures of fit. Specifically, we are able to select from a continuous range of models with increasing sparsity, examining popular measures of fit within structural equation modeling (e.g., RMSEA, BIC) in order to make our final selection. For the purposes of the current study, the BIC will be used, which will be expanded upon in Chapter 2. This approach, selecting the best model from a range of models, is in contrast to other forward-selection or stepwise model building procedures, which make use of *a priori* fixed cutoff values and halt the search when those fixed

cutoff values are reached. That is, in other competing forward- or stepwise- selection procedures, the fit of a model is compared to a fixed cutoff and not to other candidate models.

Furthermore, in the regularized uSEM, there exist the ability to handle missing data (e.g., using full information maximum likelihood), provided that data can be assumed to be missing at random. This feature stands in contrast to the graphical VAR, which requires multiple imputation in the presence of missing data. Finally, regularization has never been applied to a structural vector autoregressive model or a unified structural equation model, representing a unique contribution to the literature and a novel strategy for identifying data-driven models of directed temporal and contemporaneous network structure.

Current Study

Given the increasing interest in individual-level connectivity and in time series analysis more broadly, researchers must decide among a myriad of candidate approaches, not all of which are well-suited for identifying directed functional connectivity. The current project evaluates the ability of two existing approaches, the stepwise unified structural equation model and the graphical vector autoregressive model, as well as a new method, the regularized unified structural equation model, to recover both lagged and contemporaneous relationships that comprise directed functional connectivity. To accomplish these goals, I conduct two simulation studies.

In Chapter 2, I discuss the finite sampling behavior of each model using time series data composed of lagged and contemporaneous effects. The studies comprising this chapter, Study 1A and Study 1B, will evaluate the performance of each approach across

conditions encountered in practice. In Study 1B, the effect of mismodeling the direction of the contemporaneous structure will be evaluated. In Chapter 3, Study 2 contains selection of simulations conducted on data from Smith et al. (2011), which are considered benchmark data for evaluating any method for identifying networks representing directed functional connectivity.

CHAPTER 2: STUDY 1

Prior to discussing the relevance of these methods for functional connectivity analysis, the finite sampling behavior of each method across conditions encountered in practice must be considered. Table 1 presents the list of methods that will be considered, as well as relevant penalties and stopping criteria. Though the performance of the stepwise uSEM has been evaluated prior to this work in terms of the overall recovery of data-generating network connections (Gates et al., 2010), other outcome measures pertaining to the accuracy and precision of individual estimates have not been considered. Furthermore, given that the performance of the regularized uSEM has never before been investigated, there is a pressing need to understand its finite sampling behavior in a controlled simulation study. Finally, given the natural similarity of the graphical VAR and the regularized uSEM, it is important to understand their relative performance.

As discussed in detail below, in Study 1A, I evaluate these methods across three factors: varying number of time points, varying number of variables, and varying sparsity (or density) of the network. This study is designed to evaluate the methods across conditions encountered in time series data more broadly defined in psychological science. In Study 1A, each method will be used on data generated by the appropriate structure; that is, the regularized uSEM and stepwise uSEM will be fit to data generated by a uSEM with directed lagged and contemporaneous relationships. The graphical VAR will be fit to data generated by a sparse VAR model, with directed lagged and nondirected

contemporaneous relationships. Therefore, I am able to evaluate the performance of the models under a variety of conditions encountered in practice, when *the data-generating model and the fitted model align*.

In Study 1B, the performance of the methods are evaluated when the directionality of the contemporaneous structure is misspecified. That is, the uSEM-based methods are fit to data generated by a graphical VAR, and the graphical VAR is fit to data generated by a uSEM. Therefore, I can evaluate the performance of the regularized uSEM and stepwise uSEM when applied to data with *nondirected* contemporaneous relationships. In Study 1B, the number of time points and the sparsity of the network will again be varied, but the number of variables will be held constant at $V = 5$.

By performing these separate studies, we may evaluate the relative performance of the three methods, both when the data-generating and fitted models align (Study 1A), and when they do not (Study 1B). Further details regarding the levels of each simulation factor, as well as each outcome variable, are provided below.

Method	Stopping/Evaluation Criteria
Regularized uSEM - ALASSO	BIC
Regularized uSEM - LASSO	BIC
Stepwise uSEM	NNFI, CFI, SRMR, RMSEA
Stepwise uSEM - add BIC	NNFI, CFI, SRMR, RMSEA + BIC
Graphical VAR	BIC

Table 1: Methods Considered

Model Specifications

Stepwise uSEM. In this comparison, the stepwise model building procedure for the uSEM employs a stepwise model search using modification indices (Jöreskog & Sörbom, 1986). Here, the search will terminate when the model is "excellent" as indexed

by two of four standard fit indices used in structural equation modeling: the NNFI (Bentler & Bonnett, 1980), CFI (Bentler, 1990), RMSEA (Steiger, 1990), and SRMR (Jöreskog & Sörbom, 1981). A variation of the stepwise uSEM will also be tested, where the BIC ($\chi^2 - df * \log(N)$) is added for consideration. In this variation, the stopping rule is changed from two-of-four to three-of-five.

Regularized uSEM. Similarly, the regularized uSEM will be estimated using penalties controlled by a pre-specified range of λ values, corresponding to various degrees of regularization. As presented in Table 1, the regularized uSEM will be investigated with both the standard LASSO penalty as well as the adaptive LASSO penalty. Of the regularized unified structural equation models tested across the range of λ values, the model with the lowest BIC is chosen, consistent with current practice (Jacobucci et al., 2016).

Graphical VAR. Finally, the graphical VAR will similarly estimate models across a range of λ values, where the model with the lowest BIC is chosen. Though some variations of the graphical VAR allow the lagged and contemporaneous matrices to be penalized using different λ values, these values will be held to equality for the purpose of the current study to maintain comparability to competing methods. To ease comparison, no bidirectional contemporaneous relationships will be generated in the uSEM. These analytic approaches will again be employed in Study 1B as well as Study 2 (Chapter 3).

Here, in Study 1A and Study 1B, the number of time points will be varied, as well as the overall sparsity of the network. Only Study 1A will vary the number of variables; the number of variables will be held constant in Study 1B. The choice of these design

factors suits two purposes. First, these simulation factors represent characteristics of data that may be of general interest in examining a method for time series data collected within psychological science more broadly (e.g., ecological momentary assessment data). Second, these design factors directly relate to functional connectivity analysis in fMRI studies. Thus, in Study 2, I will be able to introduce conditions that are more specific to fMRI and less general, maintaining scope within each respective study.

Each cell in the fully-crossed simulation design will be examined across $R = 500$ replications. Finally, in order to evaluate each replication, multiple outcome measures will be considered, including both sensitivity (the ability to detect true relationships) and specificity (the ability to remove false relationships) of both nondirected and directed relationships. Additional outcome measures are considered, including the relative bias of true positive paths, the absolute bias of false positive paths, the root mean square error, and computation time. More details are provided below for each simulation factor and for each outcome measure.

Design Factors for Simulation

Number of time points. The number of time points in each replication is varied across four levels: $T = 50, 100, 200, 500$, representing a range of potential time lengths encountered in practice. At the lower bound, the stepwise unified SEM (when using shared information from the sample) has demonstrated promise in previous simulation work with as few as 60 time points (Lane et al., under revision). In an fMRI study, the number of time points is directly related to the "session length" or "session duration," which is generally reported in minutes. The number of time points is then equal to to the session duration divided by the temporal resolution, or sampling time. Thus, an fMRI

resting state or task-related session may have as many as 500 time points over the course of several minutes.

Similarly, in a daily diary study, the number of time points may relate to the number of days an individual is monitored over the course of a study (e.g., Wright et al., 2014), and may be closer to the lower bound of the chosen range here. For example, in Wright et al. (2014), individuals were kept in the study for further analysis using uSEM provided they provided at least 30 time points worth of observations, though the majority of participants provided between 30 and 100 time points worth of observations. These numbers, drawn from Wright et al. (2014), are typical within a daily diary study. Therefore, the chosen range of time series lengths in the present study is well representative of multiple conditions encountered in practice.

Number of variables. Given the iterative nature of the respective methods in this study, computational feasibility, as well as computational time, will be in part dictated by the number of variables measured at each repeated measurement. Here, the levels chosen roughly correspond to common numbers of variables that we may see in time series data more broadly defined, whether fMRI data or ecological momentary assessment data. Given the focus of this dissertation on implications for directed functional connectivity analysis, the number of variables is also informed in part by the number of ROIs that may be present within a given brain network. The number of regions of interest, in turn depends on the atlas used to select regions of interest, which are available at varying degrees of granularity. That is, different researchers and different software programs parcellate the brain differently, resulting in potentially different numbers of variables for the same network.

For example, the atlas described by Yeo et al. (2011) is implemented in the popular neuroimaging software FreeSurfer, and it defines 68 nodes representing regions of interest (ROIs) across the whole brain grouped into seven networks. In contrast, Shirer et al. (2012) utilizes 90 ROIs grouped into 14 networks, and Power et al. (2011) utilize 264 nodes, grouped into at least 11 networks. Across these various parcellations, the number of ROIs considered to be members of one network may vary from four (e.g., cerebellar network) to greater than 30 (e.g., default mode network) (Power et al., 2011). Thus, the number of variables will be varied across three levels: five, ten, and fifteen variables. For purposes of computational burden, more than fifteen variables will not be considered in this study.

Level of sparseness. Given the interest in recovering a relatively sparse network of relationships, the level of sparsity will also be varied across three levels: 15%, 20%, and 25% of possible connections. Given that each of the five methods uses stopping criteria differently, it is important to consider the recovery of the data-generating sparsity for each method, particularly as it relates to the other design factors (e.g., number of variables and number of time points). Additionally, given that it is known that regularization methods perform more optimally with the true network structure is sparse (Epskamp et al., 2015), it will be important to consider variation in performance due to sparsity. These levels of sparsity are informed by in-house empirical applications of the stepwise unified SEM, where individual-level models contained between 11% to 29% of possible relationships. The chosen levels are rounded to roughly reflect the average number of relationships, as well as one standard deviation above and below the mean.

For consistency across methods, possible connections here will be defined by the

$(p \times p) - p$ number of elements in the matrix representing the lagged relationships and the $\frac{p \times (p-1)}{2}$ number of elements in the matrix representing the contemporaneous relationships. Put differently, each directed relationship in the lagged matrix will count as a candidate path, excluding the diagonal containing autoregressive effects; in contrast, only half of the non-zero elements of the contemporaneous matrix will count as a candidate path. Again, this allows for the graphical VAR to be evaluated against these methods on a common basis, as we may assess its ability to detect the presence of a relationship regardless of its directionality. Given that the autoregressive relationships will be freed at the start of estimation in each model, these paths will not be considered in the number of candidate paths.

Factors held constant. Though many design factors are held constant in any Monte Carlo simulation study, by definition, I will delineate several factors here that will remain constant, though a future study may be interested in varying. First, for this study, the number of individuals considered will be held constant at $N = 1$; that is, no group-level structure will be generated. Consequently, no group-level inferences will be made. Though prior work has shown that improvements are possible when using shared information, (e.g., Gates & Molenaar, 2012; Varoquaux & Craddock, 2013), these methods implicitly assume some sample-level homogeneity in network structure, and I wish to avoid this assumption in the current study.

Additionally, the strength of the structural relationships among variables will be held constant over time; that is, the magnitude of the connection strength will not change across the duration of the time series. Given that neither the proposed method, the regularized uSEM, nor the competing methods, the stepwise uSEM or the graphical

VAR, are able to accommodate time-varying effects, I do not expect that these methods would perform differently from each other when faced with such unmodeled time variation.

Further, while missing data is frequently of interest as a condition in Monte Carlo simulations pertaining to structural equation modeling, it will not be investigated here. In the unified SEM, missing data may be handled by full information maximum likelihood under the assumption of missingness at random (Enders & Bandalos, 2001). However, the graphical VAR currently does not have a built-in mechanism for handling missing data, as multiple imputation must be used in an external step, prior to estimating the graphical VAR. Thus, neither the amount of missing data nor the mechanism of missing data will be varied in this study. Finally, the normality of the observations will not be varied, as all variables will be generated to be multivariate normal.

Data Generation

All data will be generated in R (R Core Team, 2016). As noted above, data will be generated according to both the unified SEM and the graphical VAR. The unified SEM will be generated in accordance with the procedure described by Gates et al. (2010). Similarly, the graphical VAR will be generated consistent with the procedure described in Yin & Li (2011) and implemented in the `graphicalVAR` (Epskamp, 2016) package in R. In generating the time series, $T + 50$ observations will be generated so that the first 50 observations may be discarded to remove fluctuations due to initialization. Additionally, prior to the generation of each time series, the matrix containing the lagged and contemporaneous effects will be checked for stationarity by ensuring that the maximum eigenvalue does not exceed a value of one.

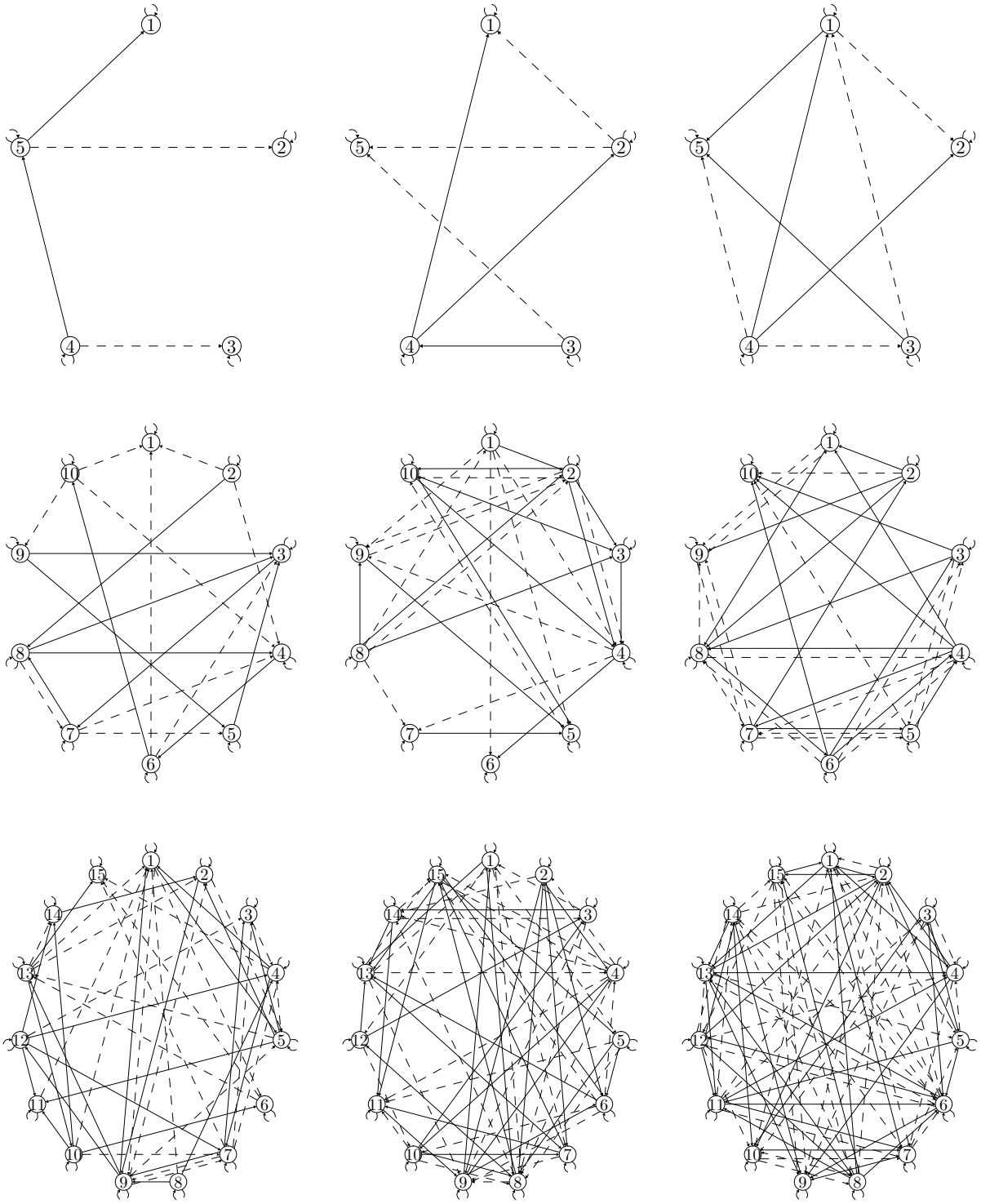

Figure 4: Study 1A: Data-generating models. Paths are drawn at random in accordance with specified simulation conditions.

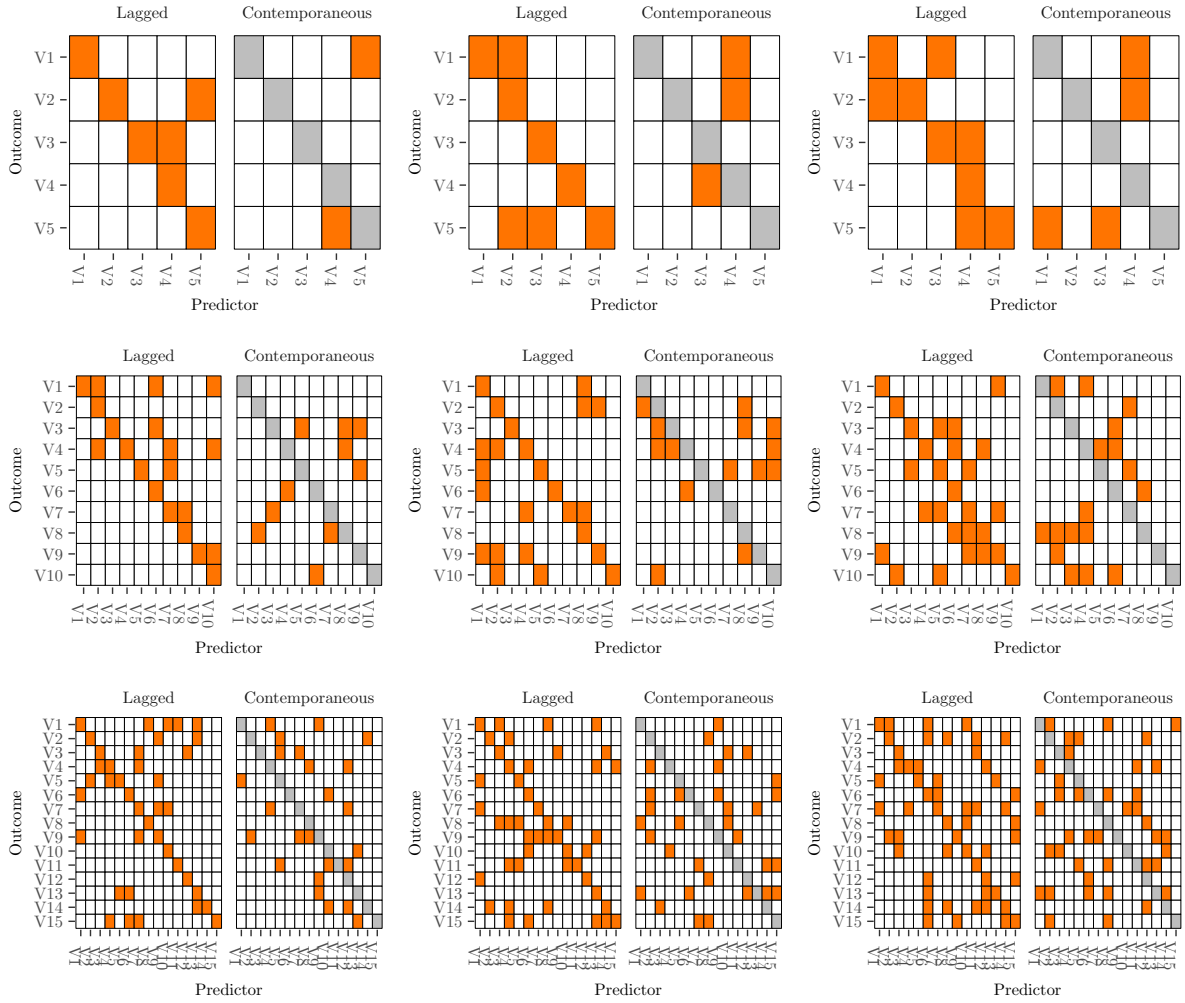

Figure 5: Study 1A: Data-generating models, Alternate Representation. Paths are drawn at random in accordance with specified simulation conditions.

Figure 4 depicts a potential data-generating connectivity structure for the nine possible combinations of the number of variables and the levels of sparsity. This structure is depicted both in the form of a simplified path diagram (Figure 4), as well as a matrix (Figure 5). In each matrix, an orange shaded cell represents a connection between the column (predictor) and row (outcome) variable, and a grey shaded cell represents a connection fixed at zero. Each replication will contain data generated from a structure that matches the specified conditions, where connections are randomly placed in the lagged

and contemporaneous matrix corresponding to the level of sparsity. In the contemporaneous matrix, no bidirectional relationships will be generated. It should be noted that the randomly generated individual-level matrices are an important feature of the simulation design, as it ensures that the generated matrices do not fit only one pattern of network connectivity (e.g., small network, random network).

Model Estimation

All models will also be estimated in R. The stepwise unified SEM will be estimated using the `indSEM` function within the `gimme` package (Lane et al., 2016), which iteratively adds relationships in a stepwise-selection procedure according to the highest modification index, terminating when a model fit is deemed "excellent," as indexed by the four previously referenced indices of fit. In another variation that will be tested, this routine will be modified to include the BIC, and estimation will halt when three of the five indices indicate "excellent" fit. The `indSEM` is specifically designed to conduct the search procedure for $N = 1$.

The graphical VAR will be estimated using the `graphicalVAR` package within R (Epskamp, 2016). In this procedure, a range of λ values will be provided, and the BIC will be used to select the optimal tuning parameter in order to arrive at a final model composed of the partial directed (lagged) correlations and the partial contemporaneous (bidirectional) correlations. To maintain consistency with the regularized uSEM, the penalty for the lagged and contemporaneous relationships will be constrained to equality.

Finally, the regularized uSEM will be estimated in a combination of two R packages: `lavaan` (Rosseel, 2012) and `regsem` (Jacobucci, 2016). First, `lavaan` will be used

to specify the unified structural equation models and provide relevant information for the next step, such as initial starting values, degrees of freedom, and model matrices expressed in RAM notation. The `regsem` package will then be used to regularize, or induce sparsity, in the structural equation models across a range of λ values controlling the LASSO and adaptive LASSO penalties.

Study Hypotheses

Multiple hypotheses guiding Study 1 are presented below:

1. *With less sparse network structures, the regularized uSEM will outperform the stepwise uSEM given the use of relative, not absolute, stopping criteria. That is, the stepwise uSEM may reach an "excellent" model before identifying all connections in a denser network.*

2. *The smallest number of converged solutions will be present in conditions when the number of time points is small relative to the number of variables.*

3. *When nondirected contemporaneous connections are present (Study 1B), the recovery of true lagged directed relationships may be poorer in the stepwise uSEM and regularized uSEM.*

4. *Less biased parameter estimates are expected for the adaptive LASSO compared to the standard LASSO given the use of parameter-specific weights in the adaptive LASSO.*

5. *Regularization-based methods (graphical VAR, regularized uSEM) are expected to perform better overall when the true network structure is more sparse.*

Outcome Measures for Study 1

Sensitivity and Specificity. In order to evaluate the recovery of data-generating connections, whether directed or nondirected in nature, both sensitivity and specificity will be evaluated. Sensitivity and specificity are both popular outcome measures for evaluating multiple aspects of recovery of connections when simulating network data (e.g., Abegaz & Wit, 2013; Epskamp et al., 2016), and are closely related to measures of "recall" and "precision" used in other literature describing the performance of various search algorithms (e.g., Ramsey et al., 2011). Sensitivity measures the ability of an algorithm to recover true paths, while specificity measures the ability of an algorithm to remove false paths. Here, we may define sensitivity as

$$\text{sensitivity} = \frac{\text{true positives}}{\text{true positives} + \text{false negatives}} \tag{27}$$

and specificity may be defined as

$$\text{specificity} = \frac{\text{true negatives}}{\text{true negatives} + \text{false positives}} \tag{28}$$

These measures allow for a global evaluation of a model's ability to recover true directed or nondirected edges and reject false directed or nondirected edges. Importantly, we may evaluate sensitivity and specificity for lagged and contemporaneous relationships separately. Additionally, as mentioned, we may evaluate these measures for directed paths and nondirected paths separately. For both of these measures, values closer to 1 are ideal, with .8 representing acceptable performance.

Relative Bias. Though researchers who make use of methods such as those proposed here are frequently interested in the identification of connectivity (e.g., the *presence*

of a connection), they are also frequently interested in the weights, or parameter estimates, associated with each relationship. Indeed, previous work has recommended that the coefficients from each individual-level final model be taken into a second-stage analysis, whether to identify potential covariates in the context of a general linear model (GLM; Kim et al., 2007), or to describe the network using measures from a graph theoretic framework. Thus, relative bias will be computed for each structural relationship. Relative bias may be computed as the difference of the true value, θ and the estimate, $\hat{\theta}$, weighted by the true estimate:

$$\text{Rel. Bias} = \frac{\hat{\theta} - \theta}{\theta} \times 100 \tag{29}$$

Bias will be important to consider for both the graphical VAR and the unified SEM, whether stepwise or regularized. First, as the graphical VAR makes use of the LASSO, it is known that regularization techniques trade some bias for increased stability and generalizability. Thus, there is reason to anticipate bias for the graphical VAR. Additionally, the unified SEM makes use of quasi-maximum likelihood estimation (or pseudomaximum likelihood). This is because a block-Toeplitz data structure is used for estimation, where additional variables are created to represent the variables at $t - 1$. In this context, we cannot assume row-wise independence of observations. Though it is known that estimates from a block-Toeplitz data structure are not true ML estimates, they have been shown to have the same asymptotic properties as ML estimates for pure AR processes (Hamaker et al., 2002). Finally, as the regularized uSEM makes use of both quasi-maximum likelihood estimation and the LASSO, bias will be an relevant outcome to consider. Within the variations tested of the regularized uSEM (standard LASSO and adaptive LASSO), it will

be important to consider differences in bias.

Absolute Bias: False Positives. Where the relative bias of true positive paths will be considered, the absolute bias of false positive paths should also be considered. That is, the absolute bias of paths which emerged in the fitted model but whose true value is $\theta = 0$. Absolute bias may simply be defined as the unsigned difference between the true and recovered path weight:

$$\text{Abs. Bias} = |\theta - \hat{\theta}| \tag{30}$$

Absolute bias is computed here in place of relative bias given that relative bias would not be defined in the presence of a true θ of 0. This measure, while not of focal interest to this study, will be useful for determining the magnitude of edges which should have been removed from the final model, but were falsely retained.

Root mean square error. Finally, root mean square error will also be computed in order to evaluate error in prediction. RMSE may be computed as:

$$\text{RMSE} = \sqrt{\frac{\Sigma(\hat{\theta} - \theta)^2}{N}} \tag{31}$$

where θ again represents the true estimate, $\hat{\theta}$ represents the recovered estimate, and N is the number of true estimates for an individual.

Computational time. Given the iterative nature of the proposed methods, the computational time will be a nontrivial factor in estimating these models. Thus, the computational time and its relationship to simulation factors such as number of variables, number of measurements, and the sparsity of the network underlying the time series will be considered. It is expected that the computational time will increase with the number of

variables.

Proper solutions. In the unified SEM, the final models will be checked for proper solutions. That is, any warnings that may indicate a solution may not be reliable (e.g., did not converge, nonpositive definite matrix) will be monitored. In the regularized unified SEM, any models within the range of models tested that possesses negative degrees of freedom or fails to converge within a given number of random starts will not be considered.

Results will be graphically examined, including the probing of any meaningfully large main effects or interaction effects.

Results

As a reminder, two sub-studies were conducted, here termed Study 1A and Study 1B. Study 1A is designed to test the performance of models under optimal conditions; for example, I evaluate the performance of the stepwise unified SEM when fit to data generated by the unified SEM. In Study 1B, the data generating model and the fitted model do not correspond. For example, the stepwise unified SEM is fit to data generated by the graphical vector autoregressive model. The importance of these sub-studies is this: we are able to assess the importance of directionality. That is, if data are generated by a unified SEM, then all connections are directed. We are able to assess the ability of the unified SEM methods (stepwise uSEM and regularized uSEM) to recover directed connections. Additionally, we are able to assess what happens when these directed models are fit to data with non-directed connections (e.g., a unified SEM fit to data generated by a graphical VAR).

In the sections that follow, the performance of each method, along with any

potential variations of each method, will be considered. Of most importance will be measures that address features of network recovery: sensitivity and specificity. For Study 1A, relative bias, absolute bias, and RMSE will also be presented. If relevant, sensitivity and specificity will be broken down across multiple levels: time-specific recovery (contemporaneous versus lagged) and direction-specific recovery (nondirected versus directed). A table of relevant outcomes for each method in Study 1A is displayed below in Table 2.

Outcome Measure	Regularized uSEM	Stepwise uSEM	Graphical VAR
Path Sensitivity	Yes	Yes	Yes
Path Specificity	Yes	Yes	Yes
Direction Sensitivity	Yes	Yes	No
Direction Specificity	Yes	Yes	No
Path Sensitivity, Lagged	Yes	Yes	Yes
Path Specificity, Lagged	Yes	Yes	Yes
Direction Sensitivity, Lagged	Yes	Yes	Yes
Direction Specificity, Lagged	Yes	Yes	Yes
Path Sensitivity, Contemp.	Yes	Yes	Yes
Path Specificity, Contemp.	Yes	Yes	Yes
Direction Sensitivity, Contemp.	Yes	Yes	No
Direction Specificity, Contemp.	Yes	Yes	No
Relative Bias	Yes	Yes	Yes
Absolute Bias	Yes	Yes	Yes
RMSE	Yes	Yes	Yes

Table 2: Study 1A: Outcome Measures by Method

Study 1A

Convergence and computational time

The number of normally terminated models varied by method. For the stepwise uSEM, 100% of cases across all conditions yielded normal solutions. The performance of the stepwise uSEM with the BIC added as a stopping criteria varied a bit more, where 21 of 36 cells yielded 100% normally terminating models. Across the remaining

cells, the lowest convergence rate was 88%. For those that did not complete estimation, the procedure was unable to arrive at a model which satisfied three-of-five fit indices. The adaptive LASSO yielded slightly more computational concern, where the cell-wise convergence rate ranged from 78% to 100%. The performance of the standard LASSO was comparable. Finally, the graphical VAR yielded 100% normally terminating models across all cells. For all subsequent analyses, complete replications will be used. Any values presented as marginal means will be adjusted for the unequal number of normally terminating replications across conditions.

Computational time differed greatly across the three general methods (regularized uSEM, stepwise uSEM, and graphical VAR), with interactive effects among the simulation factors. Overall, the stepwise uSEM and graphical VAR were much less computationally burdensome than the regularized uSEM. In contrast, the regularized uSEM, whether using the standard LASSO or adaptive LASSO, was much more computationally intensive, likely due to the size of the $\mathbf{B}$ matrix on which regularization took place.

In the most computationally burdensome situation, with a large number of variables, a less sparse network, and a short time series ($V = 15, S = 25\%, T = 50$), the regularized uSEM with standard LASSO took more than 4000 minutes to complete estimation for a single individual. The regularized uSEM with adaptive LASSO fared better, but still exceeded 3000 minutes for the same cell. With more time points, however, the regularized uSEM was much more reasonable, with the smallest differences between methods observed with a small number of variables, a sparse network, and a longer time series ($V = 5, S = 15\%, T = 500$). Figure 6 displays the computation time for each method broken down by number of variables, number of time points, and the sparsity of

the network.

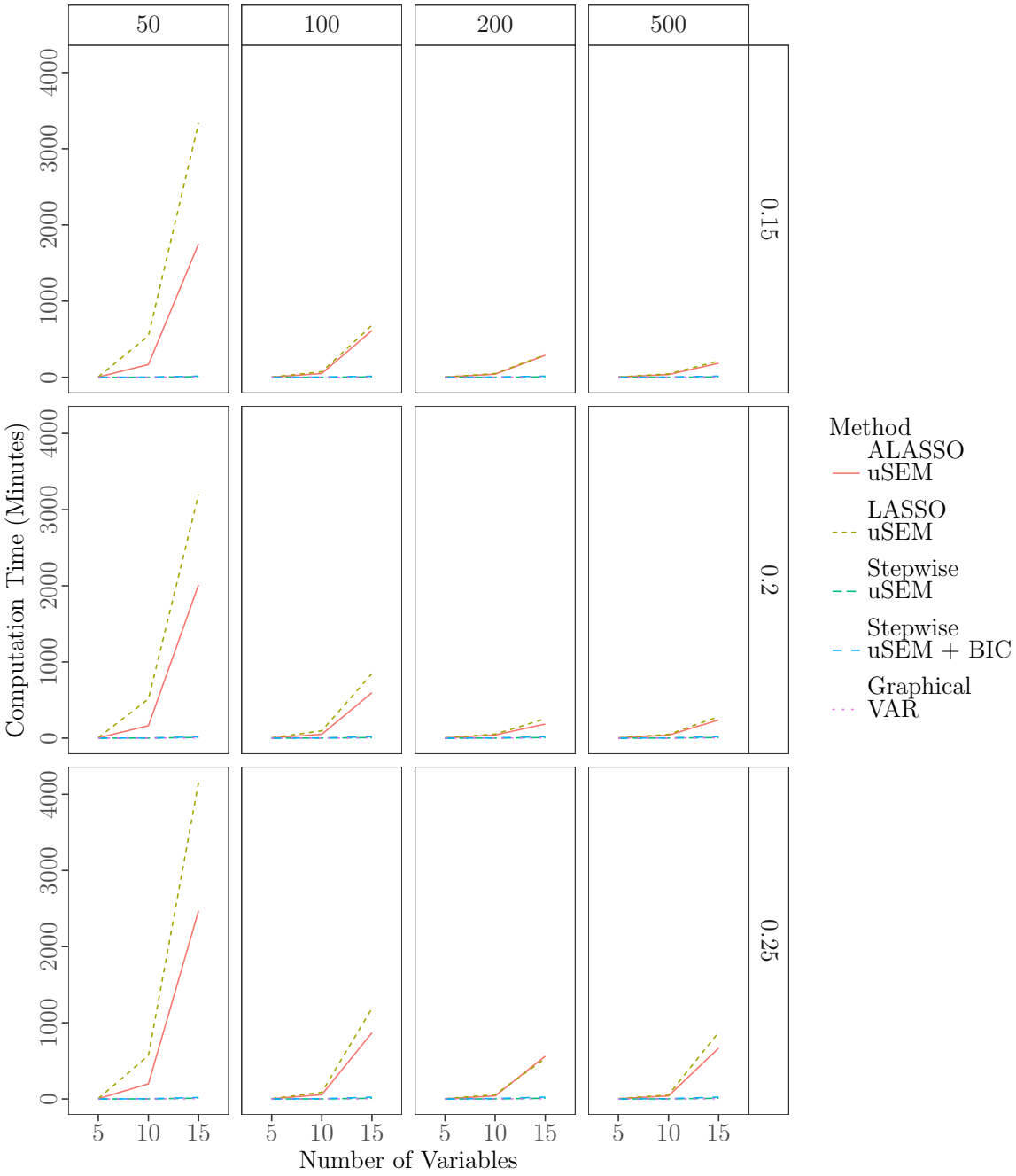

Figure 6: Study 1A: Computational Time by Number of Variables, Number of Time Points, and Sparsity of Network

Graphical VAR

Across all conditions, the performance of the graphical VAR varied widely. In many

instances, the graphical VAR adequately recovered directed lagged relationships as well as the sparse structure of nondirected contemporaneous relationships. However, of all methods, the graphical VAR was characterized by the largest RMSE values, indicating the greatest amount of prediction error. Additionally, an increased number of time points and number of variables led to dramatic decreases in the specificity of recovered relationships, indicating a tendency to retain too many false edges. Further details are provided below, broken down by relevant outcome.

Path Sensitivity

Across an increasing number of time points, the overall path sensitivity increased; for both the $T = 200$ and $T = 500$ conditions, the overall path sensitivity exceeded .98. Of the simulation factors, the number of time points most strongly related to the path sensitivity, ranging from .72 at $T = 50$ to .998 at $T = 500$. Increasing the proportion of possible connections (sparsity) was associated with quite modest increases in overall path sensitivity. Interestingly, these increases were not uniform for contemporaneous and lagged effects.

Contemporaneous versus Lagged. That is, the sensitivity of contemporaneous paths remained relatively constant across increasing network density (.83 at $S = 15\%$; .83 at $S = 25\%$), where the sensitivity of lagged paths increased mostly across increasing network density (.84 at $S = 15\%$; .91 at $S = 25\%$). The sensitivity of contemporaneous paths also remained relatively constant across an increasing number of variables; (.84 at $V = 5$; .81 at $V = 15$), where the sensitivity of lagged paths increased modestly across an increasing number of variables (.83 at $V = 5$; .93 at $V = 15$). Of the thirty-six simulation conditions, 27 conditions yielded contemporaneous path sensitivity of .8 or greater. The nine cells

yielding contemporaneous path sensitivity lower than .8 corresponded to the $T = 50$ conditions.

Path Specificity

Viewing the previous path sensitivity results, the graphical VAR demonstrated more than adequate performance in recovering true edges, regardless of directionality. However, with any data-driven search procedure, it is important to consider the balance of sensitivity and specificity. To this end, the path *specificity* was frequently below a desirable threshold (typically .8) across all varied time series lengths, and it did not vary meaningfully across increasing time series length (range $= .63 - .66$). The high sensitivity but low specificity is evidence of the method retaining too many edges in the final model. Increasing the number of variables was associated with increased path sensitivity, but decreased path specificity substantially. For illustration, Figure 7 depicts the negative correlation between path sensitivity and path specificity, broken down by the number of variables, holding the length of time series constant at $T = 200$ and the sparsity of the network constant at $S = 25\%$.

Increasing the proportion of connections was associated with dramatic *decreases* in path specificity; thus, with denser data-generating networks, the graphical VAR retained too many false edges (see Figure 8). This finding is consistent with prior work, which has found the LASSO to perform less well for variable selection if the true network structure is more dense (Epskamp et al., 2015). Marginalizing over other factors, the path specificity at $V = 5$ is .82, where the path specificity at $V = 15$ is .43. This decrease in path specificity with an increasing number of variables was present for both directed lagged relationships and nondirected contemporaneous relationships.

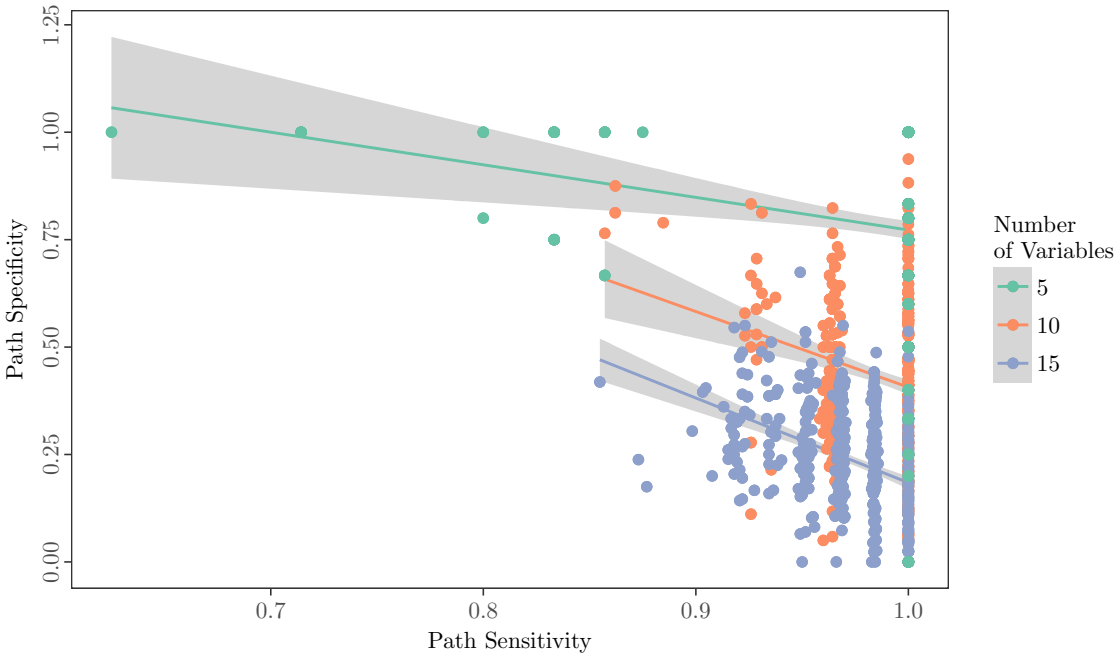

Figure 7: Graphical VAR: Path Sensitivity and Path Specificity by Number of Variables

Contemporaneous versus Lagged. For example, the contemporaneous path specificity at $V = 5$ is .94, and the contemporaneous path specificity at $V = 15$ is .76. The lagged path specificity suffers as well, where it drops from .88 at $V = 5$ to .58 at $V = 15$. Therefore, increasing the number of variables results in increased false positives in the graphical VAR.

Direction Sensitivity

Because the graphical VAR does not allow for the estimation of directed contemporaneous relationships, we may not separately evaluate the recovery of directed lagged and directed contemporaneous relationships. We may, however, consider the recovery of directed lagged relationships.

Lagged Only. In the best performing simulation condition, the graphical VAR yielded a directed lagged sensitivity of 1.0 ($V = 15, S = .25, T = 500$). Across increasing levels of network density, the sensitivity to lagged *directions* increased from

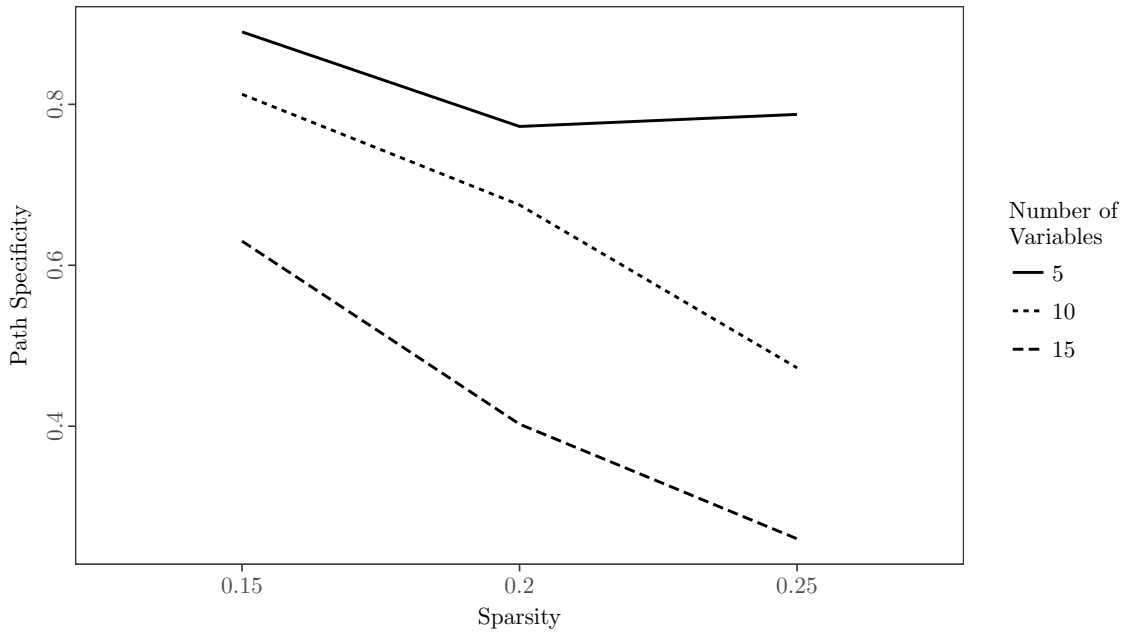

Figure 8: Graphical VAR: Path Specificity by Number of Variables and Sparsity

.83 at $S = 15\%$ to .89 at $S = 25\%$. However, this was accompanied by decreases in specificity.

Direction Specificity

Lagged Only. Increases in network density, a longer time series, and an increased number of variables all resulted in decreased performance with respect to lagged direction specificity. That is, each of these factors contributed to the graphical VAR retaining too many false edges. For example, the lagged direction specificity decreased from .93 at $S = 15\%$ to .78 at $S = 25\%$. There was a less clear effect of the number of time points on lagged direction specificity, as it dropped very slightly from .87 at $T = 50$ to .85 at $T = 500$. The most important effect pertaining to lagged direction specificity was the interaction between the number of variables and the sparsity of the network, where denser networks with a larger number of variables yielded the poorest specificity, much like the aforementioned finding for path specificity.

Bias and RMSE

Of these false positive paths, the average absolute bias was relatively small and decreased across an increasing number of time points, ranging from .08 to .03 from $T = 50$ to $T = 500$, respectively. There was more substantial relative bias of the true positive paths, where the true positive paths were heavily downwardly biased. Additionally, the RMSE was consistently high across conditions, ranging from 0.22 to 0.39 across all conditions.

Summary

Looking across all possible conditions, the best performance was observed for the cell with five variables, sparsity = 15%, and $T = 500$, where the path specificity was 1.00 and the path sensitivity was .93. Similarly, the poorest path sensitivity was observed with $V = 5$, $S = 15\%$, and $T = 50$; the poorest path specificity was observed with $V = 15$, $S = 25\%$, and $T = 500$.

Stepwise unified SEM

The performance of the stepwise unified SEM ranged varied across conditions. Overall, the best outcomes were observed with a small number of variables and a large number of time points. Compared to the performance of the graphical VAR, a more optimal balance of sensitivity and specificity was achieved, indicating improved ability to recover true edges and reject false edges. Additionally, less variability in parameter estimates was observed, as evidenced by lower RMSE values. The discussion here will focus on the standard stepwise uSEM, where estimation halts when two of four fit indices are "excellent." Any deviations observed from these results for the alternative approach, where the BIC is included, will be noted at the end of the section. Full details are

provided below.

Path Sensitivity

Collapsing over other simulation factors, there was a significant effect of number of time points on the sensitivity to data-generating relationships, without respect to direction, where the lowest condition (T = 50) experienced an average path sensitivity of .63, while the highest condition (T = 500) experienced an average path sensitivity of .86. The effect of number of time points on both path sensitivity and direction sensitivity, marginalizing over other simulation factors, is presented in Figure 10. A visual inspection of the means reveals that performance was uniformly better for a smaller number of variables ($V = 5$) compared to a larger number of variables ($V = 15$). Additionally, this difference was more pronounced when the density of the networks was greater. That is, collapsing over levels of time series length, the path sensitivity was at its lowest for the 15 variable condition with 25% of possible connections (.71). Figure 9 displays this interaction effect.

Lagged versus Contemporaneous. Breaking down path sensitivity by lagged and contemporaneous relationships, the sensitivity to lagged relationships was uniformly higher for contemporaneous relationships than lagged relationships. Factors contributing to increased lagged path sensitivity were a longer time series, a more sparse network, and a smaller number of variables. No differential effects were observed for the sensitivity of contemporaneous relationships – the same factors led to improved contemporaneous path sensitivity.

Path Specificity

There was no obvious main effect of sparsity on the ability to successfully recover

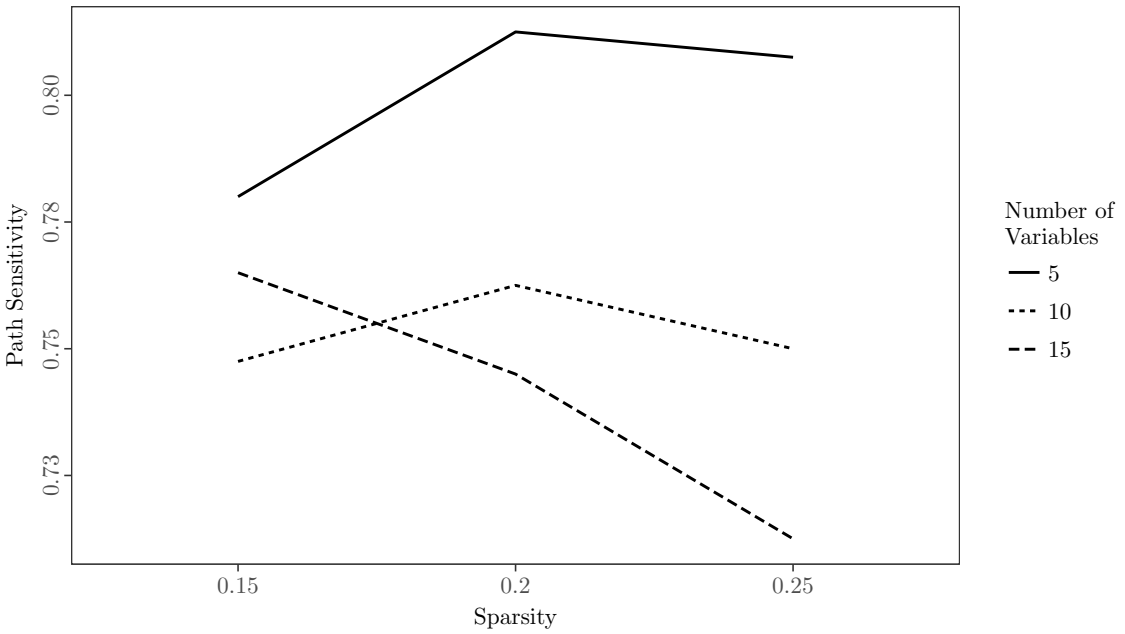

Figure 9: Stepwise uSEM: Path Sensitivity by Number of Variables and Sparsity

true paths or directions (e.g., path or direction sensitivity). There was, however, an effect of network sparsity on the overall path *specificity* (whether relationships were contemporaneous or lagged), where more sparse networks yielded greater specificity. Put differently, in more sparse networks, fewer false positives were observed. The effect of number of time points was also present for the specificity of data-generating relationships, where the specificity of the $T = 50$ condition was .77 compared to the $T = 500$ condition's sensitivity of .99. This high specificity indicates that, marginalizing over other simulation factors, very few false positives were found in the $T = 500$ condition.

Lagged versus Contemporaneous. The specificity of lagged relationships was uniformly high, where performance improved with an increased number of time points: .86 at $T = 50$ to .99 at $T = 500$. The specificity of contemporaneous relationships was similarly high, where performance varied most in accordance with time series length: .89 at $T = 50$ to .99 at $T = 500$. Increasing the network density and the number of variables

yielded detectable, but minor decreases in path specificity (e.g., .96 at $S = 15\%$ and .93 at $S = 25\%$).

Direction Sensitivity

Similar effects were seen for the direction sensitivity of the data-generating relationships as were seen for the path sensitivity. That is, the direction sensitivity ranged from .47 to .75 between the T = 50 and T = 500 conditions, respectively. As with overall path sensitivity, increasing the network density and the number of variables yielded modest decreases in direction sensitivity.

Lagged versus Contemporaneous. An interesting difference existed in the sensitivity to lagged directed relationships versus contemporaneous directed relationships. That is, lagged directions were recovered more frequently than contemporaneous directions. For example, the lagged direction sensitivity at $T = 200$ was .70, compared to the contemporaneous direction sensitivity at $T = 200$ of .57. In the best performing cell ($V = 5, S = 15\%, T = 500$), the contemporaneous direction sensitivity reached .75.

Direction Specificity

The direction specificity, while globally high, ranged in accordance with time series length, such that the direction specificity increased from .85 to .95 between the $T = 50$ and $T = 500$ conditions, respectively.

Lagged versus Contemporaneous. No differential effects were observed for the effect of the simulation factors on the direction specificity of lagged versus contemporaneous relationships. Specificity of the lagged directions was slightly, though consistently, higher than the specificity of the contemporaneous directions (e.g., lagged direction specificity

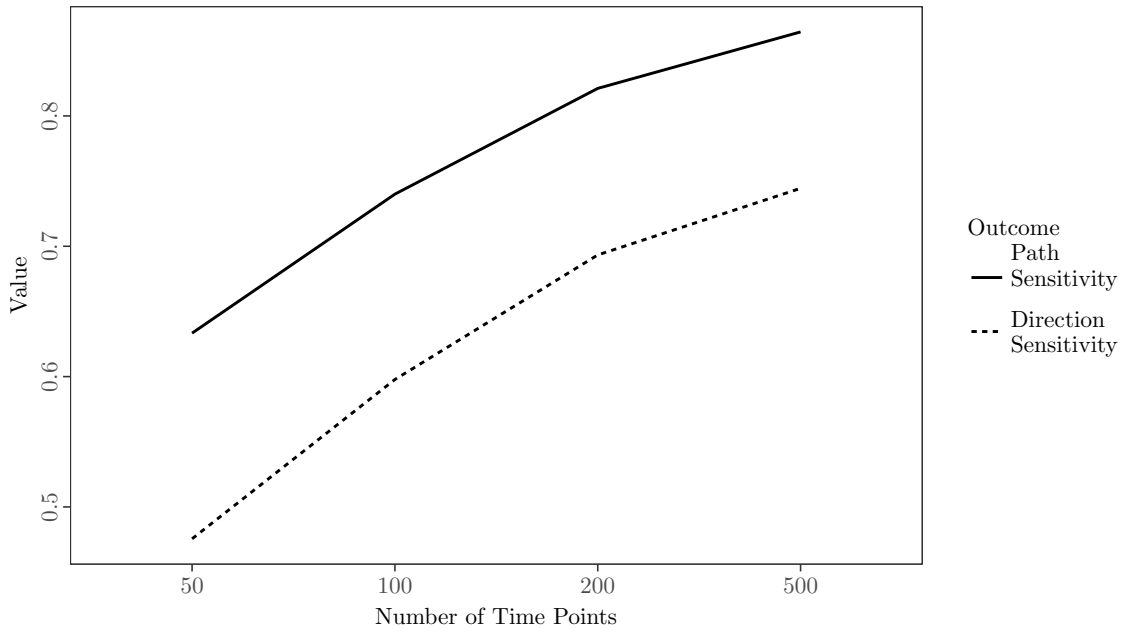

Figure 10: Stepwise uSEM: Path Sensitivity and Direction Sensitivity by Number of Time Points

of .99 at $T = 200$ compared to contemporaneous direction specificity of .95 at $T = 200$.

Bias and RMSE

As would be expected, increasing the number of time points increased the precision of the estimates, where the RMSE dropped from .21 at $T = 50$ to .08 at $T = 500$. Even with only $T = 200$, the RMSE dropped to .10, representing only slightly less precision than the condition with the largest number of time points. Additionally, increasing the number of time points decreased the moderate level of relative bias seen at $T = 50$ (10.73%) to the negligible level of bias seen at $T = 500$ (1.24%). Though bias is a known consideration when making use of a pseudo-maximum likelihood approach, the bias here remains within acceptable levels, as most individual cells remain within 10% relative bias. For the presence of relative bias across all conditions, see Figure 11.

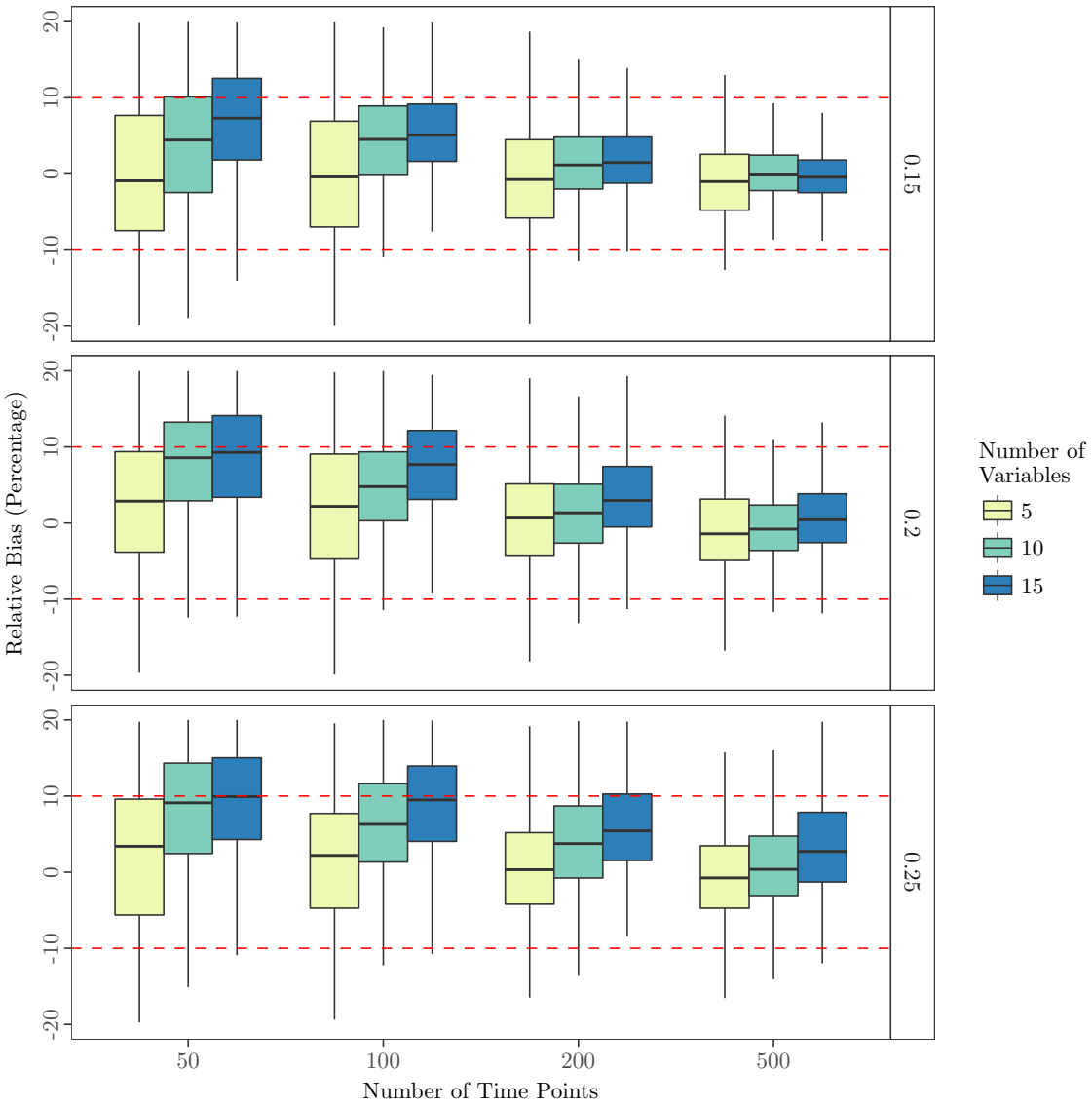

Figure 11: Stepwise uSEM: Relative Bias by Number of Variables, Number of Time Points, and Sparsity of Network

Adding BIC to stopping criteria. The oft-implemented automated unified SEM uses two of four standard SEM fit indices as stopping criteria. Here, I introduced the BIC as a stopping criteria and set estimation to terminate when three of five measures reached "excellent" according to the aforementioned criteria. Compared to the above results, very few differences were observed. Where sensitivity and specificity range from 0 to 1, no individual cell differed by more than .01.

Summary

Unlike the graphical VAR, increasing the number of time points in the stepwise uSEM yielded improved path specificity, or improved ability to reject false paths. Like the graphical VAR, increases in both the number of variables and the density of the network slightly harmed performance. Here, the ability to recover directed relationships is improved, though best performing cell yields a sensitivity of only .75 to contemporaneous directed relationships, which are frequently of interest to researchers. From this, I turn to a discussion of the regularized uSEM.

Regularized unified SEM

Two forms of regularization penalties were tested in the course of Study 1A – the standard LASSO and the adaptive LASSO. Overall, the adaptive LASSO outperformed the standard LASSO in almost every outcome measure. Though regularization with the standard LASSO penalty yielded respectable sensitivity, its specificity was poor. That is, when using the standard LASSO, the majority of true paths were retained in the final solution; however, a substantial number of false positives were also present. In contrast, the adaptive LASSO exhibited both exceptional sensitivity and specificity, representing an ideal balance.

Therefore, though my discussion will center on the performance of regularization using both methods, I will place an emphasis on the performance of the adaptive LASSO. Compared to both the graphical VAR and the stepwise uSEM, the regularized uSEM with adaptive LASSO yielded better performance with respect to sensitivity and specificity, particularly in the presence of a longer time series. Full details are provided below.

Path Sensitivity

Marginalizing over other simulation factors, increasing the number of variables yielded reduced sensitivity for the adaptive LASSO (see Figure 13) (.91 at $V = 5$ and .82 at $V = 15$). With the standard LASSO, increasing the number of variables increased path sensitivity, but reduced the path specificity (discussed below). Thus, with more variables, the standard LASSO tended to retain too many paths in general, increasing the sensitivity but decreasing the specificity. Collapsing across other factors, increasing the density of data-generating relationships led to minimal increases in path sensitivity but noticeable decreases in path specificity. The same pattern was observed with respect to direction sensitivity. Finally, increasing the length of the time series led to increases in the overall path sensitivity, regardless of whether relationships were recovered as contemporaneous or lagged. Figure 12 depicts the increase in path sensitivity for both the adaptive LASSO and standard LASSO as the length of the time series increases.

Lagged versus Contemporaneous. As with other methods, the sensitivity to lagged paths for the adaptive LASSO uSEM was slightly higher than the sensitivity to contemporaneous paths. However, this effect seemed to only be present in shorter time series. For example, at $V = 5, S = 15\%$ with $T = 50$ time points, the lagged and contemporaneous path specificity were .68 and .74, respectively. However, holding the number of variables and the sparsity of the network constant, the lagged and contemporaneous path specificity were .98 and .98, respectively, at $T = 200$.

Path Specificity

For the adaptive LASSO, increases in the density of the network did not meaningfully relate to the path specificity (.85 at $S = 15\%$ and .86 at $S = 25\%$). Increasing

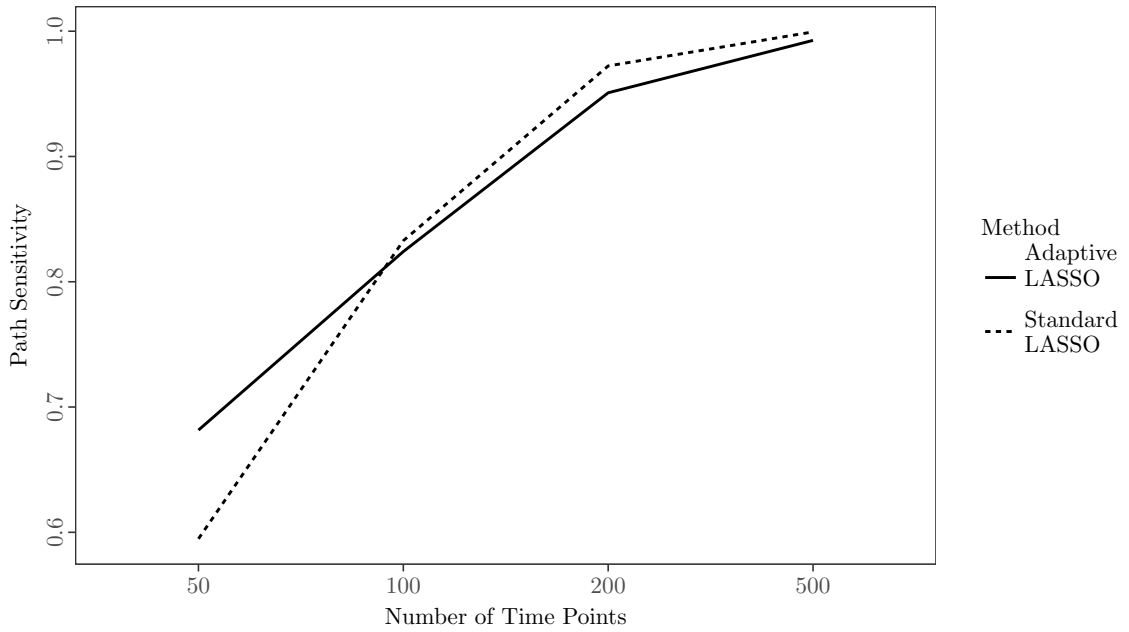

Figure 12: Path Sensitivity and Number of Time Points: Adaptive LASSO versus Standard LASSO

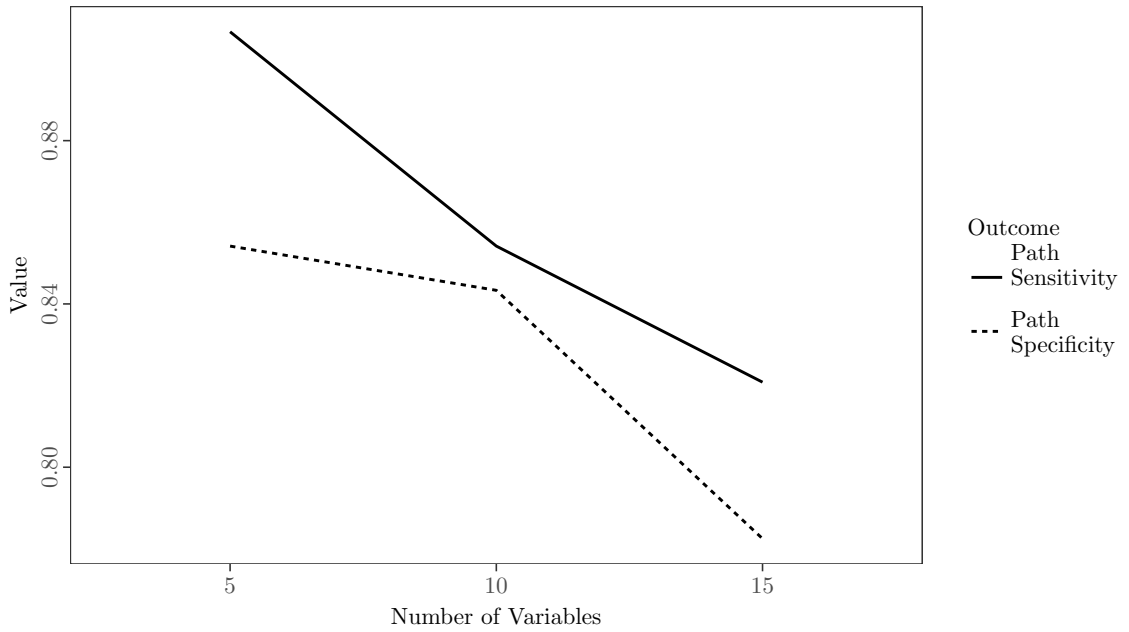

Figure 13: Adaptive LASSO: Path Sensitivity and Specificity by Number of Variables

the number of variables modestly reduced the path specificity, where the path specificity dropped from .85 at $V = 5$ to .78 at $V = 15$, representing a noticeable decrement. For the

standard LASSO, the sparsity of the network related more strongly to the path specificity, where it dropped from .79 at $S = 15\%$ to .60 at $S = 25\%$. Finally, with respect to effect of time series length on path specificity, an important discrepancy existed between the regular LASSO and the adaptive LASSO. That is, when performing regularization using the adaptive LASSO, the specificity of recovered relationships increased with increasing number of time points (specificity = .66 for $T = 50$ and specificity = .96 for $T = 500$). However, when using the standard LASSO penalty, the opposite effect occurred. That is, more false positives were produced at a higher number of time points (specificity = .76 at $T = 50$ and specificity = .63 for $T = 500$). For a depiction of this differential effect, see Figure 14.

Lagged versus Contemporaneous. The path specificity was uniformly high for lagged and contemporaneous relationships, with no noticeable differences by simulation factor. For example, at $T = 200$, the lagged path specificity was .99 and the contemporaneous path specificity was .99.

Direction Sensitivity

Marginalizing over simulation factors, increasing the number of time points improved the direction sensitivity (.50 at $T = 50$; .96 at $T = 500$), where the number of variables yielded decrements in direction sensitivity. Specifically, with $V = 5$, the direction sensitivity was .80, where with $V = 15$, the direction sensitivity was .69. Increasing the network density minimally impacted the sensitivity to directions (.75 at $S = 15\%$ compared to .73 at $S = 25\%$).

Lagged versus Contemporaneous. The sensitivity to lagged directions was again uniformly higher than the sensitivity to contemporaneous directions, as was seen in the

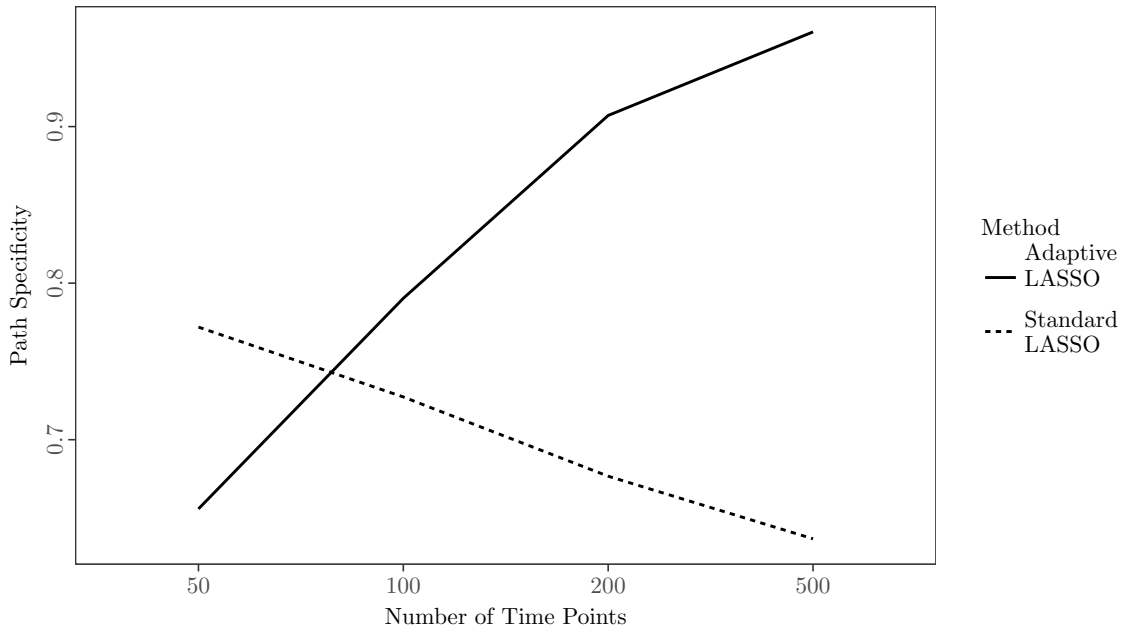

Figure 14: Path Specificity and Number of Time Points: Adaptive LASSO versus Standard LASSO

stepwise uSEM. The most striking feature of the performance by the adaptive LASSO uSEM is the sensitivity to contemporaneous directions in the presence of a longer time series. That is, the performance does not differ tremendously from the stepwise uSEM for shorter time series. However, at $T = 200$, the adaptive LASSO uSEM performs as well as the stepwise uSEM does with $T = 500$, and at $T = 500$, the adaptive LASSO uSEM far outpaces the performance of the stepwise uSEM (see Figure 15).

Direction Specificity

The specificity of the directed paths was consistently high with time series of $T = 200$ or longer. Increasing the number of variables yielded minimal impact on direction specificity, though increasing the density of the network noticeably decreased the direction specificity (e.g., .90 at $S = 15\%$ and .82 at $S = 25\%$).

Lagged versus Contemporaneous. The direction specificity of lagged and contempo-

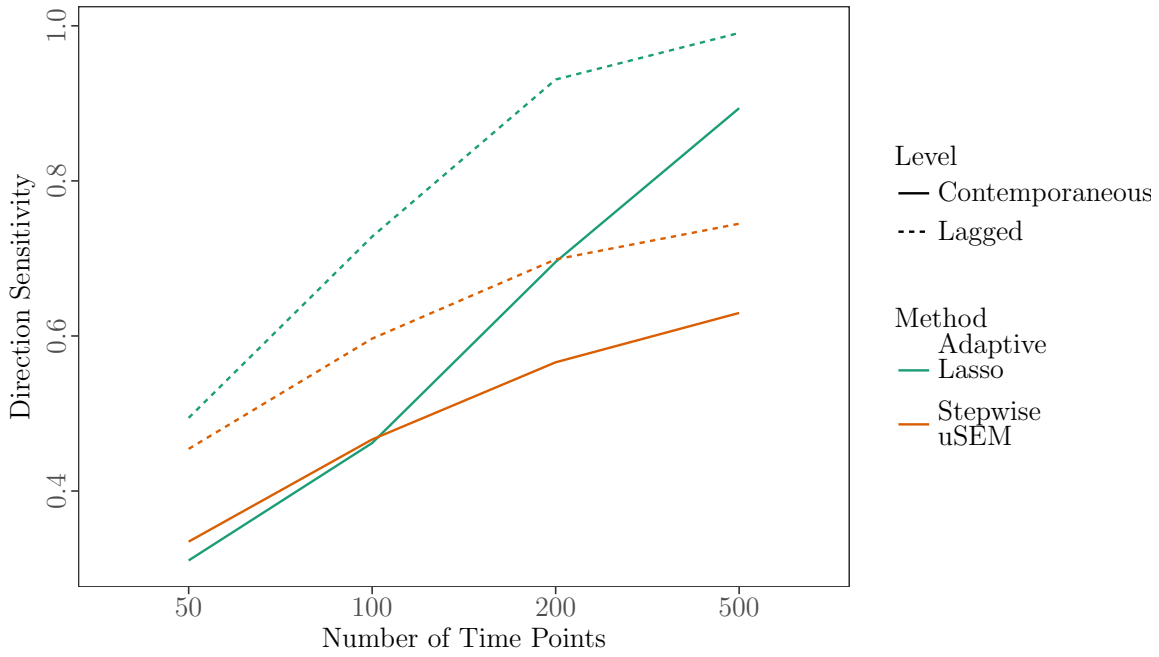

Figure 15: Direction Sensitivity and Number of Time Points: Adaptive LASSO versus Stepwise uSEM

raneous directions, considered separately, was uniformly high. When using the adaptive LASSO, no single cell yielded either a lagged or contemporaneous direction sensitivity lower than .80. When using the standard LASSO, the direction specificity was uniformly lower, though still above .60 in all cells.

Bias and RMSE

As would be expected, an increase in the number of time points was associated with decreases in RMSE (RMSE = 0.17 at $T = 50$ and RMSE = 0.07 at $T = 500$), indicating less error in prediction in the presence of a longer time series. The RMSE increased slightly with a larger number of variables, increasing from RMSE = .10 to RMSE = .14 from $V = 5$ to $V = 15$, representing a modest increase. Across all conditions, the relative bias for the true positive paths of the adaptive LASSO remained within acceptable limits. Figure 16 displays the relative bias present when using the regularized uSEM with

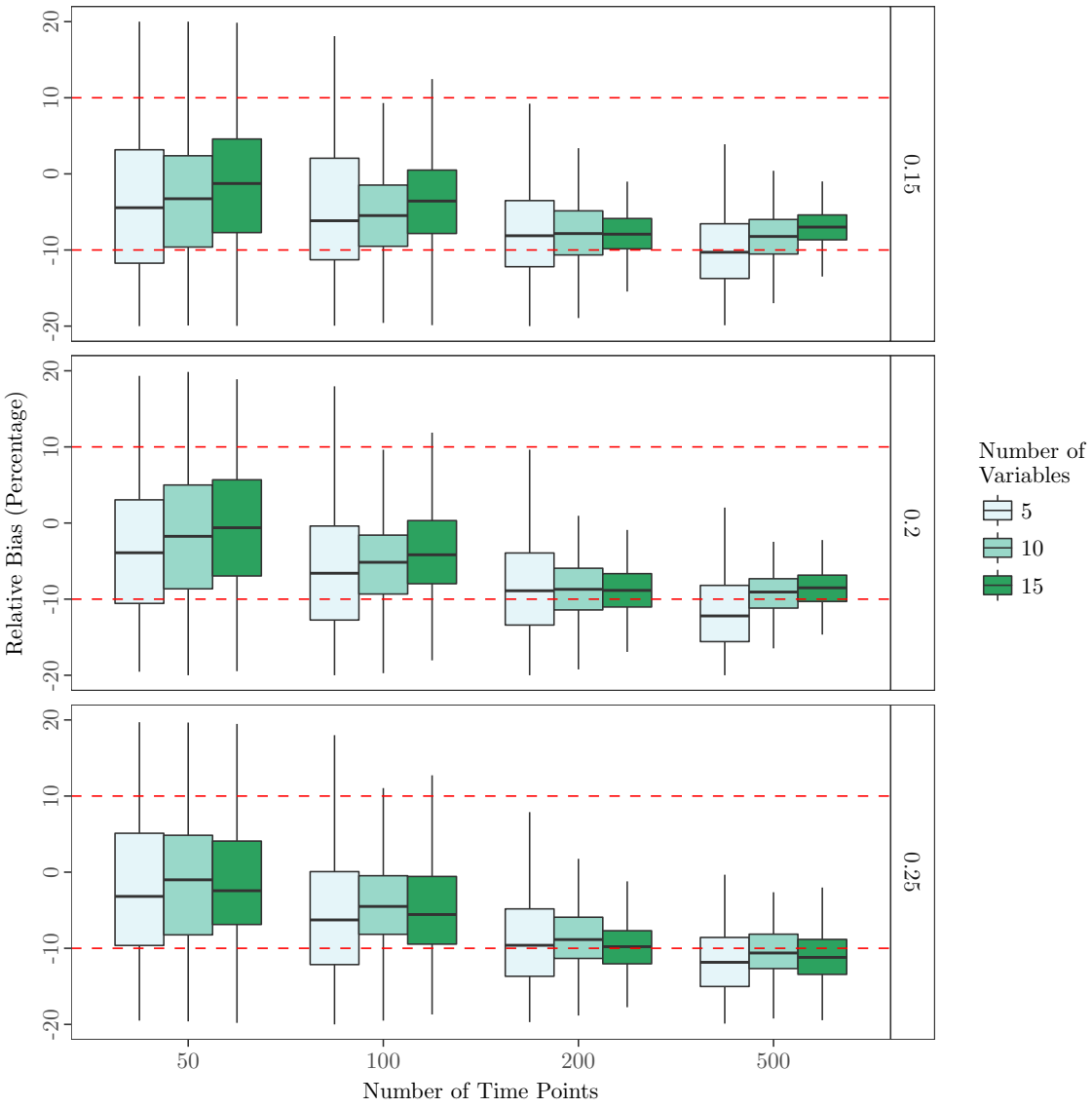

Figure 16: Adaptive LASSO: Relative Bias by Number of Variables, Number of Time Points, and Sparsity of Network

adaptive LASSO across all simulation factors: number of time points, number of variables, and sparsity of the network.

Consistent with hypothesized results, greater bias was present when using the standard LASSO, as seen in Figure 17, lending greater support for the use of the adaptive LASSO in this context. Additionally, increases in network density were associated with slight increases in both relative bias and RMSE. As previously mentioned, the standard

LASSO yielded lower specificity than the adaptive LASSO, retaining too many false edges. The absolute bias of these false positives, however, is informative. That is, when using the standard LASSO, the average absolute bias of the false positives across all conditions was less than .05. Therefore, while the adaptive LASSO clearly outperformed the standard LASSO by our indices of recovery, these false positives present in the models selected by the standard LASSO condition were not large in magnitude.

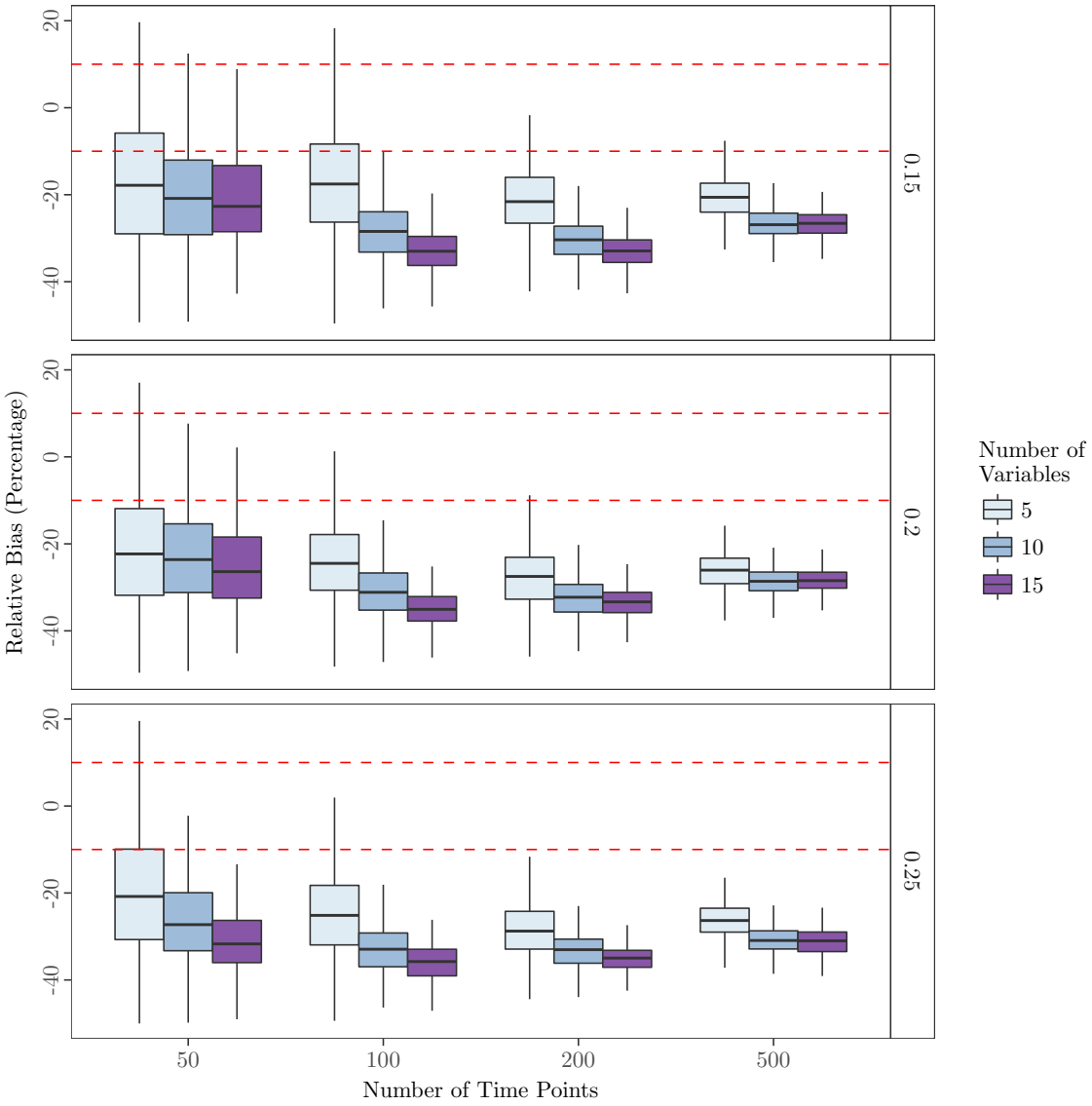

Figure 17: Standard LASSO: Relative Bias by Number of Variables, Number of Time Points, and Sparsity of Network

Study 1B

In Study 1B, the fitted model and the data-generating model are misaligned. That is, for fitting the graphical VAR, data are generated with *directed* contemporaneous relationships. For fitting the unified SEM-based models (stepwise uSEM, adaptive LASSO uSEM, standard LASSO uSEM), data are generated with *correlational* contemporaneous relationships. This study, while less central than Study 1A, provides important information regarding the performance of the models if either 1) correlational contemporaneous relationships are assumed and modeled erroneously or 2) directed contemporaneous relationships are assumed and modeled erroneously. To maintain scope, the number of variables will not be manipulated for Study 1B – it will be held constant at $V = 5$, where sparsity and length of time series will be manipulated.

For Study 1B, several outcomes are presented. In order to assess the overall recovery of connections, path sensitivity and path specificity will be examined. In order to evaluate the recovery of directed lagged relationships, lagged direction sensitivity and lagged direction specificity will be evaluated. Finally, contemporaneous path sensitivity and contemporaneous path specificity will be examined. These outcomes taken together will allow for an assessment of the influence of mismodeled contemporaneous directed relationships.

Graphical VAR

In the presence of directed contemporaneous relationships, the graphical VAR simply recovers these relationships in the form of a sparse nondirected correlation structure. The direction sensitivity and direction specificity for the lagged relationships, which remain identical to the data-generating directed lagged relationships from Study 1A, do

not change dramatically. That is, in Study 1A, the directed lagged sensitivity is .76 for the $V = 5, S = 20\%, T = 100$ cell, while in Study 1B, the directed lagged sensitivity for the same cell is .77. For this same cell, the directed lagged specificity similarly does not change. For example, the directed lagged specificity for $V = 5, S = 20\%, T = 100$ in Study 1A is .91, and the directed lagged specificity in Study 1B is .88.

Stepwise unified SEM

The overall recovery of relationships, regardless of the data-generating direction of the contemporaneous structure, remains adequate in the stepwise uSEM. Collapsing across the sparsity of the network, the path sensitivity at $T = 200$ is .90, and the path specificity at $T = 200$ is .98. Further decomposing this measure, the directed path sensitivity for lagged relationships at $T = 200$ is .79 (compared to .76 in Study 1A), and the directed path specificity for lagged relationships at $T = 200$ is .99 (compared to .99 in Study 1A). The overall contemporaneous path sensitivity *increased* slightly in Study 1B compared to Study 1A. Collapsing over other simulation factors, in the $T = 500$ conditions, the contemporaneous path sensitivity increased from .90 in Study 1A to .95 in Study 1B, indicating improved ability to retain true contemporaneous edges when the structure was generated to be correlational, not directed, in nature. The contemporaneous path specificity also remained high in Study 1B. Indeed, across all conditions in Study 1B, the contemporaneous path specificity exceeded 90% across all replications. Thus, it can be stated that the stepwise uSEM did not suffer or produce spurious relationships in the presence of a mismodeled correlational structure.

Regularized unified SEM

Performing the regularized uSEM with adaptive LASSO on data generated with

correlational contemporaneous relationships has minimal effects on measures assessing the recovery of the network structure. For example, in the cell with five variables, 20% sparsity, and $T = 200$, the sensitivity for directed lagged relationships was .94, and the specificity for directed lagged relationships was .97. These values changed minimally from Study 1A, where the outcomes for the same cell was .93 and .97, respectively. Thus, there was no evidence of spurious effects in the lagged matrix. There were differences between Study 1A and Study 1B in terms of recovering the contemporaneous structure. That is, for the $T = 50$ condition, collapsing over network sparsity, the contemporaneous path sensitivity was .72 in Study 1B compared to .52 in Study 1A. Thus, the regularized uSEM was more likely to recover that a path existed between two variables measured at *time* when the path was generated to be nondirected.

Summary: Study 1A and Study 1B

In data generated to be compatible with time series data broadly defined within psychological research, the regularized uSEM using the adaptive LASSO performed exceptionally well recovering both data-generating paths and data-generating directions. As would be expected, performance was best with a longer time series, with highest specificity and highest sensitivity observed when the number of time points was large and the network was at its most sparse. With the adaptive LASSO specifically, relative bias was lower than 15% across all cells. The stepwise uSEM also performed well, though its sensitivity was lower in general than the regularized uSEM, consistent with expectation. This effect was more pronounced when the network was less sparse, where the path sensitivity of the stepwise uSEM decreased with increasing network density. The graphical VAR demonstrated somewhat uniformly adequate sensitivity, but poor specificity, frequently

retaining too many false positive paths. In Study 1B, few differences were observed, as previously discussed. With the finite sampling behavior of these models established, I now turn to a discussion of their relative performance with data designed to emulate BOLD time series data. For the first time, the regularized uSEM is introduced and evaluated for the identification of individual-level directed functional connectivity.

CHAPTER 3: STUDY 2

In Study 2, design factors directly related to fMRI will be manipulated in a partially crossed simulation design borrowed from Smith et al. (2011). In this seminal work, researchers evaluated the performance of more than thirty methods for network modeling with fMRI data across twenty-eight conditions designed to mimic a range of network models. Smith et al. (2011) ultimately found that many competing methods perform poorly when considering measures of network recovery such as recall and precision. Of the methods tested, "Bayes net" methods were found to perform well, where lagged (lag-zero) methods were found to perform consistently poorly. All of the methods considered in the present dissertation may be thought of as Bayes net methods; none of these methods were evaluated in the original work.

Therefore, Study 2 will employ a second Monte Carlo simulation study, which will evaluate the ability of the respective methods to recover patterns of temporal dependence not just in time series data broadly, but in data generated to emulate fMRI data. Given the thoroughness of the simulation in Study 1, other relevant factors, such as number of regions and sparsity of network, will not be varied in this simulation. Instead, factors more specific to fMRI studies will be varied here. Namely, the temporal resolution (TR), the presence of backwards (i.e., reciprocal) connections, the presence of cyclic connections, inter-regional hemodynamic response function lag variability, the strength of connections, and the neural lag.

Design Factors for Simulation

Temporal resolution. The temporal resolution, or the amount of time between scans, will be varied across two levels: TR = 0.25 and 3.0. While a TR of 0.25 seconds would not practical for scanning the whole brain, it would be possible for achieving a select number of slices of data (e.g., Lindquist & Wager, 2007). Thus, this value may represent an extreme lower bound. Temporal resolution of 3 seconds represents values more typically found in standard whole-brain fMRI (see Lindquist et al., 2009 for an empirical example). Testing the ability of lag-based methods to function under different temporal resolutions is an important point of consideration, as prior work has shown methods to perform differently under varying temporal resolutions (Smith et al., 2011).

Presence of backwards connections. Within fMRI data, it is frequently the case that a given pair of brain regions may be connected in both directions, as opposed to one direction only (Smith et al., 2011). This is known as a backward, or reciprocal, connection. However, there is some ambiguity regarding the meaning of these relationships. In the context of a negative backward connection, we may infer inhibition. Here, a simulation will be introduced which adds reciprocal relationships equal in magnitude to the sending connection, but of opposite sign.

HRF lag variability. Here, the hemodynamic response function lag is defined as the time from the onset of a neural stimulus to the peak of the BOLD response. Broadly, the hemodynamic response function is the change in the magnetic resonance signal triggered by neuronal activity (Huettel et al., 2004). A schematic of between-subject variation in the HRF is depicted in Figure 29. It is known that between-person

variability is generally greater than within-person variability (Handwerker et al., 2004). Additionally, the HRF lag for individuals is important to consider against the temporal resolution (TR). In the present study, HRF lag variability is varied to be $SD = 0.5s$ and $SD = 0.0s$.

Stronger Connections. In one simulation, the magnitude of the data-generating connections will be increased from 0.4 to 0.9.

Cyclic Connections. In one condition, cyclic connections will be introduced. These connections are particularly relevant for consideration, as several modeling approaches for fMRI assume no cyclic causality. Two such methods are the PC algorithm (Meek, 1995; Spirtes & Glymour, 1991) and the Greedy Equivalence Search (GES; Chickering, 2002).

Factors held constant. Other design factors relevant to fMRI but not manipulated include the effect of inaccurate ROIs (whether mixing time series or adding random time series), the effect of nonstationary connection strength over time, the effect of strong external inputs, or the effect of shared inputs.

Data Generation and Characteristics

The source of data comes from Smith et al. (2011), which are publicly available at `http://www.fmrib.ox.ac.uk/datasets/netsim/`. In Smith et al. (2011), data were generated to mimic BOLD fMRI time series in 28 different simulations. Again, these simulations are not fully crossed; instead, each individual simulation is designed to test one plausible situation at a time that may be encountered in empirical research. Therefore, no meta-models will be used; instead, all results will be investigated graphically.

The time series data present in these simulations were based on a combination of models: a network model depicting directed relationships at the neural level, overlaid by the dynamic causal model (DCM, Friston et al., 2003) fMRI forward model, which makes use of the nonlinear balloon model to characterize vascular dynamics (Buxton et al., 1998). Specifically, DCM is a framework for identifying effective connectivity, as it seeks to infer processes at the neuronal level, instead of at the level of the BOLD time series. As such, it is based on the use of differential equations which describe dynamics at the neuronal level; this model is then combined with a hemodynamic forward model to arrive at effective connectivity (Stephan et al., 2008). Full details regarding the dynamic causal model are beyond the scope of this project, but more details may be found in Friston et al. (2003). Of most relevance here is that the data are generated in a manner considered to be most consistent with the dynamics underlying connectivity.

Here, I introduce these data for an important reason. First and foremost, these data are considered benchmark data for any method that may be brought to bear on directed functional connectivity. Further, very few approaches in the original Smith et al. (2011) study were able to accurately detect direction at the individual-level. Second, I introduce these data to avoid making use of a package that may generate data in a way that automatically prefers one method to another. That is, there are multiple methods in existing literature and software packages that one may use to generate BOLD data. Here, I evaluate the regularized uSEM, the stepwise uSEM, and the graphical VAR on fMRI on these benchmark data.

From the 28 simulations designed in Smith et al. (2011), eight were chosen to test performance in conditions that may realistically be encountered in practice. From

the original manuscript, the chosen simulations were sim1, sim5, sim13, sim14, sim15, sim18, sim19, and sim20. Table 3 details the characteristics of the chosen simulations.

Sim	Nodes	Duration	TR	Noise	HRF SD	Description
1	5	10	3.00	1.0	0.5	Start
5	5	60	3.00	1.0	0.5	Longer Session
13	5	10	3.00	1.0	0.5	Backward Connections
14	5	10	3.00	1.0	0.5	Cyclic Connections
15	5	10	3.00	0.1	0.5	Stronger Connections
18	5	10	3.00	1.0	0.0	No HRF SD
19	5	10	0.25	0.1	0.5	Fast TR, Long Neural Lag
20	5	10	0.25	0.1	0.0	Fast TR, Long Neural Lag, No HRF SD

Table 3: Study 2: Smith Simulation Conditions

Here, sim1 is considered the condition to which other conditions will be compared, as it represents typical network and scan properties. This network contains 5 nodes, a session duration of ten minutes, a temporal resolution of 3 seconds, an addition of 1% noise, and an HRF lag variability of 0.5 seconds (see Figure 18).

From this simulation, sim5 increases the session duration to 60 minutes, instead of a standard 10 minutes. This change increases the number of time points six-fold. To sim1, sim13 adds backwards (or reciprocal) connections to the data-generating process (see Figure 19). From sim1, sim14 introduces the presence of a cyclic connection (see Figure 20). For clarification, note that this cyclic connection is not a reciprocal connection. From sim1, sim15 increases the strength of the connections and decreases the amount of noise. From sim1, sim18 decreases the standard deviation of the HRF among regions to zero. From sim1, sim19 decreases the temporal resolution to 0.25 ($TR = .25$) and increases the neural lag to 100ms, as opposed to the data-generating 50ms used across other simulations. Finally, from sim19, sim20 maintains the short TR and the reduced

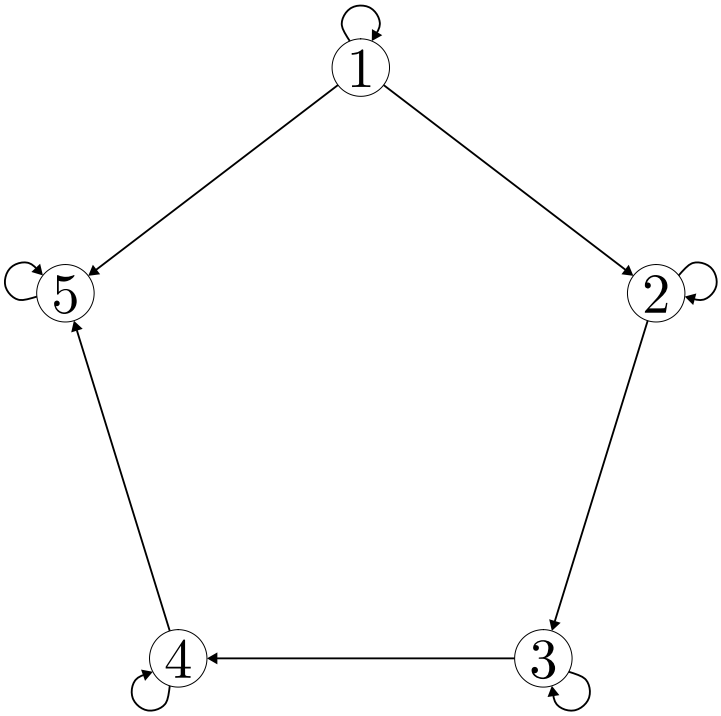

Figure 18: Smith sim1: ground truth network structure

noise, but removes the HRF standard deviation of 0.5 present in sim1, sim13, sim14, sim15, and sim19.

Outcome measures. As in Study 1A, measures of sensitivity and specificity will be evaluated in order to measure recovery and precision pertaining to the original underlying neural network structure. Measures pertaining to the estimates of the edge weights themselves will not be considered due to differences in scaling. All measures considered in Study 2 are displayed in Table 4.

Outcome Measure	Regularized uSEM	Stepwise uSEM	Graphical VAR
Path Sensitivity	Yes	Yes	Yes
Path Specificity	Yes	Yes	Yes
Direction Sensitivity	Yes	Yes	No
Direction Specificity	Yes	Yes	No

Table 4: Study 2: Outcome Measures by Method

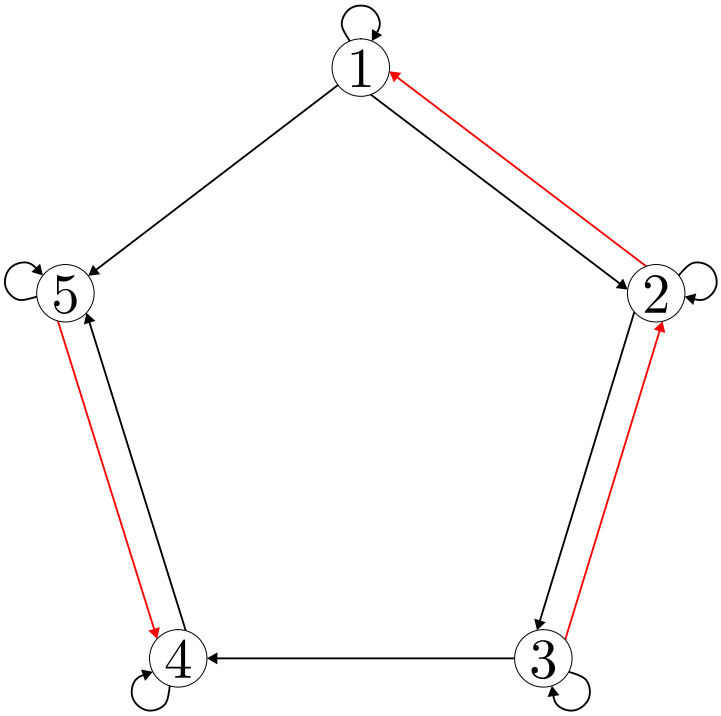

Figure 19: Smith sim13: ground truth network structure

Results

Sim1. Across the first simulation, both the sensitivity and specificity of data-generating relationships were approximately comparable. Across the methods, the highest path sensitivity was observed for the regularized uSEM using the standard LASSO. The adaptive LASSO was slightly behind with respect to path sensitivity, but outperformed the regular LASSO with respect to path *specificity*. That is, the regularized uSEM using the standard LASSO experienced a greater rate of false positives (specificity = .72); the use of the adaptive LASSO improved path specificity (specificity = .92). The stepwise uSEM fell slightly behind the adaptive LASSO uSEM in terms of path sensitivity (.81 versus .86), but outperformed the adaptive LASSO uSEM with respect to path sensitivity (.96 versus .92). The graphical VAR also performed admirably with respect to path

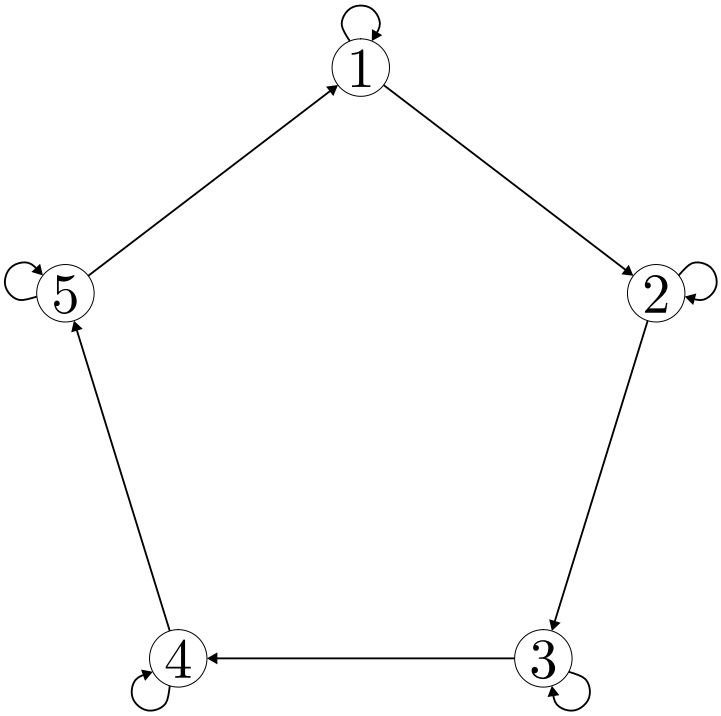

Figure 20: Smith sim14: ground truth network structure

sensitivity and specificity, (sensitivity = .86; specificity = .90). Finally, the stepwise uSEM with BIC yielded the same results as the stepwise uSEM using the standard two-of-four fixed cutoffs. These results are mostly consistent with the results of Study 1A, and demonstrate that all of the methods evaluated here exhibit promise for recovering nondirected connections in fMRI data.

Moving to direction recovery, the performance of all methods suffers. The LASSO uSEM demonstrates a direction sensitivity of .58, as the method with the best performance on this outcome. The adaptive LASSO uSEM demonstrates a direction sensitivity of only .51, though its direction specificity is .83. Across both regularized approaches and the stepwise uSEM, the modal characteristic of the results is this: very few spurious paths are estimated, and spurious directions are frequently those which represent the

opposite direction of a data-generating direction. Put differently, $V1 \rightarrow V2$ is likely to appear in a model where $V2 \rightarrow V1$ is the correct data-generating direction, but any such directed connection is unlikely to appear otherwise. The performance of each method, broken down by outcome measure, is displayed in Figure 21. For the discussion of all other Smith simulations, only variation from the aforementioned pattern of results will be presented.

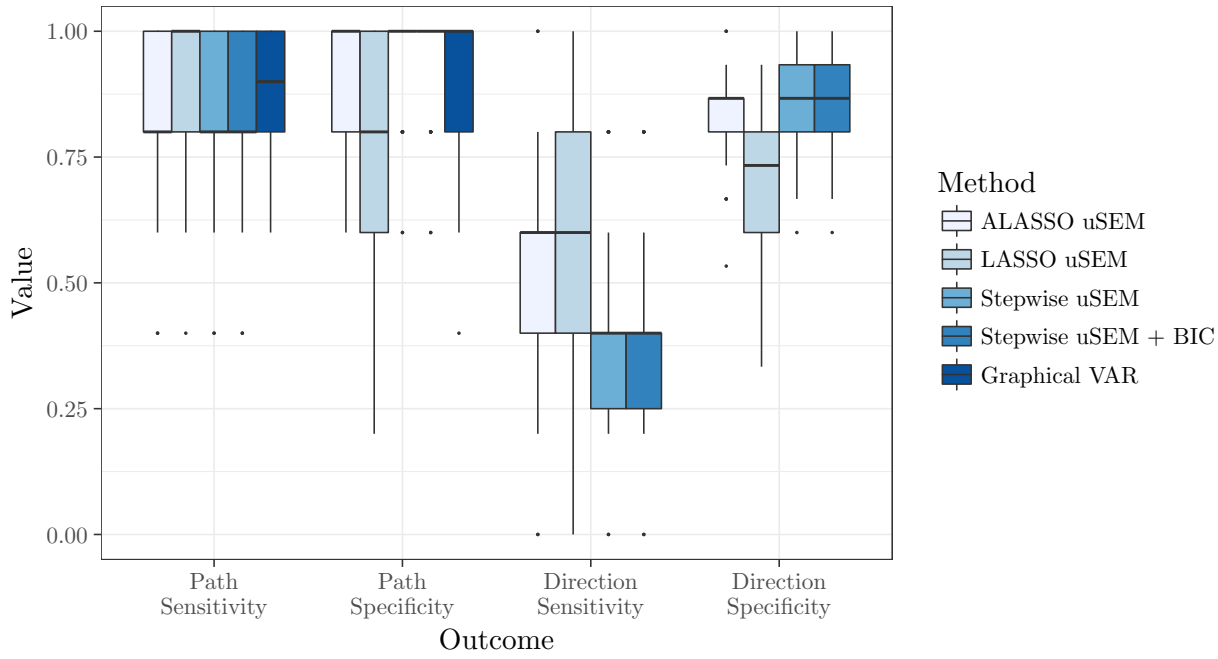

Figure 21: Sim 1: Specificity and Sensitivity by Method

Sim5: Longer Session Length. Of the set of Smith simulations, sim5 yielded arguably the most promising results. In sim5, the session duration was increased from 10 minutes to 60 minutes, representing what would be an hour-long resting state scan. The stepwise uSEM performed reasonably well in recovering that a path existed (path sensitivity = .84), and performed quite well in rejecting paths that did not exist (path specificity = 1.0). However, the stepwise uSEM performed poorly in recovering the direc-

tionality of these paths, where the direction sensitivity was .48. The regularized uSEM with adaptive LASSO outperformed the stepwise uSEM in these respects, outperforming many methods originally tested in Smith et al. (2011). For example, the overall path sensitivity for this model was 1.0, with a path specificity of 0.92. Therefore, regardless of directionality, the adaptive LASSO uSEM performs well in recovering connectivity. The recovery of directionality, however, is where the adaptive LASSO sets itself apart. The sensitivity to directed paths for the adaptive LASSO was .82, with a specificity of 0.75. Therefore, though the adaptive LASSO tends to retain a few too many false directions, it far outperforms all other competing methods in recovering the directionality. The regularized uSEM with standard LASSO performed predictably less well, exhibiting greater sensitivity but lower specificity, reflecting the tendency to over-retain edges. See Figure 22 for a full breakdown of sensitivity and specificity by method.

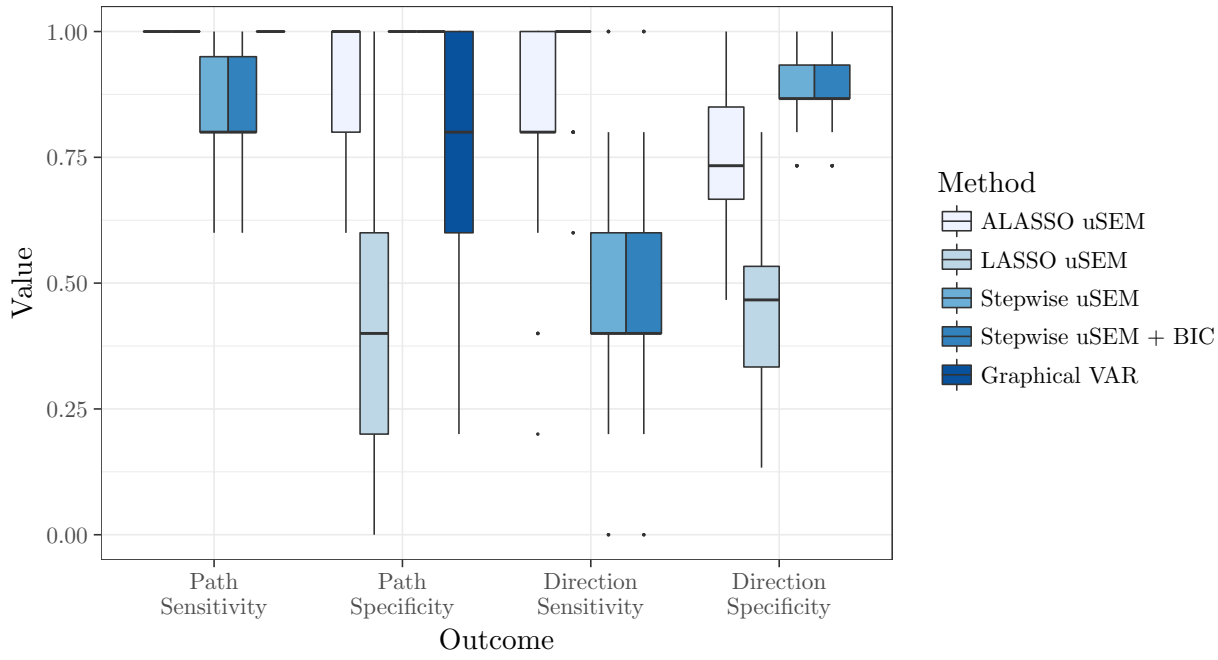

Figure 22: Sim 5: Specificity and Sensitivity by Method

Sim13: Backwards Connections. From a simulation design perspective, it is important to note that the introduction of backwards connections in this Smith simulation does not hold constant the number of overall connections with respect to the other Smith simulations. That is, the addition of a backwards connection does not result in the removal of another connection. For example, for a given individual-level data-generating matrix, there may be five directed connections. In sim13, where backwards connections are introduced, anywhere from one to three *additional* directed connections were introduced to complement the existing five directed connections. Therefore, the level of sparsity in the network is not held constant.

Across all methods, the introduction of these backwards connections hinders performance, where the path sensitivity drops from .85 to .55 (a 34% decrease) averaged across all methods. Thus, we have a reduced ability to recover true edges. The specificity of the connections does not suffer, however, with all methods performing at a specificity of .8 or higher. Given the poor performance at the level of the paths (nondirected connections), the direction sensitivity suffers as well, ranging from 0.26 to 0.31 across all methods. Note that this range does not include the graphical VAR, as it does not model directed contemporaneous connections. See Figure 23 for results.

Sim14: Cyclic Connections. In sim14, "cyclic connections" are introduced. Compared to sim1, the relationship at the level of the neural network between V1 and V5 is flipped, such that V5 predicts V1. In this way, a "causal chain" is created. This change seems to have little effect on the results, consistent with results presented by Smith et al. (2011). See Figure 24 for full details.

Sim15: Stronger Connections. In sim15, the average data-generating directed

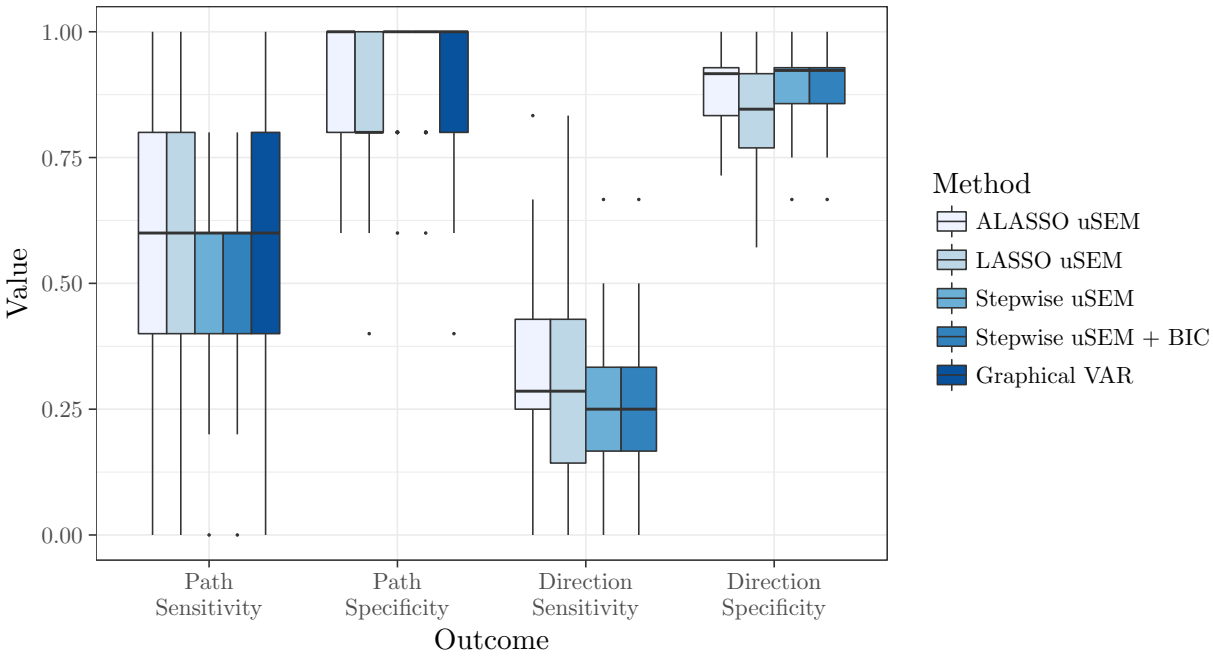

Figure 23: Sim 13: Specificity and Sensitivity by Method

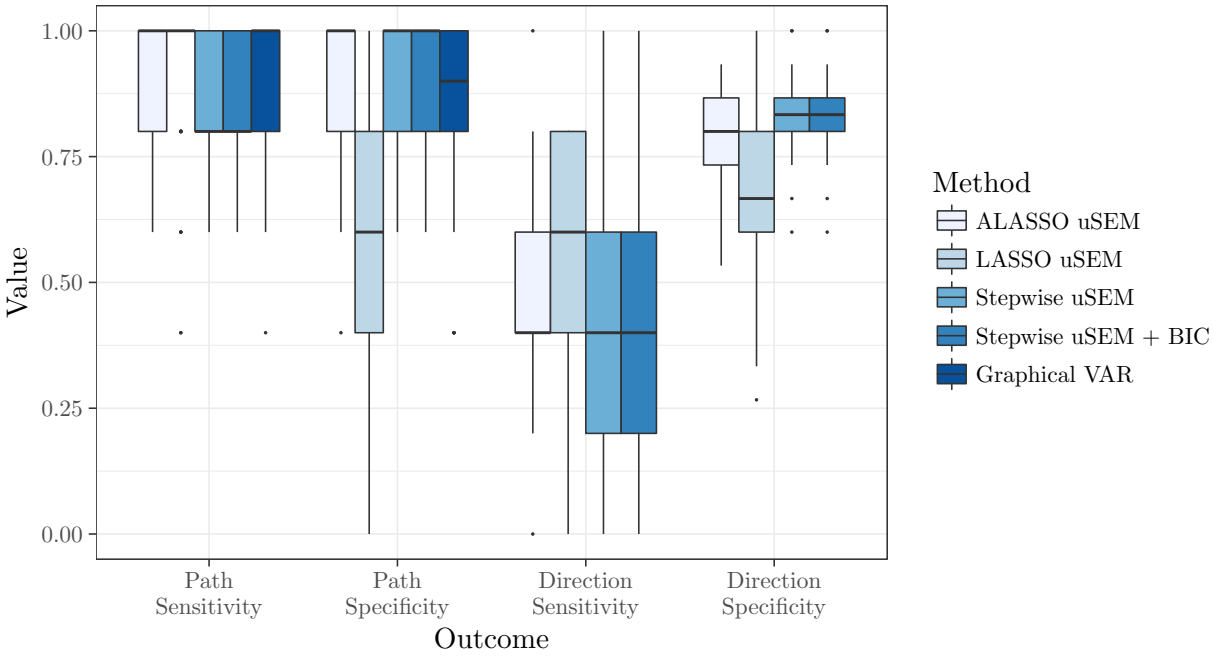

Figure 24: Sim 14: Specificity and Sensitivity by Method

connection is increased from .4 to .9. Compared to the previous two simulations, a striking finding is the relative performance of the regularized uSEM and stepwise uSEM

approaches. That is, both the LASSO and adaptive LASSO uSEM recover 100% of data-generating connections. However, while the specificity of the regularized uSEM approaches suffers in the presence of these stronger connections, the specificity of the stepwise uSEM does not. The stepwise uSEM exhibits a specificity of .81, while the adaptive LASSO uSEM and LASSO uSEM exhibit specificity values of .58 and .20, respectively. Finally, the graphical VAR offers perhaps the best balance of sensitivity (.99) and specificity (.89) for sim15 (see Figure 25). Regarding directionality, performance in sim15 did not vary meaningfully from findings already reported in sim1, as the regularized approaches outpaced the stepwise approaches in terms of path sensitivity, but not in terms of path specificity.

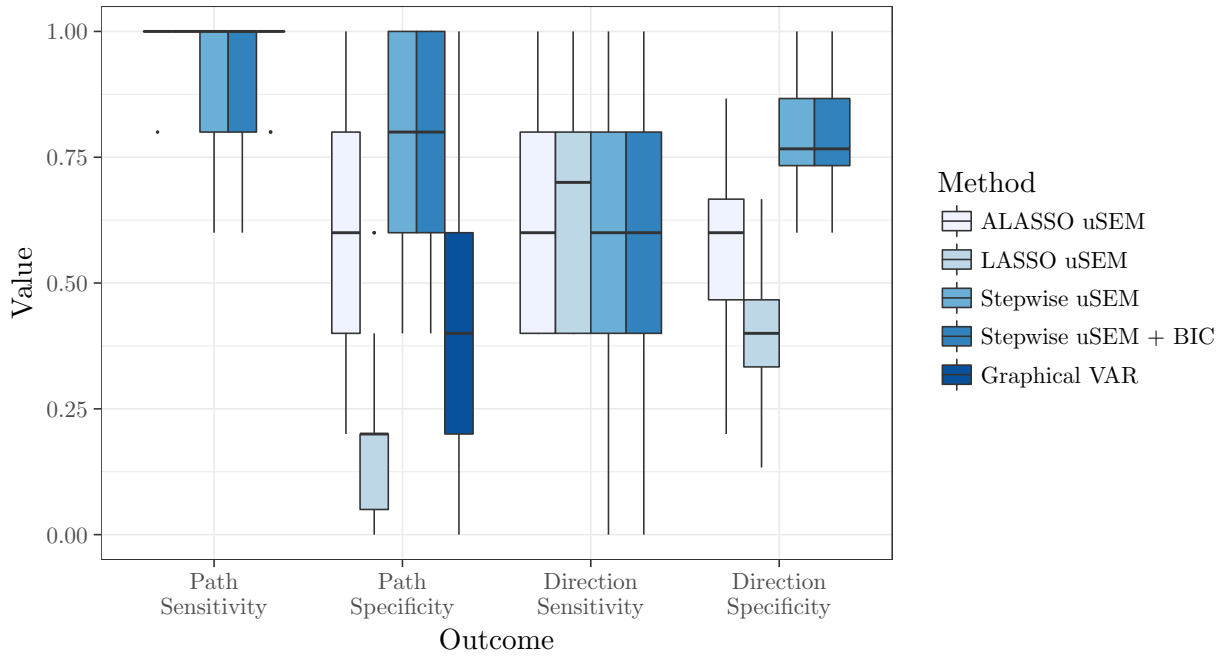

Figure 25: Sim 15: Specificity and Sensitivity by Method

Sim18: No inter-regional hemodynamic response function variability. In the original Smith et al. (2011) paper, the HRF lag across persons was not systematically

varied. Therefore, I am unable to select a simulation which mimics this specific aspect of HRF variability. Instead, the authors varied the HRF standard deviation across regions within a given person. In sim18, this inter-regional variability is dropped to 0, instead of the standard deviation of 0.5 used in other simulation conditions. Therefore, by design, sim18 is identical to sim1 other than the component representing the interregional standard deviation of the hemodynamic response funciton. Here, no meaningful differences are observed compared to sim1 (see Figure 26).

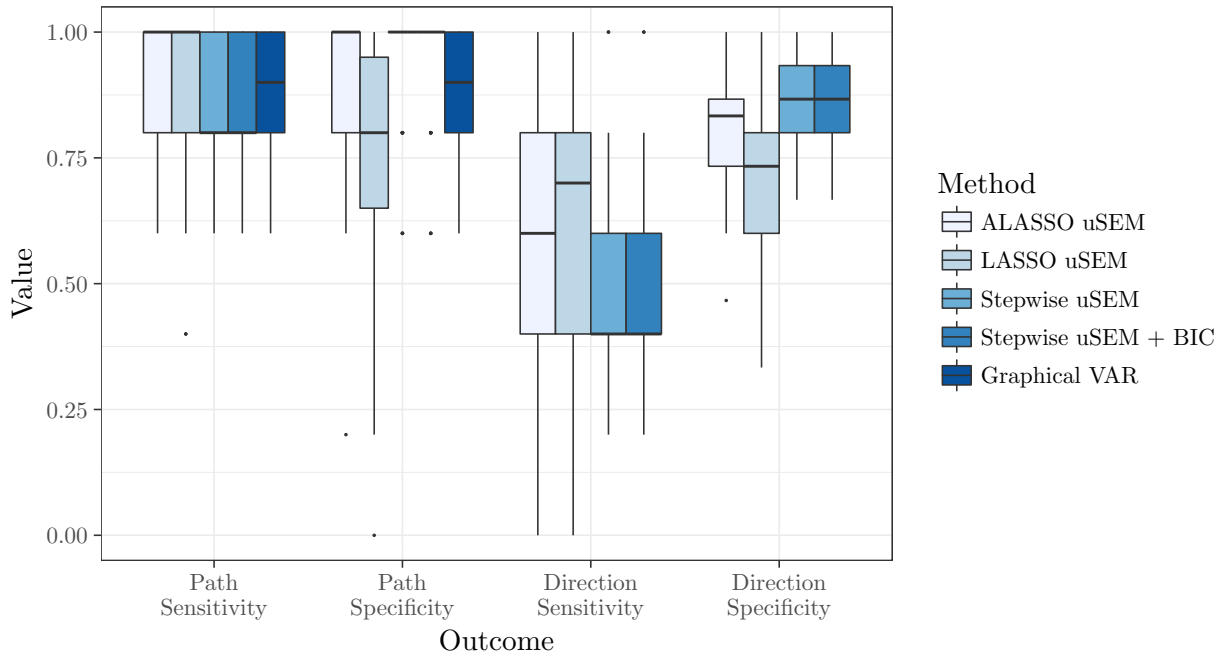

Figure 26: Sim 18: Specificity and Sensitivity by Method

Sim19: Fast TR. Finally, sim19 is comparable to sim13, with the exception that the TR is set to 0.25 instead of $TR = 3.0$ used in other conditions. Here, the number of minutes for the scan session is held constant at 10 minutes; therefore, the number of time points increases twelve-fold in this simulation study. Unfortunately, all methods perform poorly in this condition. Neither of the regularized uSEM-based methods are able to

estimate very successfully; specifically, the adaptive LASSO is able to recover only 23% of directed relationships. However, the performance of the stepwise uSEM is considerably worse. That is, neither stepwise uSEM approach (two-of-four fit or three-of-five fit including BIC) are able to detect relationships other than the diagonal of the Φ matrix containing the autoregressive components. Specifically, the path sensitivity is nearly 0 (see Figure 27), indicating that no other effects were recovered. The graphical VAR demonstrates the opposite effect, where the final model is very dense, such that sensitivity is high and specificity is low. Neither outcome is desirable.

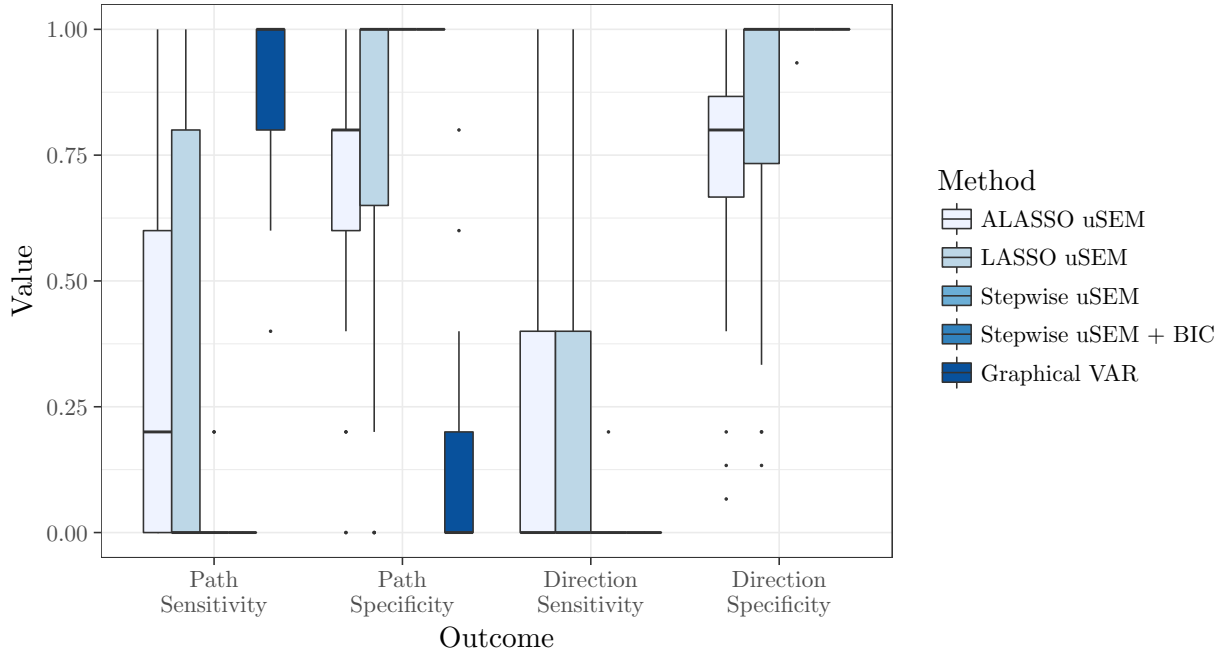

Figure 27: Sim 19: Specificity and Sensitivity by Method

Sim20: Fast TR, No HRF Lag Variability. Overall, the reduction of HRF lag variability in sim20, compared to sim19, yielded little improvement in the results. For both variations of the stepwise uSEM, largely autoregressive only effects were returned, indicating that an "excellent" model fit was achieved by freeing only the diagonal of the Φ

matrix for estimation; no additional cross-lagged or contemporaneous relationships were added. Similarly, the performance of the regularized uSEMs were again mixed for this fast TR condition, where the overall sensitivity improved but the specificity decreased (see Figure 28).

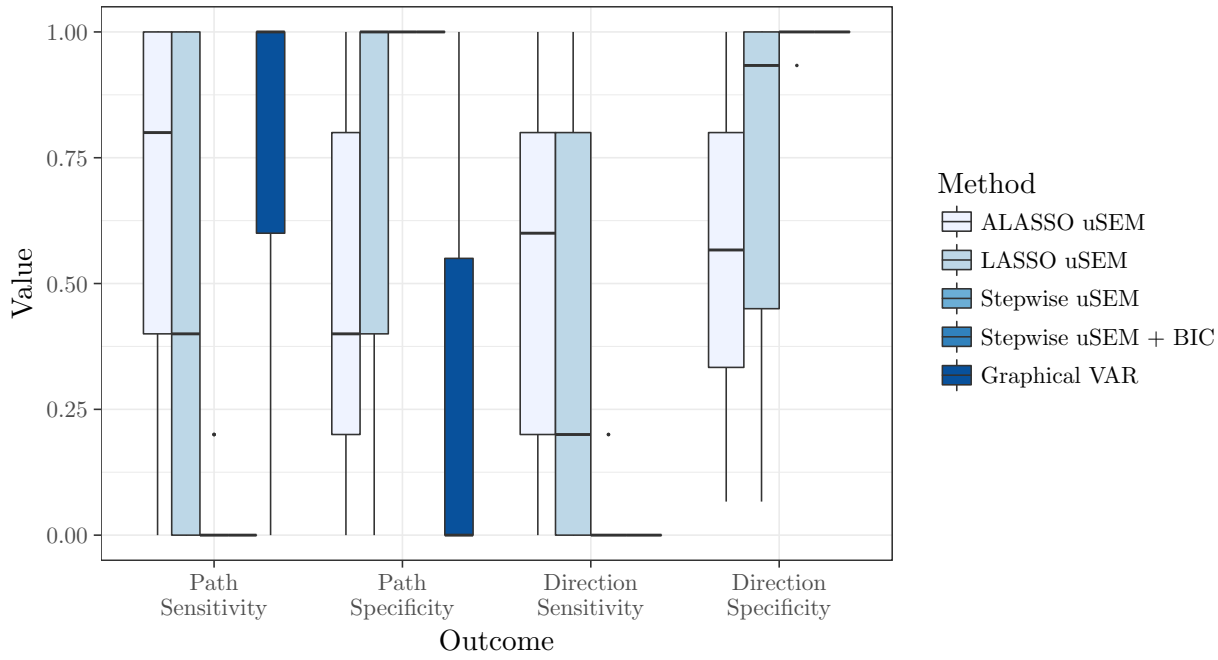

Figure 28: Sim 20: Specificity and Sensitivity by Method

Summary of Smith simulation results. Across these results, the recovery of network structure in sim5 is most encouraging. It should be noted that in the original Smith et al. (2011) paper, only three of 38 methods tested exceeded 70% direction recovery even when the length of scan session was increased to 4 hours (240 minutes). Here, adequate direction recovery (above 80%) was achieved using the adaptive LASSO when the session duration was increased to 60 minutes.

Across all methods, the recovery was uniformly poor in the fast TR condition with increased neural lag, with the stepwise uSEM recovering almost none of the data-

generating relationships other than the autoregressive effects. Though important to consider from a methodological perspective, it is useful to note that a TR as fast as $0.25s$ is not frequently used in practice. Few methods performed well in sim13, where backwards connections were introduced, though it is worth noting that the introduction of these backwards connections yielded an overall denser network. Given 1) the use of fixed cutoffs in the stepwise uSEM and 2) the assumption of a sparse network when using regularization methods, it is unsurprising that these results were not favorable. These results align with those found by Smith et al. (2011), who reported that even the best methods yielded heavily reduced sensitivity in the presence of these backwards connections.

Overall, the results of Study 2 highlight the promise of the regularized uSEM with adaptive LASSO for estimating directed functional connectivity, provided there are a sufficient number of time points. The results of Study 2 also underscore the difficulty involved for any estimation technique to recover the underlying neural network structure using the BOLD time series, and further motivate careful application of these methods.

CHAPTER 4: CONCLUSION

The intensive longitudinal data collected from a single individual offers promising insight into understanding dynamic within-person processes over time. These within person processes may characterize over time relationships between pre-defined regions of interest within networks of the brain, or these processes may pertain the over-time relationship of indicators of psychopathology (Fried et al., 2016). With the increasing presence of neuroscience within psychological research, as well as in the increased gathering of intensive longitudinal data via experience sampling, there will likely only continue to be increased interest in identifying network-like models to characterize individual-level processes. This work comes at a time when network-like characterizations of psychological outcomes have gained increasing traction in the field (Borsboom & Cramer, 2013).

Though various methods have been proposed for the data-driven identification of network-like models characterizing temporal and contemporaneous processes over time, there exists little work comparing the relative performance of these methods. Further, there exists less work evaluating the performance of these methods with data generated to specifically mimic BOLD time series data from an fMRI resting-state block. The present study sought to introduce a novel procedure, the regularized unified SEM, which bridges the strengths of the graphical VAR and the stepwise unified SEM.

In Chapter 2, the regularized uSEM was developed and investigated in the context

of a simulation study, where its finite sampling behavior was evaluated and compared to the performance of alternative methods. The regularized uSEM was shown to perform particularly well when making use of the adaptive LASSO penalty, yielding individual-level models with both exceptional sensitivity and specificity. That is, more than any other model in Study 1A, the regularized uSEM resulted in individual-level models with exceptional ability to retain true edges and remove false edges.

Also within Chapter 2, in Study 1B, it was shown that the misspecified directionality of the contemporaneous structure did not harm 1) the recovery of the directed lagged relationships or 2) the overall recovery of data-generating edges, without respect to direction. Therefore, there is not evidence that a crucial decrement in recovery of overall network structure would be observed if a researcher were to mistakenly mismodel the directionality of a sparse contemporaneous structure.

In Chapter 3, the ability of these methods to recover the underlying structure of simulated BOLD time series was evaluated. In Study 2, the relative performance of each method was considered with reference to eight simulations selected from the Smith data (Smith et al., 2011), which are considered benchmark data for evaluating the performance of methods for directed functional connectivity analysis. Given the disagreement in the literature regarding the use of methods rooted in Granger Causality for the identification of directed functional connectivity (see e.g., Smith et al., 2011; Seth et al., 2013, Friston et al., 2013), a controlled evaluation of these methods via Monte Carlo simulation was necessary. It was hoped that these methods would be particularly well-suited for this purpose, as previous work has discussed the promise of Bayes Net methods (e.g., Mumford & Ramsey, 2014).

All methods, by including either directed or nondirected contemporaneous relationships, exceeded the performance of lagged-based methods in Smith et al. (2011), where only 10% of true edges were recovered (Mumford & Ramsey, 2014). This finding underscores the importance of including not only lagged effects in the model, but also contemporaneous effects, as many of the effects surface contemporaneously. Across all methods within Study 2, the path sensitivity decreased compared to conditions observed within Study 1, though the path specificity remained adequate in many cases. That is, there was a general trend to not retain enough true edges, though the edges retained in the final model tended to be true edges, not spurious edges.

Across all methods, the ability to recover true edges and reject false edges was quite variable depending on the characteristics governing each unique simulation. Specifically, in sim13, where backwards connections are introduced, the path sensitivity of all methods suffered, and all methods uniformly suffered in sim19 and sim20, where the temporal resolution was reduced to $T = 0.25s$ in both the presence and absence of HRF lag variability. Most promise was shown in sim5, where the length of the time series was increased to reflect a 60 minute scan session, or $T = 1200$. Here, the regularized uSEM with adaptive LASSO performed as well as the best methods from Smith et al. (2011). Overall, the stepwise unified SEM and the regularized unified SEM exhibited the most promise for evaluating these data, though the ability to recover directed relationships suffered in comparison to the results of Study 1A.

Limitations

Given considerations of computational time, one limitation of the present study is the modest number of replications per cell ($R = 500$). This may have been circumvented

by removing the simulation factor with the largest number of variables ($V = 15$), or by removing the specific cell with exponentially longer computational time ($V = 15, T = 50$), which would have yielded a partially crossed simulation design. Neither decision was made, as a 15 variable condition is within the realm of possibility for both experience sampling researchers and neuroimaging researchers aiming to arrive at a network-like model of directed connectivity.

An additional limitation in the present study is that only one strategy for estimating regularized uSEMs was investigated. That is, only the BIC was considered for selection of the final model. Other research has made use of the RMSEA as one potential alternative (e.g., Jacobucci et al., 2016). Alternatively, and perhaps more commonly, the use of k-fold cross-validation has been suggested in order to select the optimal λ controlling the level of sparsity or penalization (e.g., Epskamp et al., 2015). In this process, the data would be subdivided into k blocks, where data are iteratively partitioned into training data sets (e.g., $k-1$ folds) and tests data sets (e.g., the k^{th} fold), and the λ that minimizes the cross-validation error when predicting the k^{th} fold using the model selected using data from $k-1$ folds is chosen. This approach was not used for two reasons. First, k-fold cross validation typically occurs with $k = 5$ or $k = 10$ folds, and the lower bounds of "sample size" (number of time points) manipulation in this study (e.g., $T = 50, T = 100$) would yield quite small test data sets, some of which would have more variables than time points. Thus, the BIC was used for model selection here, also to retain comparability to methods such as the graphical VAR.

An additional limitation regarding Study 2 is the use of the Smith simulation data. Though these data are considered the current "gold-standard" for evaluating methods

designed for functional connectivity analysis, the simulations are not fully crossed. Of course, this feature was intentional on the part of the researchers, as some cells that would emerge in a fully crossed design would be highly unlikely to emerge in practice, whether due to an odd crossing of scan characteristics or a nonsensical network structure. However, the lack of a fully crossed design does limit the ability to thoroughly investigate potential interactive effects.

Future Directions

As previously mentioned, prior work has found that incorporating some group- or sample-level information may improve the performance of specification searches. In the stepwise unified SEM, this has taken the form of conducting parallel specification searches and adding relationships which exist for a pre-specified majority of individuals. When considering how to incorporate group-level information into individual-level searches using regularization procedures, multiple options are possible. One option, proposed by Varoquaux & Craddock (2013), is to conduct a pooled time series analysis, concatenating time series data from all individuals into a single multivariate time series, in order to select a group-level model using the LASSO tuning parameter. Another option may be to incorporate a penalty which operates separately at the group- and individual-levels.

Additionally, more work is warranted regarding additional penalties for use with regularized uSEM. Here, most success was found using the adaptive LASSO. As the focus of this dissertation was to not only introduce the regularized uSEM, but to also evaluate its performance against competing methods, exhaustive work investigating additional penalties was not within the scope of the present study. However, many

other options exist, including the SCAD penalty, MCP penalty, and the elastic net penalty. The elastic net, which combines properties of the LASSO and ridge penalties, may be of particular interest given its known benefits for data containing correlated predictors.

Importantly, the data-driven identification of individual-level models is a first step. This process ultimate attempts to automate the model building and model selection, but still requires human judgment. In a large-scale simulation study such as this one, not every model can be manually adjusted to remove connections which do not make sense with respect to psychological theory. With any automated procedure, care must be taken to consider competing models. In the context of the stepwise uSEM, this may take the form of evaluating potential "multiple solutions" (e.g., Beltz & Molenaar, 2016), where multiple alternative models are considered when they yield functionally interchangeable solutions in terms of model fit. Similarly, in the regularized uSEM, it may be useful to consider multiple models that are within a certain range of the optimal BIC. Finally, the present study evaluated models across a standard range of λ values, but a researcher may be interested in increasing the granularity of these values. For methods such as the regularized uSEM in particular, this may have yielded fewer false positive relationships, as examining the absolute bias of these false positives revealed quite small parameter estimates which may have been set to zero with a more granular range of tuning parameters.

One final avenue for future work regards the incorporation of multiple-indicator latent factors into the framework of the regularized unified SEM. This development would allow for both the regularization of the measurement models representing the

relationship between observed variables over time and their underlying latent construct, as well as regularization of the latent variable model relating the constructs over time. The introduction of multiple-indicator latent factors would offer a unique benefit over competing network-like models, which all operate at the level of the observed variable. Careful consideration regarding the simultaneous regularization of these matrices would be necessary.

Ultimately, this research presents the timely introduction of the regularized uSEM for establishing individual-level models of directed temporal and contemporaneous effects. For time series data broadly defined, the regularized uSEM outperformed all competing methods with respect to the recovery and precision of true relationships, whether directed or nondirected. More work is warranted regarding strategies to improve the recovery of directed relationships in the context of fMRI data.

APPENDIX A: TABLES

Num. Var	Sparsity	Time	Path Sen.	Path Spec.	Rel. Bias True Pos.	Abs. Bias False Pos.	RMSE
5	0.15	50	0.60	0.83	-0.46	0.10	0.22
5	0.15	100	0.82	0.89	-0.56	0.07	0.25
5	0.15	200	0.98	0.91	-0.65	0.05	0.28
5	0.15	500	1.00	0.93	-0.69	0.03	0.31
5	0.20	50	0.66	0.78	-0.63	0.10	0.27
5	0.20	100	0.89	0.76	-0.78	0.07	0.31
5	0.20	200	0.99	0.76	-0.86	0.05	0.34
5	0.20	500	1.00	0.79	-0.91	0.03	0.36
5	0.25	50	0.66	0.79	-0.66	0.09	0.28
5	0.25	100	0.88	0.77	-0.78	0.06	0.31
5	0.25	200	0.99	0.78	-0.87	0.05	0.34
5	0.25	500	1.00	0.81	-0.90	0.03	0.36
10	0.15	50	0.61	0.82	-0.73	0.08	0.30
10	0.15	100	0.87	0.81	-0.87	0.05	0.33
10	0.15	200	0.98	0.80	-0.95	0.04	0.35
10	0.15	500	1.00	0.82	-0.99	0.02	0.38
10	0.20	50	0.68	0.73	-0.82	0.08	0.32
10	0.20	100	0.91	0.66	-0.93	0.05	0.35
10	0.20	200	0.99	0.64	-0.99	0.04	0.37
10	0.20	500	1.00	0.67	-1.03	0.03	0.38
10	0.25	50	0.81	0.53	-0.93	0.08	0.35
10	0.25	100	0.94	0.46	-1.00	0.06	0.37
10	0.25	200	0.99	0.43	-1.05	0.04	0.38
10	0.25	500	1.00	0.47	-1.08	0.03	0.39
15	0.15	50	0.71	0.69	-0.88	0.07	0.34
15	0.15	100	0.91	0.63	-0.98	0.05	0.36
15	0.15	200	0.98	0.59	-1.03	0.04	0.37
15	0.15	500	1.00	0.61	-1.08	0.03	0.39
15	0.20	50	0.84	0.46	-0.96	0.08	0.35
15	0.20	100	0.94	0.40	-1.02	0.05	0.36
15	0.20	200	0.97	0.38	-1.06	0.04	0.38
15	0.20	500	0.99	0.37	-1.12	0.03	0.39
15	0.25	50	0.88	0.32	-0.98	0.08	0.36
15	0.25	100	0.94	0.29	-1.02	0.06	0.36
15	0.25	200	0.97	0.24	-1.07	0.04	0.38
15	0.25	500	0.99	0.19	-1.15	0.03	0.39

Table 5: Study 1A: Graphical VAR Results, Part I

Mean	Path Sen.	Path Spec.	Rel. Bias True Pos.	Abs. Bias False Pos.	RMSE
T = 50	0.72	0.66	-0.78	0.08	0.31
T = 100	0.90	0.63	-0.88	0.06	0.33
T = 200	0.98	0.61	-0.95	0.04	0.35
T = 500	1.00	0.63	-0.99	0.03	0.37
S = 0.15	0.87	0.78	-0.82	0.05	0.32
S = 0.20	0.90	0.62	-0.93	0.05	0.35
S = 0.25	0.92	0.51	-0.96	0.05	0.36
V = 5	0.87	0.82	-0.73	0.06	0.30
V = 10	0.90	0.65	-0.95	0.05	0.36
V = 15	0.93	0.43	-1.03	0.05	0.37

Table 6: Study 1A: Marginal Means, Graphical VAR Results, Part I

Num. Var	Sparsity	Time	Lag Path Sen.	Lag Path Spec.	Con. Path Sen.	Con. Path Spec.	Lag Dir. Sen.	Lag Dir. Spec.
5	0.15	50	0.54	0.88	0.49	0.95	0.51	0.93
5	0.15	100	0.76	0.93	0.81	0.97	0.74	0.96
5	0.15	200	0.96	0.93	0.99	0.97	0.96	0.97
5	0.15	500	1.00	0.95	1.00	0.98	1.00	0.98
5	0.20	50	0.59	0.84	0.55	0.93	0.55	0.91
5	0.20	100	0.82	0.84	0.86	0.93	0.81	0.91
5	0.20	200	0.98	0.85	0.98	0.92	0.98	0.92
5	0.20	500	1.00	0.88	1.00	0.92	1.00	0.94
5	0.25	50	0.56	0.85	0.57	0.93	0.52	0.92
5	0.25	100	0.81	0.84	0.86	0.93	0.80	0.92
5	0.25	200	0.99	0.85	0.99	0.92	0.99	0.92
5	0.25	500	1.00	0.88	1.00	0.94	1.00	0.94
10	0.15	50	0.53	0.88	0.53	0.95	0.50	0.94
10	0.15	100	0.82	0.88	0.83	0.94	0.82	0.94
10	0.15	200	0.98	0.87	0.98	0.92	0.98	0.94
10	0.15	500	1.00	0.90	1.00	0.92	1.00	0.95
10	0.20	50	0.59	0.83	0.58	0.90	0.55	0.91
10	0.20	100	0.89	0.78	0.84	0.87	0.88	0.88
10	0.20	200	0.99	0.77	0.97	0.85	0.99	0.87
10	0.20	500	1.00	0.81	1.00	0.84	1.00	0.90
10	0.25	50	0.73	0.69	0.64	0.80	0.69	0.83
10	0.25	100	0.93	0.64	0.84	0.76	0.92	0.79
10	0.25	200	1.00	0.60	0.95	0.74	1.00	0.77
10	0.25	500	1.00	0.65	0.99	0.74	1.00	0.80
15	0.15	50	0.62	0.81	0.59	0.87	0.59	0.90
15	0.15	100	0.91	0.77	0.82	0.84	0.90	0.88
15	0.15	200	0.99	0.75	0.94	0.81	0.99	0.86
15	0.15	500	1.00	0.77	0.99	0.81	1.00	0.88
15	0.20	50	0.79	0.64	0.62	0.76	0.75	0.79
15	0.20	100	0.96	0.58	0.77	0.73	0.94	0.75
15	0.20	200	1.00	0.55	0.89	0.72	1.00	0.73
15	0.20	500	1.00	0.52	0.97	0.73	1.00	0.71
15	0.25	50	0.87	0.48	0.60	0.73	0.83	0.68
15	0.25	100	0.98	0.44	0.72	0.70	0.97	0.65
15	0.25	200	1.00	0.36	0.84	0.69	1.00	0.59
15	0.25	500	1.00	0.30	0.95	0.67	1.00	0.52

Table 7: Study 1A: Graphical VAR Results, Part II

Mean	Lag Path Sen.	Lag Path Spec.	Con. Path Sen.	Con. Path Spec.	Lag Dir. Sen.	Lag Dir. Spec.
T = 50	0.65	0.77	0.57	0.87	0.61	0.87
T = 100	0.88	0.74	0.82	0.85	0.86	0.85
T = 200	0.99	0.73	0.95	0.84	0.99	0.84
T = 500	1.00	0.74	0.99	0.84	1.00	0.85
S = 0.15	0.84	0.86	0.83	0.91	0.83	0.93
S = 0.20	0.88	0.74	0.84	0.84	0.87	0.85
S = 0.25	0.91	0.63	0.83	0.80	0.89	0.78
V = 5	0.83	0.88	0.84	0.94	0.82	0.94
V = 10	0.87	0.78	0.85	0.85	0.86	0.88
V = 15	0.93	0.58	0.81	0.76	0.91	0.74

Table 8: Study 1A: Marginal Means, Graphical VAR Results, Part II

Num. Var	Spar-sity	Time	Path Sen.	Path Spec.	Dir. Sen.	Dir. Spec.	Rel. Bias True Pos.	Abs. Bias False Pos.	RMSE
5	0.15	50	0.58	0.86	0.45	0.91	-0.00	0.35	0.15
5	0.15	100	0.76	0.93	0.64	0.95	0.01	0.25	0.09
5	0.15	200	0.87	0.98	0.76	0.97	0.00	0.21	0.07
5	0.15	500	0.91	1.00	0.82	0.99	-0.00		0.05
5	0.20	50	0.65	0.81	0.49	0.86	0.09	0.36	0.19
5	0.20	100	0.79	0.89	0.64	0.89	0.05	0.28	0.12
5	0.20	200	0.89	0.97	0.75	0.93	0.03	0.25	0.09
5	0.20	500	0.92	1.00	0.78	0.94	0.00	0.28	0.07
5	0.25	50	0.63	0.82	0.47	0.87	0.06	0.37	0.17
5	0.25	100	0.80	0.90	0.64	0.89	0.05	0.27	0.12
5	0.25	200	0.88	0.97	0.74	0.93	0.02	0.22	0.09
5	0.25	500	0.92	1.00	0.79	0.94	0.01	0.43	0.07
10	0.15	50	0.60	0.82	0.46	0.88	0.08	0.35	0.18
10	0.15	100	0.72	0.93	0.60	0.94	0.06	0.27	0.11
10	0.15	200	0.82	0.99	0.71	0.97	0.02	0.24	0.08
10	0.15	500	0.85	1.00	0.75	0.98	0.01	0.27	0.06
10	0.20	50	0.62	0.80	0.47	0.87	0.14	0.35	0.20
10	0.20	100	0.74	0.90	0.60	0.91	0.06	0.27	0.12
10	0.20	200	0.82	0.97	0.69	0.95	0.02	0.26	0.10
10	0.20	500	0.87	0.99	0.75	0.96	0.00	0.28	0.08
10	0.25	50	0.63	0.75	0.46	0.83	0.17	0.37	0.24
10	0.25	100	0.74	0.86	0.58	0.88	0.11	0.28	0.16
10	0.25	200	0.79	0.94	0.65	0.91	0.06	0.26	0.12
10	0.25	500	0.84	0.98	0.71	0.93	0.03	0.24	0.10
15	0.15	50	0.67	0.72	0.51	0.83	0.11	0.33	0.22
15	0.15	100	0.73	0.90	0.60	0.93	0.06	0.26	0.12
15	0.15	200	0.81	0.98	0.70	0.96	0.02	0.24	0.09
15	0.15	500	0.85	1.00	0.75	0.98	-0.00	0.24	0.07
15	0.20	50	0.67	0.69	0.50	0.80	0.13	0.34	0.25
15	0.20	100	0.71	0.87	0.57	0.90	0.09	0.27	0.15
15	0.20	200	0.77	0.94	0.65	0.93	0.05	0.26	0.13
15	0.20	500	0.83	0.98	0.71	0.95	0.02	0.22	0.10
15	0.25	50	0.65	0.68	0.47	0.79	0.18	0.35	0.29
15	0.25	100	0.67	0.82	0.51	0.86	0.12	0.30	0.23
15	0.25	200	0.74	0.89	0.59	0.89	0.08	0.26	0.15
15	0.25	500	0.79	0.92	0.64	0.90	0.05	0.25	0.15

Table 9: Study 1A: Stepwise uSEM Results, Part I

Mean	Path Sen.	Path Spec.	Dir. Sen.	Dir. Spec.	Rel. Bias True Pos.	Abs. Bias False Pos.	RMSE
T = 50	0.63	0.77	0.48	0.85	0.11	0.35	0.21
T = 100	0.74	0.89	0.60	0.91	0.07	0.27	0.14
T = 200	0.82	0.96	0.69	0.94	0.03	0.24	0.10
T = 500	0.86	0.99	0.74	0.95	0.01	0.28	0.08
S = 0.15	0.76	0.93	0.65	0.94	0.03	0.27	0.11
S = 0.20	0.77	0.90	0.63	0.91	0.06	0.28	0.13
S = 0.25	0.76	0.88	0.60	0.88	0.08	0.30	0.16
V = 5	0.80	0.93	0.66	0.92	0.03	0.30	0.11
V = 10	0.75	0.91	0.62	0.92	0.06	0.29	0.13
V = 15	0.74	0.87	0.60	0.89	0.08	0.28	0.16

Table 10: Study 1A: Marginal Means, Stepwise uSEM Results, Part I

Num. Var	Spar-sity	Time	Con. Path Sen.	Con. Path Spec.	Lag Path Sen.	Lag Path Spec.	Con. Dir. Sen.	Con. Dir. Spec.	Lag Dir. Sen.	Lag Dir. Spec.
5	0.15	50	0.49	0.93	0.50	0.92	0.32	0.95	0.46	0.96
5	0.15	100	0.75	0.97	0.66	0.96	0.55	0.96	0.64	0.98
5	0.15	200	0.85	0.99	0.77	0.99	0.65	0.97	0.77	0.99
5	0.15	500	0.90	1.00	0.82	1.00	0.75	0.98	0.82	1.00
5	0.20	50	0.54	0.92	0.51	0.89	0.35	0.91	0.45	0.94
5	0.20	100	0.73	0.95	0.66	0.94	0.48	0.91	0.63	0.97
5	0.20	200	0.86	0.99	0.75	0.99	0.59	0.92	0.74	0.99
5	0.20	500	0.91	1.00	0.77	1.00	0.63	0.92	0.76	1.00
5	0.25	50	0.52	0.92	0.51	0.90	0.31	0.91	0.46	0.94
5	0.25	100	0.74	0.95	0.66	0.94	0.48	0.91	0.64	0.97
5	0.25	200	0.85	0.99	0.76	0.99	0.59	0.92	0.74	0.99
5	0.25	500	0.90	1.00	0.79	1.00	0.64	0.93	0.77	1.00
10	0.15	50	0.53	0.91	0.49	0.89	0.33	0.93	0.45	0.94
10	0.15	100	0.69	0.97	0.62	0.96	0.49	0.96	0.61	0.98
10	0.15	200	0.80	0.99	0.75	0.99	0.59	0.97	0.74	1.00
10	0.15	500	0.83	1.00	0.76	1.00	0.66	0.98	0.76	1.00
10	0.20	50	0.53	0.90	0.50	0.88	0.33	0.92	0.45	0.94
10	0.20	100	0.69	0.95	0.64	0.94	0.46	0.93	0.61	0.97
10	0.20	200	0.80	0.98	0.72	0.98	0.57	0.95	0.70	0.99
10	0.20	500	0.86	1.00	0.78	1.00	0.63	0.95	0.76	1.00
10	0.25	50	0.53	0.88	0.49	0.86	0.32	0.89	0.43	0.92
10	0.25	100	0.67	0.93	0.61	0.92	0.43	0.90	0.56	0.96
10	0.25	200	0.75	0.96	0.67	0.97	0.51	0.92	0.65	0.98
10	0.25	500	0.82	0.99	0.73	0.99	0.57	0.92	0.71	0.99
15	0.15	50	0.58	0.86	0.55	0.83	0.37	0.90	0.50	0.91
15	0.15	100	0.69	0.95	0.64	0.95	0.48	0.95	0.62	0.97
15	0.15	200	0.79	0.99	0.73	0.99	0.60	0.97	0.72	0.99
15	0.15	500	0.84	1.00	0.77	1.00	0.66	0.97	0.76	1.00
15	0.20	50	0.57	0.84	0.53	0.81	0.35	0.88	0.47	0.90
15	0.20	100	0.65	0.93	0.60	0.93	0.44	0.92	0.57	0.96
15	0.20	200	0.75	0.97	0.68	0.97	0.53	0.94	0.65	0.98
15	0.20	500	0.81	0.99	0.74	0.99	0.61	0.95	0.72	0.99
15	0.25	50	0.54	0.83	0.49	0.81	0.33	0.87	0.42	0.90
15	0.25	100	0.61	0.91	0.54	0.90	0.39	0.90	0.49	0.95
15	0.25	200	0.69	0.94	0.61	0.94	0.46	0.91	0.57	0.97
15	0.25	500	0.76	0.95	0.67	0.96	0.52	0.91	0.64	0.98

Table 11: Study 1A: Stepwise uSEM Results, Part II

Mean	Con. Path Sen.	Con. Path Spec.	Lag Path Sen.	Lag Path Spec.	Con. Dir. Sen.	Con. Dir. Spec.	Lag Dir. Sen.	Lag Dir. Spec.
T = 50	0.54	0.89	0.51	0.87	0.33	0.91	0.45	0.93
T = 100	0.69	0.95	0.63	0.94	0.47	0.93	0.60	0.97
T = 200	0.79	0.98	0.72	0.98	0.57	0.94	0.70	0.99
T = 500	0.85	0.99	0.76	0.99	0.63	0.95	0.74	1.00
S = 0.15	0.73	0.96	0.67	0.96	0.54	0.96	0.65	0.98
S = 0.20	0.72	0.95	0.66	0.94	0.50	0.92	0.63	0.97
S = 0.25	0.70	0.94	0.63	0.93	0.46	0.91	0.59	0.96
V = 5	0.75	0.97	0.68	0.96	0.53	0.93	0.66	0.98
V = 10	0.71	0.95	0.65	0.95	0.49	0.94	0.62	0.97
V = 15	0.69	0.93	0.63	0.92	0.48	0.92	0.59	0.96

Table 12: Study 1A: Marginal Means, Stepwise uSEM Results, Part II

Num. Var	Spar-sity	Time	Path Sen.	Path Spec.	Dir. Sen.	Dir. Spec.	Rel. Bias True Pos.	Abs. Bias False Pos.	RMSE
5	0.15	50	0.58	0.86	0.45	0.91	0.00	0.35	0.15
5	0.15	100	0.76	0.93	0.64	0.95	0.01	0.25	0.10
5	0.15	200	0.87	0.98	0.76	0.97	0.00	0.21	0.07
5	0.15	500	0.91	1.00	0.83	0.99	-0.00		0.05
5	0.20	50	0.65	0.81	0.49	0.86	0.09	0.37	0.19
5	0.20	100	0.79	0.90	0.64	0.90	0.05	0.28	0.12
5	0.20	200	0.88	0.97	0.74	0.93	0.03	0.26	0.09
5	0.20	500	0.92	1.00	0.78	0.94	0.00	0.28	0.07
5	0.25	50	0.63	0.83	0.47	0.87	0.06	0.37	0.17
5	0.25	100	0.80	0.89	0.64	0.89	0.05	0.27	0.12
5	0.25	200	0.88	0.97	0.74	0.93	0.03	0.25	0.09
5	0.25	500	0.92	1.00	0.79	0.95	0.01	0.42	0.07
10	0.15	50	0.60	0.82	0.45	0.88	0.09	0.35	0.18
10	0.15	100	0.72	0.93	0.60	0.94	0.06	0.27	0.12
10	0.15	200	0.82	0.99	0.71	0.97	0.02	0.24	0.08
10	0.15	500	0.84	1.00	0.75	0.98	0.01	0.28	0.06
10	0.20	50	0.62	0.80	0.47	0.87	0.14	0.35	0.20
10	0.20	100	0.74	0.90	0.59	0.91	0.07	0.28	0.12
10	0.20	200	0.82	0.97	0.69	0.95	0.03	0.27	0.10
10	0.20	500	0.87	0.99	0.75	0.96	0.01	0.31	0.08
10	0.25	50	0.63	0.75	0.46	0.83	0.16	0.37	0.23
10	0.25	100	0.73	0.86	0.58	0.88	0.11	0.29	0.16
10	0.25	200	0.79	0.94	0.65	0.91	0.06	0.27	0.12
10	0.25	500	0.84	0.98	0.71	0.94	0.03	0.24	0.10
15	0.15	50	0.67	0.72	0.51	0.83	0.09	0.35	0.25
15	0.15	100	0.72	0.91	0.60	0.93	0.07	0.27	0.12
15	0.15	200	0.81	0.98	0.71	0.97	0.02	0.26	0.11
15	0.15	500	0.84	1.00	0.75	0.98	0.00	0.25	0.07
15	0.20	50	0.67	0.69	0.50	0.81	0.14	0.33	0.24
15	0.20	100	0.71	0.87	0.57	0.90	0.10	0.27	0.15
15	0.20	200	0.77	0.95	0.65	0.94	0.05	0.26	0.13
15	0.20	500	0.83	0.98	0.72	0.96	0.02	0.23	0.10
15	0.25	50	0.65	0.69	0.47	0.79	0.17	0.35	0.29
15	0.25	100	0.67	0.83	0.51	0.87	0.14	0.29	0.19
15	0.25	200	0.73	0.90	0.59	0.90	0.08	0.26	0.15
15	0.25	500	0.78	0.93	0.64	0.91	0.05	0.26	0.15

Table 13: Study 1A: Stepwise uSEM + BIC Results, Part I

Mean	Path Sen.	Path Spec.	Dir. Sen.	Dir. Spec.	Rel. Bias True Pos.	Abs. Bias False Pos.	RMSE
T = 50	0.63	0.77	0.47	0.85	0.10	0.35	0.21
T = 100	0.74	0.89	0.60	0.91	0.07	0.27	0.13
T = 200	0.82	0.96	0.69	0.94	0.04	0.25	0.10
T = 500	0.86	0.99	0.75	0.96	0.01	0.28	0.08
S = 0.15	0.76	0.93	0.65	0.94	0.03	0.28	0.11
S = 0.20	0.77	0.90	0.63	0.91	0.06	0.29	0.13
S = 0.25	0.75	0.88	0.60	0.89	0.08	0.30	0.15
V = 5	0.80	0.93	0.66	0.92	0.03	0.30	0.11
V = 10	0.75	0.91	0.62	0.92	0.07	0.29	0.13
V = 15	0.74	0.87	0.60	0.90	0.08	0.28	0.16

Table 14: Study 1A: Marginal Means, Stepwise uSEM + BIC Results, Part I

Num. Var	Sparsity	Time	Con. Path Sen.	Con. Path Spec.	Lag Path Sen.	Lag Path Spec.	Con. Dir. Sen.	Con. Dir. Spec.	Lag Dir. Sen.	Lag Dir. Spec.
5	0.15	50	0.49	0.93	0.50	0.92	0.32	0.95	0.46	0.96
5	0.15	100	0.75	0.97	0.65	0.96	0.54	0.96	0.64	0.98
5	0.15	200	0.85	0.99	0.77	0.99	0.65	0.97	0.76	0.99
5	0.15	500	0.89	1.00	0.82	1.00	0.75	0.98	0.82	1.00
5	0.20	50	0.54	0.92	0.51	0.89	0.35	0.91	0.45	0.94
5	0.20	100	0.73	0.95	0.66	0.94	0.48	0.91	0.62	0.97
5	0.20	200	0.85	0.99	0.75	0.99	0.59	0.93	0.73	0.99
5	0.20	500	0.91	1.00	0.77	1.00	0.64	0.93	0.76	1.00
5	0.25	50	0.52	0.92	0.51	0.90	0.31	0.91	0.45	0.95
5	0.25	100	0.74	0.95	0.66	0.94	0.48	0.91	0.63	0.97
5	0.25	200	0.85	0.99	0.76	0.98	0.59	0.93	0.74	0.99
5	0.25	500	0.90	1.00	0.78	1.00	0.65	0.93	0.77	1.00
10	0.15	50	0.53	0.92	0.49	0.89	0.33	0.93	0.45	0.94
10	0.15	100	0.69	0.97	0.62	0.96	0.49	0.96	0.60	0.98
10	0.15	200	0.80	0.99	0.75	0.99	0.60	0.97	0.74	1.00
10	0.15	500	0.83	1.00	0.76	1.00	0.67	0.98	0.75	1.00
10	0.20	50	0.53	0.90	0.50	0.88	0.33	0.92	0.45	0.94
10	0.20	100	0.69	0.95	0.63	0.94	0.46	0.93	0.60	0.97
10	0.20	200	0.79	0.99	0.71	0.98	0.57	0.95	0.70	0.99
10	0.20	500	0.85	1.00	0.77	1.00	0.64	0.96	0.76	1.00
10	0.25	50	0.53	0.88	0.49	0.86	0.32	0.89	0.43	0.93
10	0.25	100	0.66	0.93	0.61	0.93	0.43	0.90	0.57	0.96
10	0.25	200	0.75	0.97	0.67	0.97	0.51	0.92	0.65	0.98
10	0.25	500	0.82	0.99	0.73	0.99	0.58	0.93	0.71	0.99
15	0.15	50	0.58	0.86	0.55	0.83	0.38	0.90	0.50	0.91
15	0.15	100	0.69	0.95	0.64	0.95	0.48	0.95	0.62	0.97
15	0.15	200	0.79	0.99	0.73	0.99	0.61	0.97	0.72	0.99
15	0.15	500	0.83	1.00	0.77	1.00	0.67	0.98	0.76	1.00
15	0.20	50	0.57	0.84	0.53	0.81	0.35	0.89	0.47	0.90
15	0.20	100	0.65	0.93	0.60	0.93	0.44	0.93	0.57	0.96
15	0.20	200	0.74	0.97	0.68	0.97	0.54	0.95	0.65	0.99
15	0.20	500	0.81	0.99	0.74	0.99	0.62	0.96	0.73	0.99
15	0.25	50	0.54	0.83	0.49	0.82	0.33	0.87	0.41	0.90
15	0.25	100	0.61	0.91	0.53	0.91	0.39	0.90	0.49	0.95
15	0.25	200	0.69	0.94	0.61	0.95	0.46	0.92	0.58	0.97
15	0.25	500	0.75	0.96	0.67	0.97	0.53	0.92	0.64	0.98

Table 15: Study 1A: Stepwise uSEM + BIC Results, Part II

Mean	Con. Path Sen.	Con. Path Spec.	Lag Path Sen.	Lag Path Spec.	Con. Dir. Sen.	Con. Dir. Spec.	Lag Dir. Sen.	Lag Dir. Spec.
T = 50	0.54	0.89	0.51	0.87	0.33	0.91	0.45	0.93
T = 100	0.69	0.95	0.63	0.94	0.47	0.93	0.60	0.97
T = 200	0.79	0.98	0.72	0.98	0.57	0.94	0.70	0.99
T = 500	0.85	0.99	0.76	0.99	0.63	0.95	0.74	1.00
S = 0.15	0.73	0.96	0.67	0.96	0.54	0.96	0.65	0.98
S = 0.20	0.72	0.95	0.66	0.94	0.50	0.92	0.63	0.97
S = 0.25	0.70	0.94	0.63	0.93	0.46	0.91	0.59	0.96
V = 5	0.75	0.97	0.68	0.96	0.53	0.93	0.66	0.98
V = 10	0.71	0.95	0.65	0.95	0.49	0.94	0.62	0.97
V = 15	0.69	0.93	0.63	0.92	0.48	0.92	0.59	0.96

Table 16: Study 1A: Marginal Means, Stepwise uSEM + BIC Results, Part II

Num. Var	Spar-sity	Time	Path Sen.	Path Spec.	Dir. Sen.	Dir. Spec.	Rel. Bias True Pos.	Abs. Bias False Pos.	RMSE
5	0.15	50	0.79	0.63	0.63	0.77	-0.10	0.21	0.14
5	0.15	100	0.86	0.87	0.73	0.90	-0.07	0.17	0.09
5	0.15	200	0.97	0.95	0.88	0.95	-0.09	0.14	0.08
5	0.15	500	1.00	0.99	0.99	0.96	-0.10	0.10	0.07
5	0.20	50	0.82	0.62	0.63	0.73	-0.07	0.22	0.14
5	0.20	100	0.87	0.85	0.73	0.85	-0.07	0.18	0.10
5	0.20	200	0.95	0.95	0.87	0.90	-0.09	0.14	0.08
5	0.20	500	1.00	0.98	0.97	0.92	-0.13	0.10	0.08
5	0.25	50	0.80	0.63	0.63	0.73	-0.07	0.21	0.14
5	0.25	100	0.86	0.86	0.73	0.85	-0.07	0.18	0.10
5	0.25	200	0.96	0.94	0.86	0.90	-0.10	0.14	0.08
5	0.25	500	1.00	0.98	0.97	0.92	-0.12	0.10	0.07
10	0.15	50	0.59	0.73	0.42	0.83	-0.05	0.24	0.15
10	0.15	100	0.84	0.85	0.69	0.89	-0.06	0.18	0.10
10	0.15	200	0.96	0.94	0.87	0.94	-0.08	0.13	0.08
10	0.15	500	1.00	0.99	0.98	0.97	-0.08	0.09	0.06
10	0.20	50	0.62	0.69	0.44	0.80	-0.02	0.24	0.16
10	0.20	100	0.84	0.82	0.69	0.85	-0.06	0.18	0.10
10	0.20	200	0.96	0.92	0.87	0.91	-0.09	0.13	0.08
10	0.20	500	1.00	0.98	0.97	0.96	-0.09	0.09	0.06
10	0.25	50	0.67	0.62	0.48	0.74	-0.02	0.25	0.17
10	0.25	100	0.84	0.76	0.68	0.81	-0.05	0.19	0.11
10	0.25	200	0.94	0.88	0.84	0.87	-0.09	0.14	0.09
10	0.25	500	0.99	0.94	0.94	0.91	-0.11	0.11	0.08
15	0.15	50	0.55	0.72	0.39	0.83	-0.03	0.26	0.17
15	0.15	100	0.74	0.78	0.58	0.85	-0.04	0.19	0.12
15	0.15	200	0.96	0.91	0.87	0.92	-0.08	0.13	0.08
15	0.15	500	1.00	0.98	0.97	0.97	-0.07	0.09	0.05
15	0.20	50	0.60	0.66	0.42	0.78	-0.03	0.27	0.19
15	0.20	100	0.78	0.69	0.61	0.78	-0.05	0.20	0.13
15	0.20	200	0.94	0.86	0.84	0.88	-0.10	0.15	0.10
15	0.20	500	0.99	0.94	0.94	0.93	-0.09	0.11	0.08
15	0.25	50	0.64	0.60	0.43	0.73	-0.09	0.34	0.27
15	0.25	100	0.77	0.61	0.59	0.72	-0.10	0.26	0.20
15	0.25	200	0.91	0.79	0.78	0.81	-0.14	0.19	0.15
15	0.25	500	0.97	0.85	0.89	0.85	-0.13	0.14	0.11

Table 17: Study 1A: Adaptive LASSO uSEM Results, Part I

Mean	Path Sen.	Path Spec.	Dir. Sen.	Dir. Spec.	Rel. Bias True Pos.	Abs. Bias False Pos.	RMSE
T = 50	0.68	0.66	0.50	0.77	-0.05	0.25	0.17
T = 100	0.82	0.79	0.67	0.83	-0.06	0.19	0.12
T = 200	0.95	0.90	0.85	0.90	-0.10	0.14	0.09
T = 500	0.99	0.96	0.96	0.93	-0.10	0.10	0.07
S = 0.15	0.85	0.86	0.75	0.90	-0.07	0.16	0.10
S = 0.20	0.86	0.83	0.75	0.86	-0.07	0.17	0.11
S = 0.25	0.86	0.79	0.73	0.82	-0.09	0.19	0.13
V = 5	0.91	0.85	0.80	0.86	-0.09	0.16	0.10
V = 10	0.85	0.84	0.74	0.87	-0.07	0.16	0.10
V = 15	0.82	0.78	0.69	0.84	-0.08	0.19	0.14

Table 18: Study 1A: Marginal Means, Adaptive LASSO uSEM, Part I

Num. Var	Spar-sity	Time	Con. Path Sen.	Con. Path Spec.	Lag Path Sen.	Lag Path Spec.	Con. Dir. Sen.	Con. Dir. Spec.	Lag Dir. Sen.	Lag Dir. Spec.
5	0.15	50	0.68	0.86	0.74	0.73	0.38	0.90	0.69	0.85
5	0.15	100	0.81	0.96	0.84	0.90	0.53	0.95	0.84	0.95
5	0.15	200	0.95	0.99	0.95	0.96	0.75	0.96	0.95	0.98
5	0.15	500	1.00	1.00	1.00	0.99	0.96	0.97	1.00	0.99
5	0.20	50	0.67	0.86	0.75	0.71	0.36	0.86	0.69	0.84
5	0.20	100	0.79	0.95	0.83	0.88	0.51	0.90	0.80	0.94
5	0.20	200	0.93	0.98	0.93	0.95	0.70	0.91	0.93	0.97
5	0.20	500	0.99	1.00	0.99	0.98	0.90	0.92	0.99	0.99
5	0.25	50	0.64	0.86	0.73	0.72	0.34	0.86	0.67	0.84
5	0.25	100	0.78	0.95	0.82	0.88	0.49	0.90	0.80	0.94
5	0.25	200	0.93	0.98	0.94	0.95	0.69	0.92	0.93	0.97
5	0.25	500	1.00	1.00	1.00	0.97	0.90	0.92	1.00	0.99
10	0.15	50	0.53	0.86	0.45	0.83	0.28	0.90	0.40	0.91
10	0.15	100	0.78	0.94	0.80	0.90	0.49	0.93	0.78	0.95
10	0.15	200	0.94	0.98	0.96	0.95	0.74	0.95	0.95	0.97
10	0.15	500	1.00	1.00	1.00	0.99	0.94	0.98	1.00	0.99
10	0.20	50	0.55	0.84	0.47	0.81	0.28	0.88	0.40	0.90
10	0.20	100	0.76	0.93	0.80	0.87	0.47	0.91	0.77	0.93
10	0.20	200	0.93	0.97	0.95	0.93	0.71	0.94	0.94	0.96
10	0.20	500	0.99	0.99	1.00	0.98	0.91	0.97	1.00	0.99
10	0.25	50	0.56	0.80	0.52	0.76	0.30	0.85	0.44	0.87
10	0.25	100	0.75	0.90	0.79	0.83	0.44	0.87	0.75	0.91
10	0.25	200	0.90	0.96	0.93	0.91	0.64	0.90	0.92	0.95
10	0.25	500	0.98	0.98	0.99	0.94	0.84	0.93	0.99	0.97
15	0.15	50	0.49	0.85	0.39	0.84	0.26	0.90	0.34	0.91
15	0.15	100	0.69	0.89	0.64	0.86	0.40	0.90	0.60	0.93
15	0.15	200	0.93	0.96	0.96	0.93	0.73	0.95	0.95	0.97
15	0.15	500	0.99	0.99	1.00	0.98	0.93	0.98	1.00	0.99
15	0.20	50	0.51	0.81	0.43	0.80	0.27	0.87	0.36	0.89
15	0.20	100	0.70	0.83	0.67	0.80	0.41	0.86	0.62	0.89
15	0.20	200	0.90	0.94	0.93	0.90	0.67	0.92	0.92	0.95
15	0.20	500	0.98	0.97	0.98	0.95	0.84	0.95	0.98	0.97
15	0.25	50	0.53	0.77	0.44	0.77	0.28	0.83	0.35	0.87
15	0.25	100	0.69	0.78	0.63	0.76	0.39	0.82	0.57	0.87
15	0.25	200	0.85	0.89	0.87	0.85	0.59	0.87	0.85	0.92
15	0.25	500	0.94	0.93	0.96	0.88	0.75	0.89	0.95	0.94

Table 19: Study 1A: Adaptive LASSO uSEM Results, Part II

Mean	Con. Path Sen.	Con. Path Spec.	Lag Path Sen.	Lag Path Spec.	Con. Dir. Sen.	Con. Dir. Spec.	Lag Dir. Sen.	Lag Dir. Spec.
T = 50	0.54	0.89	0.51	0.87	0.34	0.91	0.45	0.93
T = 100	0.69	0.95	0.62	0.94	0.47	0.93	0.59	0.97
T = 200	0.79	0.98	0.71	0.98	0.57	0.95	0.70	0.99
T = 500	0.84	0.99	0.76	0.99	0.64	0.95	0.74	1.00
S = 0.15	0.73	0.96	0.67	0.96	0.54	0.96	0.65	0.98
S = 0.20	0.72	0.95	0.65	0.94	0.50	0.93	0.62	0.97
S = 0.25	0.70	0.94	0.63	0.93	0.46	0.91	0.59	0.96
V = 5	0.75	0.97	0.68	0.96	0.53	0.94	0.65	0.98
V = 10	0.71	0.96	0.64	0.95	0.49	0.94	0.62	0.97
V = 15	0.69	0.93	0.63	0.93	0.48	0.93	0.59	0.96

Table 20: Study 1A: Marginal Means, Adaptive LASSO uSEM Results, Part II

Num. Var	Sparsity	Time	Path Sen.	Path Spec.	Dir. Sen.	Dir. Spec.	Rel. Bias True Pos.	Abs. Bias False Pos.	RMSE
5	0.15	50	0.57	0.80	0.40	0.87	-0.17	0.08	0.14
5	0.15	100	0.70	0.88	0.56	0.90	-0.16	0.06	0.12
5	0.15	200	0.93	0.85	0.86	0.85	-0.21	0.04	0.12
5	0.15	500	1.00	0.77	1.00	0.78	-0.20	0.03	0.10
5	0.20	50	0.65	0.75	0.48	0.81	-0.21	0.09	0.15
5	0.20	100	0.83	0.75	0.68	0.77	-0.24	0.06	0.14
5	0.20	200	0.97	0.71	0.91	0.69	-0.28	0.04	0.13
5	0.20	500	1.00	0.57	1.00	0.57	-0.26	0.03	0.12
5	0.25	50	0.63	0.76	0.45	0.81	-0.20	0.08	0.15
5	0.25	100	0.82	0.77	0.68	0.78	-0.24	0.06	0.14
5	0.25	200	0.97	0.68	0.91	0.68	-0.28	0.04	0.13
5	0.25	500	1.00	0.59	1.00	0.58	-0.26	0.03	0.12
10	0.15	50	0.48	0.86	0.33	0.90	-0.20	0.07	0.16
10	0.15	100	0.80	0.82	0.64	0.86	-0.28	0.05	0.15
10	0.15	200	0.98	0.77	0.90	0.81	-0.30	0.03	0.14
10	0.15	500	1.00	0.78	0.99	0.79	-0.27	0.02	0.12
10	0.20	50	0.57	0.80	0.40	0.85	-0.22	0.07	0.16
10	0.20	100	0.85	0.73	0.70	0.79	-0.31	0.05	0.15
10	0.20	200	0.98	0.68	0.92	0.73	-0.33	0.04	0.14
10	0.20	500	1.00	0.68	0.99	0.71	-0.29	0.02	0.12
10	0.25	50	0.65	0.70	0.46	0.79	-0.26	0.08	0.17
10	0.25	100	0.90	0.60	0.75	0.69	-0.33	0.05	0.16
10	0.25	200	0.98	0.56	0.92	0.63	-0.33	0.04	0.14
10	0.25	500	1.00	0.53	0.99	0.58	-0.31	0.03	0.13
15	0.15	50	0.49	0.84	0.34	0.89	-0.19	0.06	0.17
15	0.15	100	0.83	0.75	0.68	0.82	-0.33	0.05	0.16
15	0.15	200	0.98	0.70	0.92	0.78	-0.33	0.03	0.14
15	0.15	500	1.00	0.71	1.00	0.77	-0.27	0.02	0.11
15	0.20	50	0.61	0.75	0.42	0.82	-0.25	0.07	0.18
15	0.20	100	0.89	0.63	0.75	0.73	-0.35	0.05	0.16
15	0.20	200	0.98	0.57	0.93	0.68	-0.34	0.04	0.14
15	0.20	500	1.00	0.58	0.99	0.66	-0.28	0.03	0.12
15	0.25	50	0.73	0.62	0.51	0.73	-0.31	0.08	0.18
15	0.25	100	0.91	0.52	0.76	0.64	-0.36	0.06	0.16
15	0.25	200	0.98	0.48	0.93	0.59	-0.35	0.04	0.15
15	0.25	500	1.00	0.45	0.99	0.55	-0.31	0.03	0.13

Table 21: Study 1A: Standard LASSO uSEM Results, Part I

Mean	Path Sen.	Path Spec.	Dir. Sen.	Dir. Spec.	Rel. Bias True Pos.	Abs. Bias False Pos.	RMSE
T = 50	0.60	0.76	0.42	0.83	-0.22	0.08	0.16
T = 100	0.84	0.72	0.69	0.78	-0.29	0.05	0.15
T = 200	0.97	0.67	0.91	0.72	-0.31	0.04	0.14
T = 500	1.00	0.63	0.99	0.67	-0.27	0.03	0.12
S = 0.15	0.81	0.79	0.72	0.83	-0.24	0.04	0.14
S = 0.20	0.86	0.68	0.76	0.73	-0.28	0.05	0.14
S = 0.25	0.88	0.60	0.78	0.67	-0.29	0.05	0.15
V = 5	0.84	0.74	0.74	0.76	-0.23	0.05	0.13
V = 10	0.85	0.71	0.75	0.76	-0.29	0.05	0.14
V = 15	0.87	0.63	0.77	0.72	-0.31	0.05	0.15

Table 22: Study 1A: Marginal Means, Standard LASSO uSEM Results, Part I

Num. Var	Spar-sity	Time	Con. Path Sen.	Con. Path Spec.	Lag Path Sen.	Lag Path Spec.	Con. Dir. Sen.	Con. Dir. Spec.	Lag Dir. Sen.	Lag Dir. Spec.
5	0.15	50	0.53	0.90	0.48	0.88	0.29	0.92	0.44	0.94
5	0.15	100	0.72	0.94	0.62	0.92	0.47	0.93	0.61	0.96
5	0.15	200	0.94	0.93	0.90	0.90	0.79	0.89	0.89	0.95
5	0.15	500	1.00	0.90	1.00	0.82	0.99	0.85	1.00	0.91
5	0.20	50	0.59	0.88	0.55	0.84	0.34	0.87	0.49	0.91
5	0.20	100	0.80	0.88	0.73	0.84	0.54	0.83	0.71	0.91
5	0.20	200	0.97	0.84	0.93	0.80	0.83	0.76	0.93	0.89
5	0.20	500	1.00	0.80	1.00	0.66	0.99	0.67	1.00	0.81
5	0.25	50	0.56	0.89	0.52	0.85	0.31	0.88	0.46	0.92
5	0.25	100	0.80	0.88	0.73	0.86	0.54	0.83	0.71	0.92
5	0.25	200	0.97	0.85	0.94	0.79	0.82	0.76	0.93	0.89
5	0.25	500	1.00	0.79	1.00	0.67	0.99	0.67	1.00	0.82
10	0.15	50	0.46	0.93	0.39	0.92	0.25	0.93	0.35	0.96
10	0.15	100	0.78	0.91	0.72	0.89	0.52	0.90	0.70	0.94
10	0.15	200	0.97	0.88	0.96	0.86	0.82	0.87	0.95	0.93
10	0.15	500	1.00	0.88	1.00	0.86	0.98	0.84	1.00	0.92
10	0.20	50	0.53	0.90	0.46	0.88	0.29	0.90	0.41	0.94
10	0.20	100	0.82	0.86	0.77	0.83	0.57	0.86	0.74	0.91
10	0.20	200	0.98	0.83	0.96	0.80	0.84	0.81	0.95	0.89
10	0.20	500	1.00	0.82	1.00	0.79	0.97	0.78	1.00	0.88
10	0.25	50	0.58	0.84	0.52	0.82	0.33	0.86	0.45	0.90
10	0.25	100	0.86	0.79	0.82	0.76	0.60	0.79	0.78	0.86
10	0.25	200	0.97	0.76	0.96	0.72	0.83	0.74	0.94	0.84
10	0.25	500	1.00	0.74	1.00	0.68	0.96	0.69	1.00	0.82
15	0.15	50	0.47	0.92	0.38	0.91	0.26	0.93	0.35	0.95
15	0.15	100	0.82	0.87	0.75	0.86	0.57	0.88	0.72	0.92
15	0.15	200	0.98	0.84	0.96	0.82	0.86	0.85	0.95	0.91
15	0.15	500	1.00	0.84	1.00	0.83	0.98	0.84	1.00	0.91
15	0.20	50	0.56	0.86	0.46	0.85	0.32	0.89	0.40	0.92
15	0.20	100	0.86	0.80	0.81	0.78	0.63	0.82	0.78	0.88
15	0.20	200	0.98	0.76	0.96	0.74	0.86	0.79	0.95	0.86
15	0.20	500	1.00	0.76	1.00	0.74	0.98	0.76	1.00	0.85
15	0.25	50	0.65	0.79	0.57	0.77	0.37	0.83	0.49	0.88
15	0.25	100	0.87	0.74	0.82	0.70	0.63	0.77	0.77	0.83
15	0.25	200	0.97	0.71	0.95	0.67	0.85	0.72	0.93	0.81
15	0.25	500	1.00	0.67	0.99	0.64	0.97	0.68	0.99	0.80

Table 23: Study 1A: Standard LASSO uSEM Results, Part II

Mean	Con. Path Sen.	Con. Path Spec.	Lag Path Sen.	Lag Path Spec.	Con. Dir. Sen.	Con. Dir. Spec.	Lag Dir. Sen.	Lag Dir. Spec.
T = 50	0.57	0.83	0.55	0.77	0.31	0.87	0.48	0.88
T = 100	0.75	0.90	0.76	0.85	0.46	0.89	0.73	0.92
T = 200	0.92	0.96	0.94	0.93	0.69	0.92	0.93	0.96
T = 500	0.99	0.98	0.99	0.96	0.89	0.95	0.99	0.98
S = 0.15	0.82	0.94	0.81	0.90	0.62	0.94	0.79	0.95
S = 0.20	0.81	0.92	0.81	0.88	0.59	0.91	0.78	0.93
S = 0.25	0.80	0.90	0.80	0.85	0.55	0.88	0.77	0.92
V = 5	0.85	0.95	0.88	0.88	0.63	0.91	0.86	0.94
V = 10	0.81	0.93	0.80	0.89	0.59	0.92	0.78	0.94
V = 15	0.77	0.88	0.74	0.86	0.54	0.90	0.71	0.92

Table 24: Study 1A: Marginal Means, Standard LASSO uSEM Results, Part II

Num. Var	Sparsity	Time	Path Sen.	Path Spec	Lag Dir. Sen.	Lag Dir. Spec.	Con. Path Sen.	Con. Path Spec.
5	0.15	50	0.58	0.83	0.51	0.93	0.47	0.95
5	0.15	100	0.79	0.88	0.74	0.95	0.75	0.97
5	0.15	200	0.97	0.89	0.94	0.95	0.97	0.97
5	0.15	500	1.00	0.90	1.00	0.93	1.00	0.98
5	0.20	50	0.65	0.78	0.55	0.90	0.47	0.95
5	0.20	100	0.85	0.75	0.77	0.88	0.75	0.94
5	0.20	200	0.98	0.72	0.94	0.84	0.96	0.93
5	0.20	500	1.00	0.66	0.99	0.77	1.00	0.92
5	0.25	50	0.61	0.76	0.54	0.89	0.43	0.94
5	0.25	100	0.86	0.77	0.79	0.88	0.75	0.95
5	0.25	200	0.98	0.72	0.95	0.85	0.95	0.94
5	0.25	500	1.00	0.67	1.00	0.78	1.00	0.92

Table 25: Study 1B: Graphical VAR Results

Num. Var	Sparsity	Time	Path Sen.	Path Spec	Lag Dir. Sen.	Lag Dir. Spec.	Con. Path Sen.	Con. Path Spec.
5	0.15	50	0.59	0.84	0.46	0.95	0.50	0.92
5	0.15	100	0.79	0.93	0.70	0.98	0.74	0.97
5	0.15	200	0.88	0.98	0.80	1.00	0.86	0.99
5	0.15	500	0.95	1.00	0.86	1.00	0.94	1.00
5	0.20	50	0.67	0.79	0.46	0.94	0.59	0.91
5	0.20	100	0.82	0.86	0.65	0.96	0.79	0.94
5	0.20	200	0.91	0.97	0.78	0.99	0.89	0.99
5	0.20	500	0.96	0.98	0.81	1.00	0.96	1.00
5	0.25	50	0.68	0.79	0.46	0.94	0.61	0.90
5	0.25	100	0.82	0.89	0.65	0.96	0.80	0.95
5	0.25	200	0.90	0.97	0.78	0.99	0.88	0.98
5	0.25	500	0.96	0.99	0.82	0.99	0.96	1.00

Table 26: Study 1B: Stepwise uSEM Results

Num. Var	Sparsity	Time	Path Sen.	Path Spec	Lag Dir. Sen.	Lag Dir. Spec.	Con. Path Sen.	Con. Path Spec.
5	0.15	50	0.59	0.84	0.46	0.95	0.50	0.92
5	0.15	100	0.79	0.93	0.69	0.98	0.74	0.97
5	0.15	200	0.87	0.98	0.80	1.00	0.86	0.99
5	0.15	500	0.95	1.00	0.86	1.00	0.94	1.00
5	0.20	50	0.67	0.79	0.46	0.94	0.59	0.90
5	0.20	100	0.82	0.87	0.65	0.96	0.79	0.94
5	0.20	200	0.91	0.97	0.77	0.99	0.89	0.99
5	0.20	500	0.95	0.99	0.80	1.00	0.96	1.00
5	0.25	50	0.68	0.79	0.46	0.95	0.61	0.90
5	0.25	100	0.82	0.89	0.65	0.96	0.79	0.95
5	0.25	200	0.90	0.97	0.77	0.99	0.88	0.98
5	0.25	500	0.96	0.99	0.82	0.99	0.96	1.00

Table 27: Study 1B: Stepwise uSEM + BIC Results

Num. Var	Sparsity	Time	Path Sen.	Path Spec	Lag Dir. Sen.	Lag Dir. Spec.	Con. Path Sen.	Con. Path Spec.
5	0.15	50	0.81	0.62	0.70	0.84	0.69	0.85
5	0.15	100	0.88	0.87	0.86	0.95	0.83	0.96
5	0.15	200	0.97	0.97	0.95	0.98	0.96	0.99
5	0.15	500	1.00	0.97	1.00	0.98	1.00	0.99
5	0.20	50	0.84	0.58	0.70	0.83	0.73	0.84
5	0.20	100	0.90	0.83	0.82	0.93	0.85	0.95
5	0.20	200	0.97	0.95	0.94	0.97	0.96	0.99
5	0.20	500	1.00	0.94	0.99	0.95	1.00	0.99
5	0.25	50	0.84	0.58	0.71	0.84	0.75	0.83
5	0.25	100	0.89	0.87	0.82	0.94	0.84	0.96
5	0.25	200	0.97	0.95	0.93	0.97	0.95	0.98
5	0.25	500	1.00	0.93	1.00	0.95	1.00	0.99

Table 28: Study 1B: Adaptive LASSO uSEM Results

Num. Var	Sparsity	Time	Path Sen.	Path Spec	Lag Dir. Sen.	Lag Dir. Spec.	Con. Path Sen.	Con. Path Spec.
5	0.15	50	0.52	0.83	0.40	0.95	0.48	0.91
5	0.15	100	0.74	0.88	0.65	0.96	0.73	0.94
5	0.15	200	0.95	0.84	0.93	0.95	0.95	0.93
5	0.15	500	1.00	0.80	1.00	0.93	1.00	0.90
5	0.20	50	0.66	0.75	0.48	0.92	0.61	0.86
5	0.20	100	0.86	0.70	0.72	0.92	0.85	0.83
5	0.20	200	0.99	0.69	0.96	0.91	0.98	0.81
5	0.20	500	1.00	0.56	1.00	0.82	1.00	0.76
5	0.25	50	0.66	0.74	0.45	0.93	0.63	0.85
5	0.25	100	0.86	0.73	0.74	0.91	0.86	0.85
5	0.25	200	0.98	0.68	0.95	0.90	0.98	0.81
5	0.25	500	1.00	0.55	1.00	0.82	1.00	0.75

Table 29: Study 1B: Standard LASSO uSEM Results

Condition	Path Sen.	Path Spec.	Dir. Sen.	Dir. Spec.
sim1	0.86	0.90	0.86	0.65
sim5	1.00	0.74	1.00	0.50
sim13	0.56	0.91	0.45	0.78
sim14	0.92	0.86	0.91	0.61
sim15	0.99	0.40	0.99	0.29
sim18	0.88	0.89	0.88	0.65
sim19	0.90	0.09	0.86	0.19
sim20	0.78	0.24	0.74	0.29

Table 30: Study 2: Graphical VAR Results

Condition	Path Sen.	Path Spec.	Dir. Sen.	Dir. Spec.
sim1	0.81	0.96	0.42	0.85
sim5	0.84	1.00	0.48	0.88
sim13	0.52	0.95	0.26	0.91
sim14	0.83	0.94	0.40	0.84
sim15	0.92	0.81	0.54	0.78
sim18	0.82	0.94	0.48	0.87
sim19	0.00	1.00	0.00	1.00
sim20	0.00	1.00	0.00	1.00

Table 31: Study 2: Stepwise uSEM Results

Condition	Path Sen.	Path Spec.	Dir. Sen.	Dir. Spec.
sim1	0.81	0.96	0.42	0.85
sim5	0.84	1.00	0.48	0.88
sim13	0.52	0.95	0.26	0.91
sim14	0.83	0.94	0.40	0.84
sim15	0.92	0.81	0.55	0.78
sim18	0.82	0.94	0.48	0.87
sim19	0.01	1.00	0.00	1.00
sim20	0.01	1.00	0.01	1.00

Table 32: Study 2: Stepwise uSEM + BIC Results

Condition	Path Sen.	Path Spec.	Dir. Sen.	Dir. Spec.
sim1	0.86	0.92	0.51	0.83
sim5	1.00	0.92	0.82	0.75
sim13	0.59	0.93	0.30	0.88
sim14	0.89	0.90	0.50	0.80
sim15	1.00	0.58	0.62	0.57
sim18	0.92	0.91	0.58	0.82
sim19	0.31	0.68	0.23	0.74
sim20	0.64	0.45	0.50	0.55

Table 33: Study 2: Adaptive LASSO Results

Condition	Path Sen.	Path Spec.	Dir. Sen.	Dir. Spec.
sim1	0.91	0.72	0.58	0.69
sim5	1.00	0.46	0.96	0.45
sim13	0.58	0.85	0.31	0.83
sim14	0.92	0.64	0.58	0.66
sim15	1.00	0.20	0.68	0.39
sim18	0.92	0.74	0.65	0.70
sim19	0.34	0.81	0.25	0.83
sim20	0.45	0.72	0.35	0.74

Table 34: Study 2: Standard LASSO Results

APPENDIX B: FIGURES

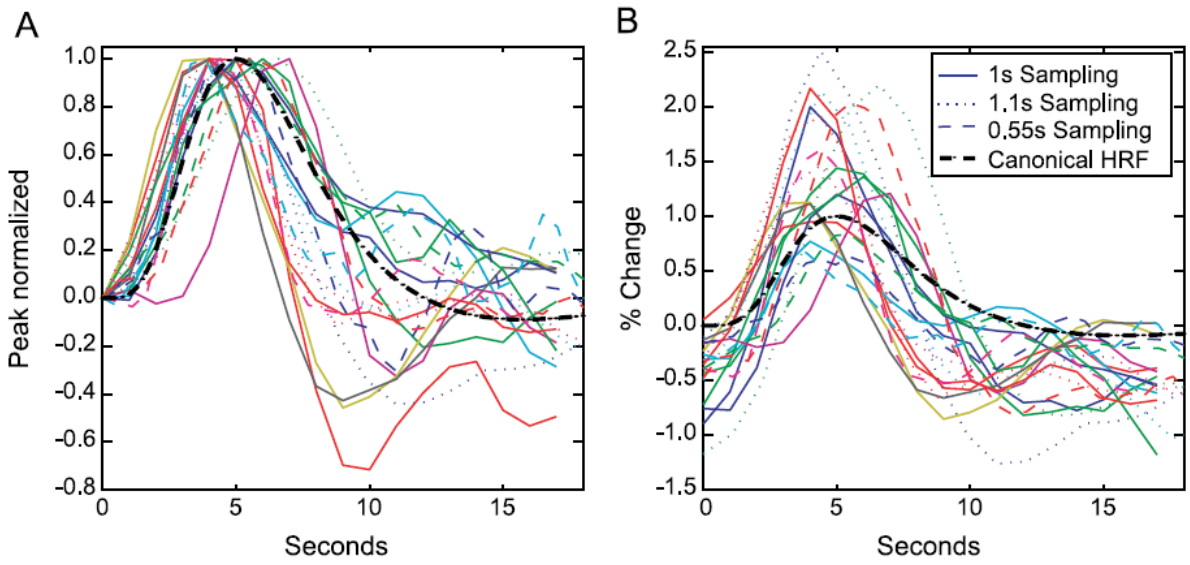

Figure 29: Hemodynamic response function across 20 subjects, as depicted in Handwerker et al., 2004, demonstrating both between-subject variability and sensitivity of HRF to sampling rate (TR). Panel A shows the normalized HRF. Panel B shows the HRF scaled by % change, allowing us to see between-subject amplitude variability.

REFERENCES

Abegaz, F. & Wit, E. (2013). Sparse time series chain graphical models for reconstructing genetic networks. *Biostatistics*, 14, 586–599.

Barch, D. M., Burgess, G. C., Harms, M. P., Petersen, S. E., Schlaggar, B. L., Corbetta, M., Glasser, M. F., Curtiss, S., Dixit, S., Feldt, C., et al. (2013). Function in the human connectome: Task-fMRI and individual differences in behavior. *NeuroImage*, 80, 169–189.

Beltz, A. M. & Molenaar, P. C. (2016). Dealing with multiple solutions in structural vector autoregressive models. *Multivariate Behavioral Research*, 51, 357–373.

Beltz, A. M., Wright, A. G., Sprague, B. N., & Molenaar, P. C. (2016). Bridging the nomothetic and idiographic approaches to the analysis of clinical data. *Assessment*, 23, 447–458.

Bentler, P. M. (1990). Comparative fit indexes in structural models. *Psychological Bulletin*, 107, 238–246.

Bentler, P. M. & Bonnett, D. G. (1980). Significance tests and goodness of fit in the analysis of covariance structures. *Psychological Bulletin*, 88, 588–606.

Borsboom, D. & Cramer, A. O. (2013). Network analysis: An integrative approach to the structure of psychopathology. *Annual Review of Clinical Psychology*, 9, 91–121.

Buxton, R. B., Wong, E. C., & Frank, L. R. (1998). Dynamics of blood flow and oxygenation changes during brain activation: The balloon model. *Magnetic Resonance In Medicine*, 39(6), 855–864.

Cattell, R. B. (1966). The data box: Its ordering of total resources in terms of possible relational systems. In *Handbook of Multivariate Experimental Psychology* (pp. 69–130). Springer Science.

Chen, G., Glen, D. R., Saad, Z. S., Hamilton, J. P., Thomason, M. E., Gotlib, I. H., & Cox, R. W. (2011). Vector autoregression, structural equation modeling, and their synthesis in neuroimaging data analysis. *Computers in Biology and Medicine*, 41(12), 1142–1155.

Chen, J. & Chen, Z. (2008). Extended bayesian information criteria for model selection with large model spaces. *Biometrika*, 95(3), 759–771.

Chickering, D. M. (2002). Optimal structure identification with greedy search. *Journal of Machine Learning Research*, 3, 507–554.

Eichler, M. (2005). A graphical approach for evaluating effective connectivity in neural systems. *Philosophical Transactions of the Royal Society of London B: Biological Sciences*, 360(1457), 953–967.

Enders, C. K. & Bandalos, D. L. (2001). The relative performance of full information maximum likelihood estimation for missing data in structural equation models. *Structural Equation Modeling*, 8(3), 430–457.

Epskamp, S. (2016). *graphicalVAR: Graphical VAR for Experience Sampling Data*. R package version 0.1.4.

Epskamp, S. & Fried, E. I. (2016). A primer on estimating regularized psychological networks. *arXiv preprint arXiv:1607.01367*.

Epskamp, S., Maris, G., Waldorp, L., & Borsboom, D. (2015). Network psychometrics. In P. Irwing, D. Hughes, & T. Booth (Eds.), *Handbook of Psychometrics*. New York, NY: Wiley.

Epskamp, S., Rhemtulla, M., & Borsboom, D. (2016). Generalized network psychometrics: Combining network and latent variable models. *arXiv preprint arXiv:1605.09288*.

Finn, E. S., Shen, X., Scheinost, D., Rosenberg, M. D., Huang, J., Chun, M. M., Papademetris, X., & Constable, R. T. (2015). Functional connectome fingerprinting: Identifying individuals using patterns of brain connectivity. *Nature Neuroscience*, 18, 1664–1671.

Fried, E. I., Epskamp, S., Nesse, R. M., Tuerlinckx, F., & Borsboom, D. (2016). What are "good" depression symptoms? Comparing the centrality of DSM and non-DSM symptoms of depression in a network analysis. *Journal of Affective Disorders*, 189, 314–320.

Friedman, J., Hastie, T., & Tibshirani, R. (2008). Sparse inverse covariance estimation with the graphical lasso. *Biostatistics*, 9(3), 432–441.

Friston, K., Moran, R., & Seth, A. K. (2013). Analysing connectivity with granger causality and dynamic causal modelling. *Current Opinion in Neurobiology*, 23(2), 172–178.

Friston, K. J., Harrison, L., & Penny, W. (2003). Dynamic causal modelling. *NeuroImage*, 19(4), 1273–1302.

Gates, K. M., Lane, S. T., Varangis, E., Giovanello, K., & Guskiewicz, K. (2016). Unsupervised classification during time series model building. *Multivariate Behavioral Research*, (pp. 1–20).

Gates, K. M. & Molenaar, P. C. (2012). Group search algorithm recovers effective connectivity maps for individuals in homogeneous and heterogeneous samples. *NeuroImage*, 63(1), 310–319.

Gates, K. M., Molenaar, P. C., Hillary, F. G., Ram, N., & Rovine, M. J. (2010). Automatic search for fMRI connectivity mapping: An alternative to granger causality testing using formal equivalences among SEM path modeling, VAR, and unified SEM. *NeuroImage*, 50(3), 1118–1125.

Granger, C. W. J. (1969). Investigating causal relations by econometric models and cross-spectral methods. *Econometrica*, 37(3), 424–438.

Hamaker, E. L., Dolan, C. V., & Molenaar, P. C. (2002). On the nature of SEM estimates of ARMA parameters. *Structural Equation Modeling*, 9(3), 347–368.

Handwerker, D. A., Ollinger, J. M., & D'Esposito, M. (2004). Variation of BOLD hemodynamic responses across subjects and brain regions and their effects on statistical analyses. *NeuroImage*, 21(4), 1639–1651.

Hoerl, A. E. & Kennard, R. W. (1970). Ridge regression: Biased estimation for nonorthogonal problems. *Technometrics*, 12(1), 55–67.

Hsu, H.-Y., Troncoso Skidmore, S., Li, Y., & Thompson, B. (2014). Forced zero cross-loading misspecifications in measurement component of structural equation models: Beware of even "small" misspecifications. *Methodology: European Journal of Research Methods for the Behavioral and Social Sciences*, 10(4), 138.

Huettel, S. A., Song, A. W., & McCarthy, G. (2004). *Functional magnetic resonance imaging*, volume 1. Sinauer Associates Sunderland.

Jacobucci, R. (2016). *regsem: Performs Regularization on Structural Equation Models*. R package version 0.2.0.

Jacobucci, R., Grimm, K. J., & McArdle, J. J. (2016). Regularized structural equation modeling. *Structural Equation Modeling: A Multidisciplinary Journal*, 23(4), 555–566.

Jöreskog, K. & Sörbom, D. (1981). LISREL V: Analysis of linear structural relationships by maximum likelihood and least squares methods (Research Report 81-8). Uppsala, Sweden: University of Uppsala, Department of Statistics.

Jöreskog, K. G. & Sörbom, D. (1986). *LISREL VI: Analysis of linear structural relationships by maximum likelihood, instrumental variables, and least squares methods*. Scientific Software.

Kim, J., Zhu, W., Chang, L., Bentler, P. M., & Ernst, T. (2007). Unified structural equation modeling approach for the analysis of multisubject, multivariate functional MRI data. *Human Brain Mapping*, 28(2), 85–93.

Lane, S., Gates, K., & Molenaar, P. (2016). *gimme: Group Iterative Multiple Model Estimation*. R package version 0.1-7.

Lane, S. T., Gates, K., Pike, H., Beltz, A., & Wright, A. (under revision). Uncovering general, shared, and unique temporal patterns in ambulatory assessment data. *Psychological Methods*.

Lindquist, M. A., Loh, J. M., Atlas, L. Y., & Wager, T. D. (2009). Modeling the hemodynamic response function in fMRI: efficiency, bias and mis-modeling. *NeuroImage*, 45(1), S187–S198.

Lindquist, M. A. & Wager, T. D. (2007). Validity and power in hemodynamic response modeling: A comparison study and a new approach. *Human Brain Mapping*, 28(8), 764–784.

Lütkepohl, H. (2005). *New introduction to multiple time series analysis*. Springer Science & Business Media.

MacCallum, R. C. (1986). Specification searches in covariance structure modeling. *Psychological Bulletin*, 100, 107–120.

MacCallum, R. C., Roznowski, M., & Necowitz, L. B. (1992). Model modifications in covariance structure analysis: The problem of capitalization on chance. *Psychological Bulletin*, 111, 490–504.

McArdle, J. J. (2005). The development of the RAM rules for latent variable structural equation modeling. *Contemporary psychometrics: A festschrift for Roderick P. McDonald*, (pp. 225–273).

McIntosh, A. & Gonzalez-Lima, F. (1994). Structural equation modeling and its application to network analysis in functional brain imaging. *Human Brain Mapping*, 2(1-2), 2–22.

McNeish, D. M. (2015). Using lasso for predictor selection and to assuage overfitting: A method long overlooked in behavioral sciences. *Multivariate Behavioral Research*, 50(5), 471–484.

Meek, C. (1995). Causal inference and causal explanation with background knowledge. In *Proceedings of the Eleventh Conference on Uncertainty in Artificial Intelligence* (pp. 403–410).: Morgan Kaufmann Publishers Inc.

Molenaar, P. C. (2004). A manifesto on psychology as idiographic science: Bringing the person back into scientific psychology, this time forever. *Measurement*, 2(4), 201–218.

Mumford, J. A. & Ramsey, J. D. (2014). Bayesian networks for fMRI: A primer. *NeuroImage*, 86, 573–582.

Nesselroade, J. R. & Ford, D. H. (1985). P-technique comes of age multivariate, replicated, single-subject designs for research on older adults. *Research on Aging*, 7(1), 46–80.

Power, J. D., Cohen, A. L., Nelson, S. M., Wig, G. S., Barnes, K. A., Church, J. A., Vogel, A. C., Laumann, T. O., Miezin, F. M., & Schlaggar, B. L. (2011). Functional network organization of the human brain. *Neuron*, 72(4), 665–678.

Price, R. B., Lane, S. T., Gates, K. M., Kraynak, T. E., Horner, M. S., Thase, M. E., & Siegle, G. J. (2016). Parsing heterogeneity in the brain connectivity of depressed and healthy adults during positive mood. *Biological Psychiatry*.

R Core Team (2016). *R: A Language and Environment for Statistical Computing*. R Foundation for Statistical Computing, Vienna, Austria.

Ramsey, J. D., Hanson, S. J., & Glymour, C. (2011). Multi-subject search correctly identifies causal connections and most causal directions in the DCM models of the smith et al. simulation study. *NeuroImage*, 58(3), 838–848.

Rosseel, Y. (2012). lavaan: An R package for structural equation modeling. *Journal of Statistical Software*, 48(2), 1–36.

Rothman, A. J., Levina, E., & Zhu, J. (2010). Sparse multivariate regression with covariance estimation. *Journal of Computational and Graphical Statistics*, 19(4), 947–962.

Schwarz, G. et al. (1978). Estimating the dimension of a model. *The Annals of Statistics*, 6(2), 461–464.

Seth, A. K., Barrett, A. B., & Barnett, L. (2015). Granger causality analysis in neuroscience and neuroimaging. *The Journal of Neuroscience*, 35(8), 3293–3297.

Seth, A. K., Chorley, P., & Barnett, L. C. (2013). Granger causality analysis of fMRI BOLD signals is invariant to hemodynamic convolution but not downsampling. *NeuroImage*, 65, 540–555.

Shirer, W., Ryali, S., Rykhlevskaia, E., Menon, V., & Greicius, M. (2012). Decoding subject-driven cognitive states with whole-brain connectivity patterns. *Cerebral Cortex*, 22(1), 158–165.

Smith, S. M., Miller, K. L., Salimi-Khorshidi, G., Webster, M., Beckmann, C. F., Nichols, T. E., Ramsey, J. D., & Woolrich, M. W. (2011). Network modelling methods for fMRI. *NeuroImage*, 54(2), 875–891.

Sörbom, D. (1989). Model modification. *Psychometrika*, 54(3), 371–384.

Spirtes, P. & Glymour, C. (1991). An algorithm for fast recovery of sparse causal graphs. *Social Science Computer Review*, 9(1), 62–72.

Steiger, J. H. (1990). Structural model evaluation and modification: An interval estimation approach. *Multivariate Behavioral Research*, 25, 173–180.

Stephan, K. E., Kasper, L., Harrison, L. M., Daunizeau, J., den Ouden, H. E., Breakspear, M., & Friston, K. J. (2008). Nonlinear dynamic causal models for fMRI. *NeuroImage*, 42(2), 649–662.

Tibshirani, R. (1996). Regression shrinkage and selection via the lasso. *Journal of the Royal Statistical Society. Series B (Methodological)*, (pp. 267–288).

van den Heuvel, M. P., Stam, C. J., Kahn, R. S., & Pol, H. E. H. (2009). Efficiency of functional brain networks and intellectual performance. *The Journal of Neuroscience*, 29(23), 7619–7624.

Van Essen, D. C., Smith, S. M., Barch, D. M., Behrens, T. E., Yacoub, E., Ugurbil, K., Consortium, W.-M. H., et al. (2013). The WU-Minn human connectome project: An overview. *NeuroImage*, 80, 62–79.

Varoquaux, G. & Craddock, R. C. (2013). Learning and comparing functional connectomes across subjects. *NeuroImage*, 80, 405–415.

Wild, B., Eichler, M., Friederich, H.-C., Hartmann, M., Zipfel, S., & Herzog, W. (2010). A graphical vector autoregressive modelling approach to the analysis of electronic diary data. *BMC Medical Research Methodology*, 10(1), 1–13.

Wright, A., Beltz, A. M., Gates, K. M., Molenaar, P., & Simms, L. J. (2014). Examining the dynamic structure of daily internalizing and externalizing behavior at multiple levels of analysis. *Frontiers in Psychology*, 6, 1–20.

Yeo, B. T., Krienen, F. M., Sepulcre, J., Sabuncu, M. R., Lashkari, D., Hollinshead, M., Roffman, J. L., Smoller, J. W., Zöllei, L., Polimeni, J. R., et al. (2011). The organization of the human cerebral cortex estimated by intrinsic functional connectivity. *Journal of Neurophysiology*, 106(3), 1125–1165.

Yin, J. & Li, H. (2011). A sparse conditional gaussian graphical model for analysis of

genetical genomics data. *The Annals of Applied Statistics*, 5(4), 2630.

Zou, H. (2006). The adaptive lasso and its oracle properties. *Journal of the American Statistical Association*, 101(476), 1418–1429.